2019

THE ROLE OF EPHEMERAL STRATIFICATION, ANOXIA, AND ENTRAINMENT IN MEDIATING SPATIOTEMPORAL TROPHIC STATE DYNAMICS IN A LAKE MICHIGAN DROWNED RIVER MOUTH SYSTEM (MONA LAKE, MI)

Hayden Henderson
Michigan Technological University, hmhender@mtu.edu

THE ROLE OF EPHEMERAL STRATIFICATION, ANOXIA, AND ENTRAINMENT IN MEDIATING SPATIOTEMPORAL TROPHIC STATE DYNAMICS IN A LAKE MICHIGAN DROWNED RIVER MOUTH SYSTEM (MONA LAKE, MI)

By

Hayden M. Henderson

A THESIS

Submitted in partial fulfillment of the requirements for the degree of

MASTER OF SCIENCE

In Environmental Engineering

MICHIGAN TECHNOLOGICAL UNIVERSITY

2019

This thesis has been approved in partial fulfillment of the requirements for the Degree of MASTER OF SCIENCE in Environmental Engineering.

Department of Civil & Environmental Engineering

Thesis Advisor:	*Dr. Martin T. Auer*
Committee Member:	*Dr. Cory McDonald*
Committee Member:	*Dr. Amy Marcarelli*
Department Chair:	*Dr. Audra Morse*

Table of Contents

List of figures

List of tables

Acknowledgements

Many thanks to CEE and GLRC personnel: Rashelle Sandell, Angela Keranen, Lisa Cunard, Jamey Anderson, Chris Pinnow, Ryan Williams, Mike Abbott, and Dr. Guy Meadows for supporting my research and laboratory operations - as well as past and present students Dr. Anika Kuczynski, Nathan Zgnilec, Anya Leach, Dani Cummins, Sara Gustafson, Jacob Hernandez, Tristan Odekirk, Jimmy Peterman, Chenfu Huang and Emily Shaw for your help in field efforts, laboratory efforts, and, well, life efforts.

External personnel involved in this project's success include: Dr. Steve Charpa (Tufts University), Michelle Storey (MDEQ), Josh and Mark Kieser (Kieser and Associates), Clayton Yochum, and active members of the Mona Lake Watershed Council: George Cannon, Don Trygstad, Thomas Hillstrom, and Joel Jarvis.

Furthermore, it was by an anonymous donation to Michigan Tech for the purposes of graduate student funding in surface water research that this experience was made available to me – and for that I will be forever grateful.

Another wholehearted thank you to my committee: Dr. Cory McDonald, Dr. Amy Marcarelli, and my advisor and mentor in areas ranging from heartbreak to Henry's law - Dr. Martin T. Auer.

I could not have accomplished and grown so much in this period of my life without the support of many friends and family members – and especially my dog, Frank, who always reminds me when it is time to go to the woods and remember why we do this in the first place.

"You become. It takes a long time. That's why it doesn't happen often to people who break easily, or have sharp edges, or who have to be carefully kept. Generally, by the time you are Real, most of your hair has been loved off, and your eyes drop out and you get loose in the joints and very shabby. But these things don't matter at all, because once you are Real you can't be µgly, except to people who don't understand."

The Velveteen Rabbit

Abstract

Mona Lake, MI (a drowned river mouth system) has become eutrophic as result of cultural eutrophication. The integrated monitoring effort and subsequent modeling (LAKE2K) reported on here has shifted the management focus to internal phosphorus loads (60 percent of annual load, 90 percent of load during the stratified and anoxic period) as a necessary precursor to trophic state change. Sediment phosphorus release can yield extreme elevations (> 1 mgSRP/L) of bottom water soluble reactive phosphorus (SRP), with blooms of potentially toxic cyanobacteria (largely Microcystis) occurring annually. Such blooms are ascribable to stochastic mixing and phosphorus entrainment to the surface waters, with entrainment forces shown to be significant as a result of this lakes geographic proximity to large fetch events across Lake Michigan. Intrusion events from Lake Michigan are shown to strengthen stratification in Mona Lake, increasing hypolimnetic phosphorus accumulation prior to mixing events. Hypothetical phosphorus reduction strategies applied to the calibrated model indicate treatment of internal loading and a 25 percent reduction in external loading would allow Mona Lake to remain below 20 ug/L total phosphorus (eutrophic threshold).

1 Introduction

Eutrophication of inland waters in the Great Lakes basin has steadily increased as urbanization and growing agricultural intensity deliver phosphorus loads exceeding the assimilation capacity of the watersheds and their receiving water bodies (Smith et al. 1999). Resulting algal blooms often include cyanobacteria, often capable of producing a toxin that is a threat to both human and aquatic life (Jacoby et al. 2000). This and other manifestations of eutrophication (e.g. reduced water clarity, hypoxia) place increasing importance on mitigating potential impacts through management plans that address both causes and impacts.

Implementations of plans and methods addressing *causes* of eutrophic conditions can be seen throughout the Great Lakes basin. For example, in the Madison Lakes (WI), wastewater diversion in 1958 reduced the algae composition from 99 percent *Microcystis* to as low as 25 percent just one year later (Sonzgoni et al. 1975). Ongoing efforts to manage agricultural land use in the same region through efficient fertilizer application have been successful in reducing phosphorus loads between 30 and 50 percent. An adaptive watershed management plan implemented for Lake Mendota (WI) resulted in a phosphorus load reduction of nearly 33 percent from 2013 to 2015 (Yahara WINS Final Report 2016).

Addressing *symptoms* of eutrophication often requires an engineering approach. For example, implementation of artificial mixing devices (physical mixing and/or aeration) is known to suppress the release of phosphorus from lake bottom sediments (Cook et al. 2005). Chaffrey Reservoir (Australia) saw a reduction in the internal loading of soluble reactive phosphorus of nearly 80 percent when artificial destratification was employed to enhance oxygen transport to the hypolimnion (Sherman et al. 2000).

Chemical treatment of lakes to suppress phosphorus-based eutrophication is another common management practice. This method and associated chemicals (i.e. aluminum sulfate, poly-aluminum chloride, lanthanum-modified bentonite clay) function on the same principle, wherein the chemical is applied to the lake surface and precipitates with phosphates in the water column, then settles out as a floc and creates a barrier in the pore water incapable of releasing phosphorus. The urban, predominantly internal phosphorus loading in hyper-eutrophic Swan Lake (Toronto) resulted in total phosphorus (TP) concentrations decrease 60 and 76 percent, respectively, in years one and two of Phoslock treatment, the commercial name for lanthanum-modified bentonite clay (Nurnberg et al. 2016). These and other methodologies are continually evolving implementations with promising success rates, used throughout the world in inland lakes with eutrophication issues, with certain methods being more appropriate for given ecosystems. In choosing an appropriate method, or combination thereof, it should be noted that the percent contribution of phosphorus from internal versus external loads differs for every waterbody. Wastewater treatment plants (pre-diversion) once delivered massive phosphorus loads to tributaries and thus surface waters. Although modern technologies and management techniques have reduced the external loading of phosphorus, including these wastewater sources, much of it remains in the watershed, commonly referred to as ‘legacy’ phosphorus deposits (James 2013), and quantified as an *internal* load.

To understand the impact of these deposits, we must study the phosphorus cycle and its respective role as the limiting nutrient in a given watershed or lake as it relates to biogeochemical processes. While external loading has historically been the dominating contributor of phosphorus to eutrophic lakes, it is generally delivered in forms not entirely bioavailable. Internal phosphorus loading is often significant or dominant in lakes that vertically stratify. Solar radiation causes at-depth density differences in the water column (stratification), resulting in decreased rates of mass transfer across layers. In productive lakes, the resulting decomposition creates a high oxygen demand in the sediments, capable of completely depleting the bottom layer (hypolimnion) of oxygen, termed anoxia. With large amounts of historic phosphorus loading and subsequent settling, and no process capable of diffusing sufficient oxygen into the hypolimnion, phosphorus-binding ferric iron is reduced to ferrous iron, releasing SRP, the most bioavailable form of phosphorus. This phosphorus is brought to the surface by wind-driven mixing forces, known as entrainment, where algae now have the components required for photosynthesis. Seasonally, this phenomenon often coincides with nitrate and other nutrient depletions. Algae capable of nitrogen fixation (i.e. some cyanobacteria) often lack competition for nutrients at this time in the seasonal succession. This allows them to become the dominant algal species by consuming SRP brought to the surface by wind-driven entrainment. Hypolimnetic anoxia and attendant sediment phosphorus release can occur for upwards of 6 months in northern temperate lakes (Nurnberg 2004), a feature of their bathymetry and therefore stratification regime, as well as sediment chemistry.

Drowned river mouth lakes, such as those common along the eastern shore of Lake Michigan, are hydrodynamically linked to the larger Great Lakes system, potentially exposing them to intrusions under certain meteorological conditions. Carved by glaciers and flooded by water-level rise after the last ice age, drowned river mouth lakes are ravine-like in their bathymetry with large length to width ratios. Furthermore, their riverine formation often features a minimal mean depth and seasonally variable hydraulic residence times. These unique characteristics play intricately into the biogeochemical cycle of drowned river mouth lakes, increasing their susceptibility to stochastic wind events and associated disturbances in stratification regime and nutrient cycling. We seek to understand how historical impacts, as well as current features of a specific drowned river mouth system (hydrology, biogeochemistry) impact and inform management, both historically (wastewater diversion, celery flat discharge structures) and in the future (external and internal nutrient loads).

1.1 Study Site Description

Mona Lake, a drowned river mouth system discharging to Lake Michigan, is oriented largely east-west, aligning it with prevailing westerly winds (Figure 1-1). The lake has a length of 6.5 km and an average width of 0.5 km with mean and maximum depths of 4.5 and 8.5 m, respectively. Hydraulic residence time can vary from 105 to 160 days during low tributary flows, decreasing to less than 35 days during high tributary flows (Evans 1992). The mean annual retention time in this study was calculated to be 69 and 54 days in 2017 and 2018, respectively.

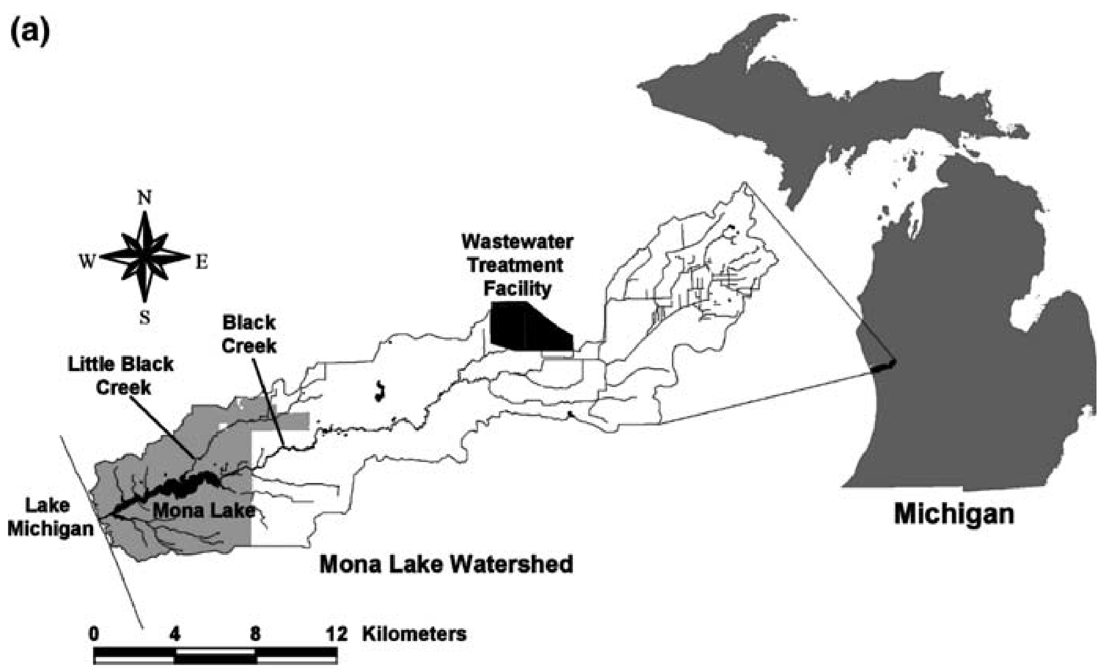

Figure 1-1 Mona Lake watershed location and orientation with respect to the wastewater treatment plant and major tributaries. Gray shaded area indicates municipal boundaries within watershed (Annis Water Resources Institute 2003).

The Mona Lake watershed has an area of 2 km^2 and is predominantly agricultural in its eastern portion, forested in mid-watershed and residential/commercial to the west (Figure 1-2). Mona Lake, comprising less than 2 percent of the total watershed area, receives inputs from four tributaries (Black Creek, Little Black Creek, Cress Creek, and Ellis Drain; Table 1-1) with Black Creek representing the largest percentage of watershed area and hydrologic contribution. Black Creek receives input from large ponds, called the 'celery flats', about 1 km upstream from the mouth at Mona Lake. These ponds were once agricultural fields that now represent attempts to return the area to wetlands. Once contributing phosphorus-rich water to Black Creek through levees (2.6x downstream increase; Steinman and Ogdahl 2011), discharge limiting structures were installed and levees filled in 2015 with the intention to suppress phosphorus loading from the flats. Their current magnitude and frequency of influence on Black Creek and therefore Mona Lake are presently not well understood. The effort herein will aim to update, elaborate upon, and synthesize previous and new studies of the lake, its watershed, and its tributaries.

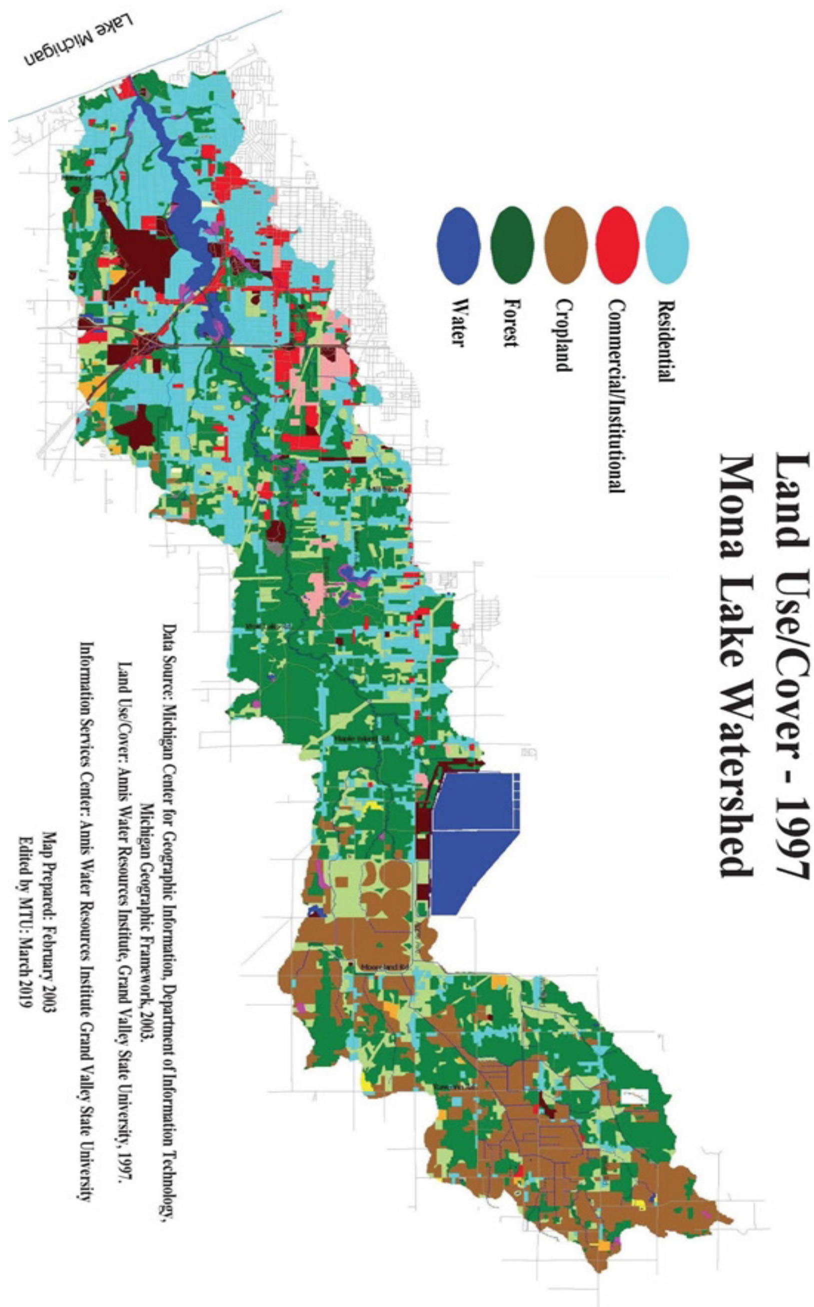

Figure 1-2 Mona Lake watershed land use in 1997, illustrating the dominance of agricultural/forested lands to the east and commercial/residential land uses in the west (Annis Water Resources Institute 2003, edited to highlight major land use types).

Table 1-1 Contribution, of the four major tributaries to Mona Lake to watershed area and hydrologic contribution, as a percentage of the total.

Tributary	Watershed Area	Hydrologic Contribution
Black Creek	68	77
Little Black Creek	9	9
Cress Drain	6	6
Ellis Drain	6	6
Other	11	2

2 Objectives and Approach

The Mona Lake Watershed Council is representing stakeholders to the Michigan Department of Environmental Quality (MDEQ) in recommending a management framework for eliminating manifestations of eutrophication. The plan would include a review of previous studies, a monitoring program to characterize tributary and lake conditions, and modeling exercises providing guidance for restorative actions, e.g. reductions in internal and external phosphorus loads. Several studies have quantified these loads for Mona Lake, documenting significant reductions over a period of decades (Freedman et al. 1979, Limnotech 1982, Steinman et al. 2006; Steinman et al. 2009). However, phosphorus loads have not been quantified in the last decade, and load estimates have not been integrated to support development of the engineered designs required for implementation of management solutions.

Historically, the TP load to Mona Lake was well beyond the assimilation capacity of the system (water quality heavily impaired). Legacy deposits of phosphorus and oxygen demanding materials reflected decades of agricultural runoff and municipal wastewater discharge. Mona Lake once represented a classic example of a hypereutrophic water body (Figure 2-1) with manifestations of eutrophication including high levels of algal biomass, poor water clarity, and hypolimnetic oxygen depletion. Following wastewater diversion in 1972 (and continuing through 1981), external loading to Mona Lake was reduced 75-80 percent (Limnotech 1982); however, the annual mean TP for Mona Lake remained above the eutrophic threshold when modeled via trophic state (Chapra et al. 1981; Carlson 1977; Figures 2-2 and 2-3). Internal phosphorus loading, previously estimated to constitute 73 to 82 percent of the total phosphorus load to Mona Lake (Steinman et al. 2009), results from legacy deposits in lake sediments that serve to sustain eutrophic conditions. In this study, internal phosphorus loading was found to constitute 60 percent of the annual total phosphorus load, and 90 percent of the total phosphorus load during the stratified and anoxic period (June to September). Loading models (Vollenweider 1975; Figure 2-1), based on external total phosphorus loading and retention time, support this hypothesis. Based solely on external loads, Mona Lake should have exhibited mesotrophic behavior following wastewater diversion (1982 study). The total phosphorus trophic state index (TSI), constructed from mean lake total phosphorus concentrations, more accurately represents the current eutrophic state (compare Figure 2-2 with Figures 2-3 and 2-4), pointing to the significance of internal phosphorus loading.

Mona Lake stakeholders seek to reduce and or eliminate symptoms of eutrophication through reductions in phosphorus loading. Discrepancies between external load-based projections of trophic state and those observed at the lake today point to the need for further consideration of the importance of both external and internal loading management. Our primary objective is to integrate results from field monitoring and mathematical modeling of trophic state conditions to identify engineered actions allowing Mona Lake stakeholders to meet their goals. The results and proposed management implications will serve as the basis for development of a planning proposal submitted to MDEQ for consideration of funding and implementation assistance. The approach includes a field program in support of a modeling efforts, with insights from both informing the recommended survey of management techniques and focus areas.

In this research, two hypotheses will be tested using a one-dimensional (vertical) model, capable of simulating both current and potential water quality in Mona Lake. With the ability to modify internal and external loading independently, the model will allow for prediction of trophic state impacts by reducing external loads as well as further quantification of internal loading influence, hypothesized to be the driving factor in the still-eutrophic Mona Lake. Field sampling data collection was designed to provide model inputs: tributary loads, particle settling velocity analysis via sediment traps and photosynthetically active radiation monitoring at both the lake surface and subsurface, as well as conductivity, temperature, and dissolved oxygen profiles at multiple locations. In addition to satisfying needs for model inputs and calibration data, the specific assemblage of monitoring components allowed for a robust spatiotemporal analysis of both lake and tributary biogeochemical influences. Field data analysis and accompanying model application accomplished here are intended to be complementary to previous watershed research efforts while attempting to further summarize and confirm previous hypotheses about the relative importance of external and internal loading to Mona Lake.

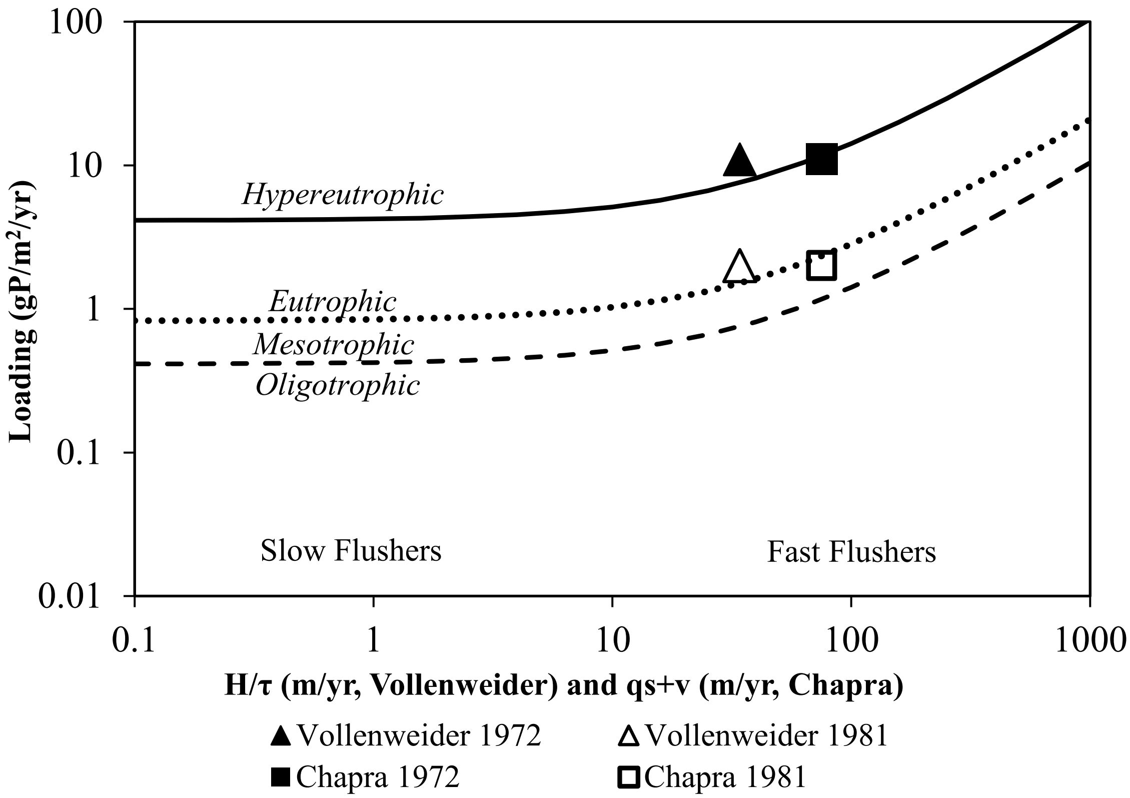

Figure 2-1 Vollenweider Loading Plot (1975 Model) 2017 for years 1972 (Freedman et al 1979), 1981 (Limnotech 1982).

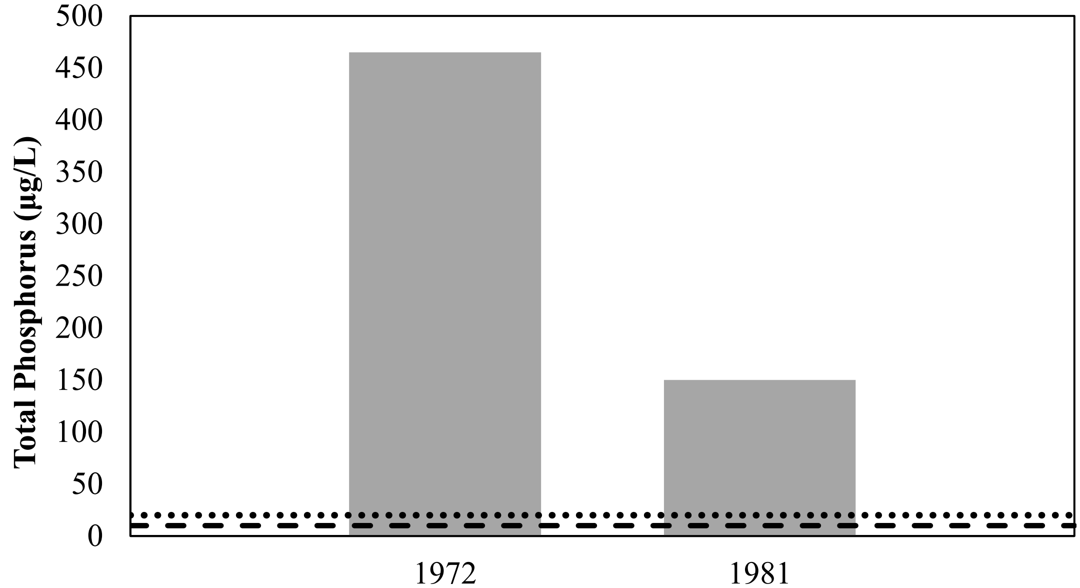

Figure 2-2 Composite of Total Phosphorus in Mona Lake for years 1972 (Freedman et al 1979), 1981 (Limnotech 1982). Dangerous and permissible trophic state boundary lines are shown (20 and 10 µg/L; Wetzel 2001).

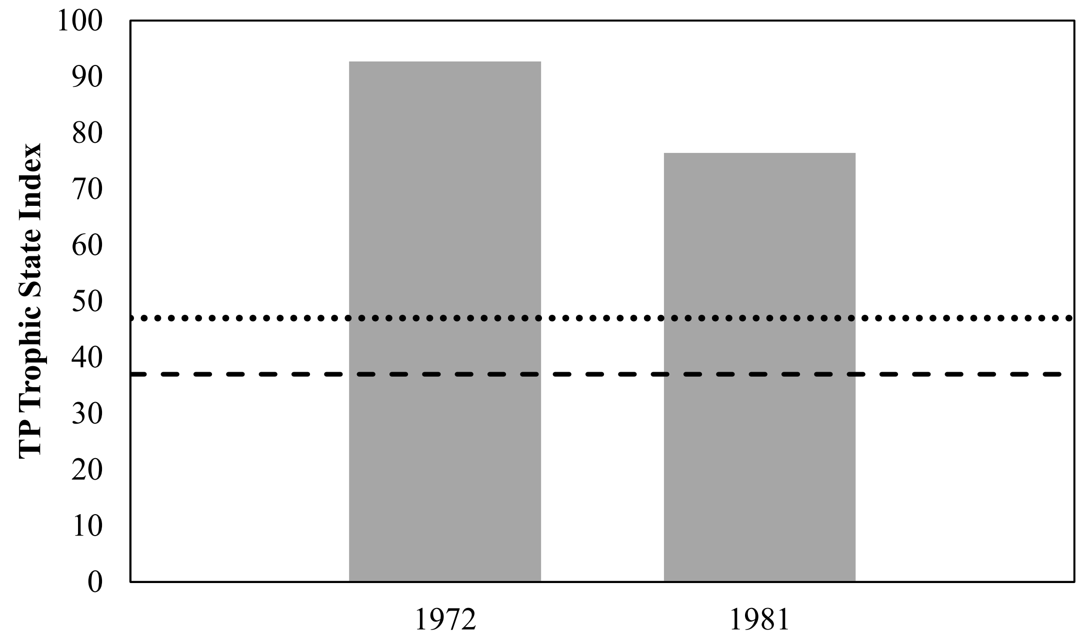

Figure 2-3 Composite of Carlson's TP Trophic State Index (Carlson 1977) in Mona Lake for years 1972 (Freedman et al. 1979), 1981 (Limnotech 1982). Dangerous and permissible trophic state boundary lines are shown (Wetzel 2001) as applied to Carlson's TP TSI (47 and 37).

3 Monitoring and Modeling Methods

The monitoring program was designed to complement previous research regarding external and internal loading of phosphorus to Mona Lake and attendant water quality conditions. The field program was executed at multiple stations over June-September 2017 and March-October 2018, at approximately twice-monthly intervals. Profiling was performed for conductivity, temperature, and dissolved oxygen, and discrete samples were collected for phosphorus, chlorophyll, and nitrate. These parameters support examination of spatiotemporal patterns and model calibration. Three tributaries were monitored for phosphorus and discharge in support of loading calculations. Additional monitoring components are detailed below, in relation to specific asset deployments and process studies (settling velocity, intrusion detection) in support of modeling. The biokinetic model applied in this research (LAKE2K) simulates the physical structure (3-layer system: epilimnion, metalimnion, and hypolimnion) typical of dimictic lakes in temperate climates. Vertical diffusion coefficients (driven by seasonal and meteorological mixing activity) mediate the thermal balance and mass transfer through the water column. The water balance assumes that inflow equals outflow, and that precipitation balances evaporation. The model's modest computational requirements yet robust biogeochemical simulation and calibration capability offer an ideal platform for application of overall project objectives.

3.1 Monitoring Methods

3.1.1 Field Sampling

3.1.1.1 Lake Monitoring

The bathymetry of Mona Lake is spatially non-uniform, but generally, deeper from east to west, a property of its heritage as a drowned river mouth system. A bathymetric survey (Restorative Lake Sciences, LLC) was contracted by the Mona Lake Watershed Council prior to the beginning of lake sampling in 2017 (Figure 3-1). Those data were then used to determine the area of specified water column layers and their volume. Important in understanding its estuary-like nature and associated hydrodynamics, it should be noted that ~90 percent of the inflow to Mona Lake enters at the east end of the system, flowing westerly to its discharge into Lake Michigan. Five lake sampling sites (Figure 3-2) were chosen along the primary east-west axis, with the addition of conductivity, temperature, and dissolved oxygen profiles in the channel in 2018 to better understand the characteristics of water introduced to Mona Lake through intrusions from Lake Michigan.

Lake sampling sites were selected to best represent the expected spatial differences in depth-driven phenomena (thermocline, oxycline) as they relate to the stability of stratification, degree of anoxia and therefore rate of sediment phosphorus release. Samples for a full phosphorus series (SRP, TP and total dissolved phosphorus, TDP) were collected from the surface and 1 m above bottom; yielding particulate phosphorus (PP) and dissolved organic phosphorus (DOP) by calculation. Discrete conductivity, temperature, and dissolved oxygen profiles were also generated at each site

(~0.3m resolution). Time-continuous discrete depth (1 m below surface, mid-depth ~4 m, 1 m above bottom ~8 m) water column temperature, and discrete depth Chl-*a* concentrations (surface) and nitrate levels (bottom) were monitored at the 'East Deep' site. Sediment traps were deployed via buoy at the East Deep and West Deep stations during 2017 for determination of particle (chlorophyll and particulate phosphorus) settling velocity. The 2017 field program included an acoustic doppler current profiler (ADCP) deployed midway down the ~0.5 km channel to Lake Michigan to measure the magnitude and frequency of intrusion into Mona Lake from Lake Michigan. Given the channel's shallow depth, frequent recreational boat traffic and submerged aquatic vegetation, the ADCP was not deployed in 2018 and instead replaced by an Onset HOBO temperature logger post (surface, middle and bottom in ~6 m) at the confluence of Mona Lake and the channel to more simply detect the presence of intrusions from Lake Michigan.

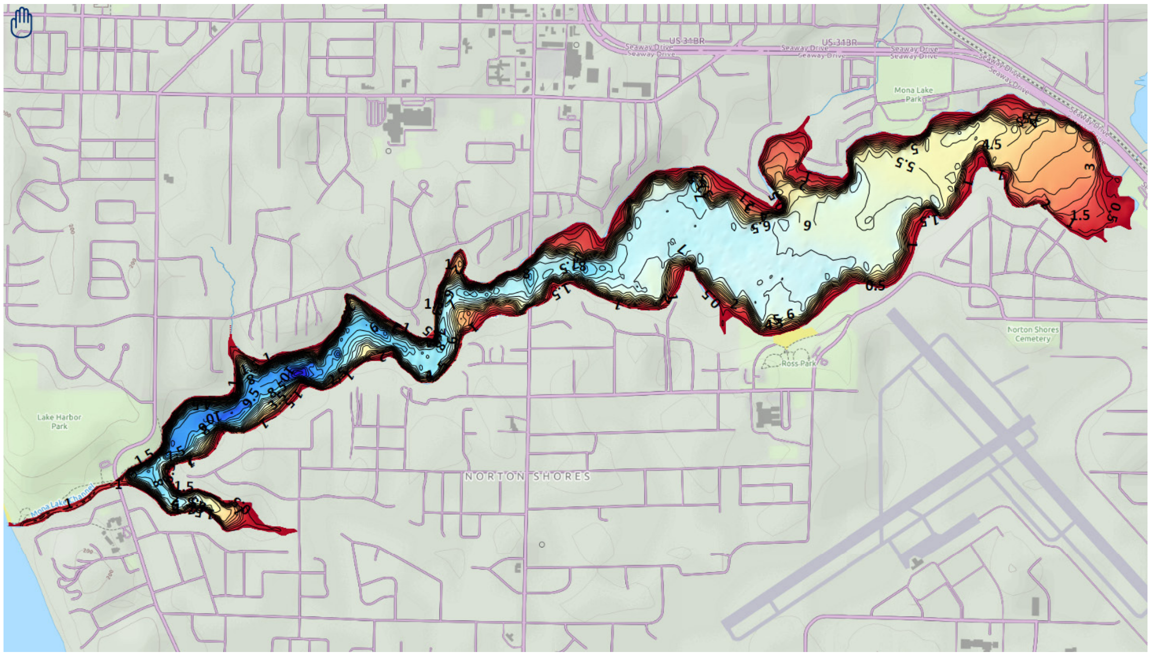

Figure 3-1 Bathymetry of Mona Lake, illustrating the overall depth gradient from east to west, as well as the channel with Lake Michigan. Bathymetric Survey: Restorative Lake Sciences/Mona Lake Watershed Council, Map: Jamey Anderson, Great Lakes Research Center at Michigan Tech.

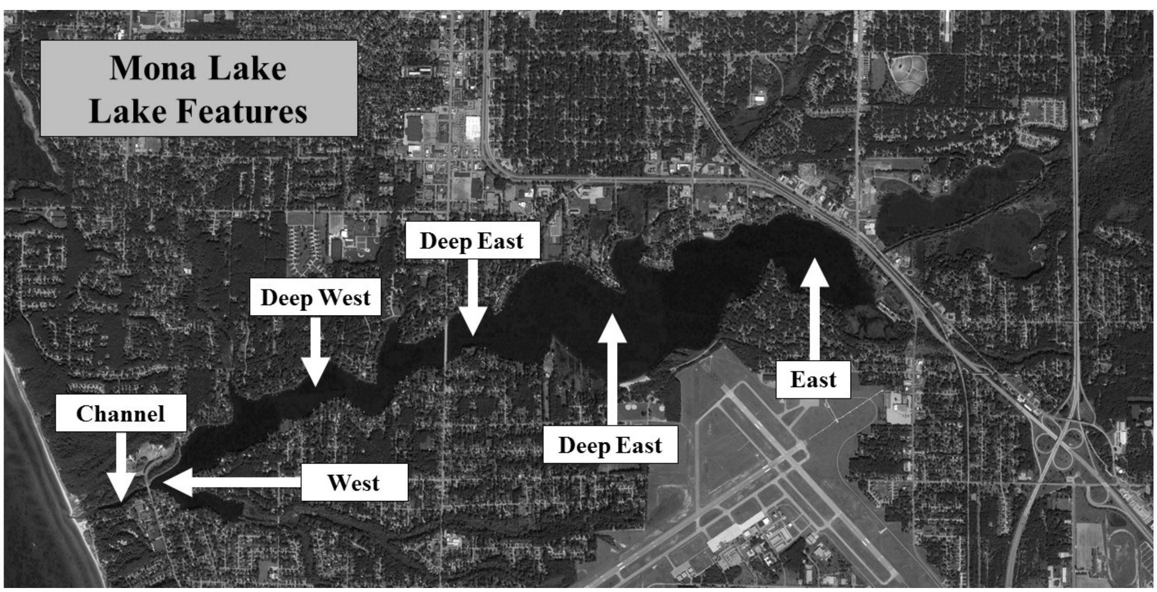

Figure 3-2 Mona Lake Sampling Station Map.

3.1.1.2 Tributary Monitoring

Three tributaries (Cress Creek, Black Creek, Little Black Creek; Figure 3-3) were sampled for discharge and phosphorus concentrations (SRP, TP, TDP, yielding PP and DOP by calculation) so that tributary loads could be calculated. Tributaries were monitored on 12 and 10 occasions in 2017 and 2018, respectively, capturing a broad range of discrete flows with the intent of identifying relationships between discharge (precipitation) and phosphorus concentrations. Discharge was measured as the product of velocity (Swoffer 2100 Velocity Meter) and stream cross-sectional area (based on water level, collected via staff gages and Onset HOBO U20L). Sampling was performed near the stream entrances to Mona Lake, with enough distance upstream to avoid potential intrusions of lake water. In 2017, monitoring of Black Creek included sites upstream and downstream of the celery flats as a means of assessing the phosphorus contribution from this P-rich source (Steinman and Ogdahl 2011). An upstream site was added on Little Black Creek in 2018 to further explore a potential point source of phosphorus observed in 2017. Ellis Drain, a fourth named tributary, was not monitored as its drainage basin represents less than 5 percent of the load to Mona Lake (Steinman et al. 2009). Ellis drain was assumed to possess area-proportional discharge characteristics and phosphorus concentrations to Cress Creek and was accounted for in the external loading calculation as such.

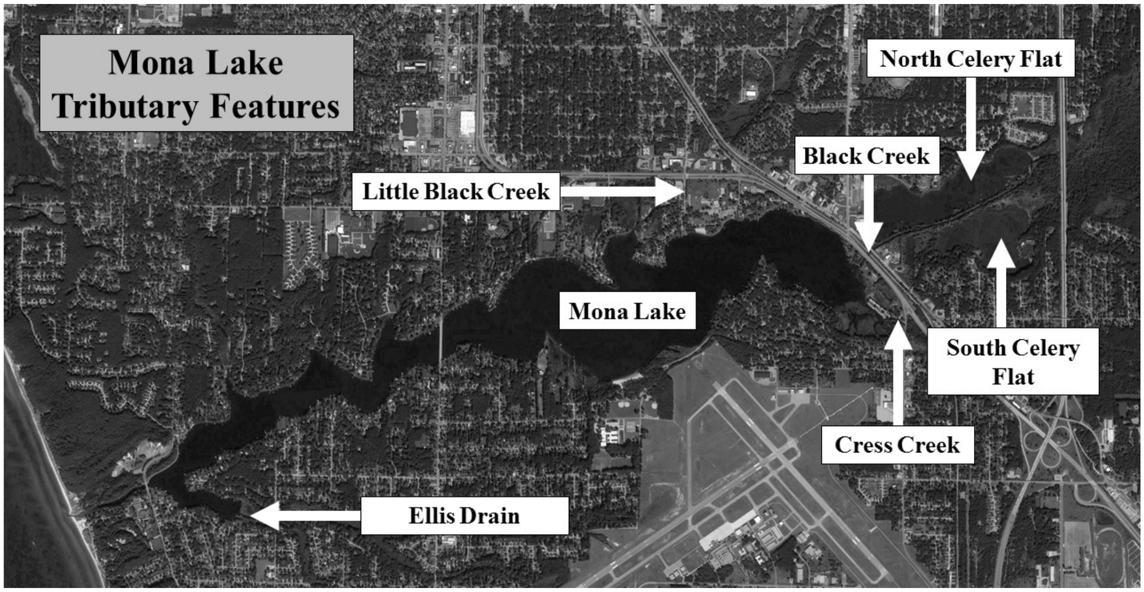

Figure 3-3 Mona Lake Tributary Site Map.

3.1.1.3 Celery Flats

Outflow from the flats enters Black Creek through drainage structures preceded by discharge restrictors. Measuring discharge through the restrictors proved to be difficult and the hydrologic cycle of the celery flats was not well understood in the context of this monitoring effort. However, with a sampling site both upstream and downstream of the drain entrances to Black Creek, the 2017 field program was able to quantify the phosphorus loading from the celery flats. The sampling site upstream of the celery flats and downstream of the celery flats, this sampling site was omitted from the field program for 2018 for logistic/cost reasons.

3.1.2 Laboratory Analysis

Samples were analyzed for SRP (field filtered), TDP (field filtered), and TP (unfiltered). Respective pools of PP and DOP were then calculated. SRP concentrations were determined via the ascorbic acid method within 48 hours of sample collection while

TDP and TP samples were frozen upon collection and later digested with ammonium persulfate, followed by analysis via the ascorbic acid method (APHA, 2005, 4500-P B) on a Lambda Spectrophotometer with a concentration appropriate path length. Nitrate and Chl-*a* samples from a single lake station (East Deep) were field filtered and frozen upon collection, then sent to Upstate Freshwater Institute (UFI) in Syracuse, NY to be analyzed (US EPA 353.2 Rev 2.0, US EPA 445.0 Rev 1.2). Sediment traps, deployed 1 m above lake bottom at the East Deep and West Deep lake stations, were retrieved at ~monthly intervals. The samples were frozen upon collection and sent to UFI to be analyzed for Chl-*a* and total suspended solids (US EPA 445.0 Rev 1.2, Standard Methods 2540-D-97).

3.1.3 Data Analysis

3.1.3.1 Loading Calculation

Mass balance surface water modeling requires a continuous time series of constituent (phosphorus) loads, which are calculated as the product of concentration (C) and discharge (Q). No tributaries in the Mona Lake watershed are gaged or monitored, yielding continuous discharge data. It is impractical to collect continuous concentration data. Thus, continuous discharge estimates were sought by methods other than direct measurement and concentration values through relationships with discharge (C/Q plots).

Tributary velocity and cross-sectional area data were collected regularly for all three monitored tributaries, yielding discrete discharge values. Statistical fitting methods (least squares) were used to relate field-measured Black Creek discharge values with continuous measurements for Bear Creek (USGS gauge, Muskegon, MI). This relationship was then used to generate daily, annual, and historical discharge data for Black Creek, based on the Bear Creek USGS database. Watershed area ratios to Black Creek (Mona Lake Watershed Resource Atlas, Annis Water Resources Institute 2003) were applied to the remaining Mona Lake tributaries (Little Black Creek, Cress Creek, Ellis Drain, Other), with the respective discrete discharge measurements for Little Black Creek and Cress Creek used for validation. Paired measurements of concentration (SRP, TP) and discharge for each tributary were regressed to explore relationships between discharge and concentration (construct C/Q plots). Continuous discharge data (Bear Creek/Black Creek relationship) can then be used with concentration estimates to produce time-continuous load estimates.

3.1.3.2 Settling Velocity

In a surface water mass balance, the rate of particle settling is a term required in identifying the quantity (phosphorus) lost to lake sediments, and thus not present in the outflow. Sediment trap contents were used to calculate the rate of particulate phosphorus settling (Chapra and Martin 2004) in Mona Lake as,

$$J = \frac{C_T.V}{A \cdot t} = \frac{C_T.H}{t}$$

$$v = \frac{J}{C_w}$$

where J = particulate phosphorus flux (mgPP/m^2/d), C_T = sediment trap total phosphorus concentration (mg/m^3), V = sediment trap volume (m^3), A = sediment trap entry area (m^2), H = sediment trap height (m), t = deployment time (d), C_w = water column total phosphorus (mg/m^3), and v = settling velocity (m/yr).

3.2 Modeling Methods

Two types of modeling approaches are utilized here: a screening model (Vollenweider/Chapra Plots) to provide rapid assessment of phosphorus – phosphorus trophic state relationships and a more complex NDPZ model (LAKE2K) to support management projections.

3.2.1 Screening Model

In his book on *Surface Water Quality Modeling*, Chapra (1997) outlines the development and evolution of phosphorus loading plots (Vollenweider) and budget models (Chapra) useful in relating phosphorus inputs to lakes with the resultant trophic state. Vollenweider (1975), building on ideas set forth by Rawson (1956), recognized that the susceptibility of a lake to eutrophication was impacted by the system's morphometric and hydraulic characteristics. More specifically, lakes that were deep and those with short hydraulic residence times (fast-flushing) were observed to be less susceptible to eutrophication than shallow lakes and those with long hydraulic residence times (slow-flushing). The significance of these observations is that lakes with low susceptibility can assimilate more phosphorus (higher loading) while maintaining a trophic state similar to that for lakes with high susceptibility.

Vollenweider (1975) developed a database of lake depth (H, m), hydraulic residence time (τ, yr) and areal total phosphorus loading (L_p, gP m^{-2} yr^{-1}) to examine these relationships. The resulting 'plot' placed a lake's areal phosphorus loading on the y-axis and a term (H/τ_w, m yr^{-1}) characterizing morphometric and hydraulic properties on the x-axis (Figure 3-4). From an examination of H/τ_w, increasing depth (H) and decreasing hydraulic residence time (τ_w, fast-flushing) serve to position a lake further to the right along the x-axis, reflecting the observed reduction in susceptibility to eutrophication and the ability to assimilate a larger phosphorus loading. For the depth and hydraulic retention times characteristic of most lakes, hydraulic retention time is the dominant term, with endpoints on the x-axis that may be termed 'fast flushers' and 'slow flushers', as illustrated here for four lakes with differing morphometric and hydraulic properties (Table 3-1 and Figure 3-4).

Table 3-1 Morphometric and hydraulic characteristics of Lake Superior, Lake Erie, Mona Lake and Lake Pepin in the context of a Vollenweider Plot.

System	**Depth** **H (m)**	**Retention Time** **τ (yr)**	**H/τ_w** **($m\ yr^{-1}$)**
Lake Superior	**149**	**191**	**0.78**
Lake Erie	**19**	**2.6**	**7.31**
Mona Lake	**6**	**0.2**	**32.1**
Lake Pepin	**6**	**0.04**	**136.88**

Chapra (1997) presents a derivation demonstrating that the term H/τ_w in the Vollenweider Plot (Figure 1) is equivalent to q_s, the areal hydraulic loading ($m^3\ m^{-2}\ yr^{-1}$ or $m\ yr^{-1}$). Chapra and Tarapchak (1976) developed a derivation of a phosphorus budget model where the steady state phosphorus concentration (p, $mg\ m^{-3}$) was given by,

$$p = \frac{L_p}{q_s + v}$$

with v being the apparent (TP-based) settling velocity ($m\ yr^{-1}$). The budget model approach explicitly recognizes one source term (areal loading, L_p) and two sink terms (flushing (q_s) and settling (v). Rearrangement of the steady state solution yields the applied in development of, what is termed here, a Chapra Plot,

$$L_p = p \cdot (q_s + v)$$

with the source term (loading) on the y-axis and the sum of the sink terms (flushing and settling) on the x-axis (Figure 3-5). This format also accommodates inclusion of total phosphorus concentrations representing the boundaries between oligotrophy and mesotrophy (10 $mgP\ m^{-3}$) and mesotrophy and eutrophy (20 $mgP\ m^{-3}$; Figure 3-5). Both Vollenweider and Chapra Plots are utilized in this work to explore trophic state associated with historical and contemporary external TP-based loadings to Mona Lake.

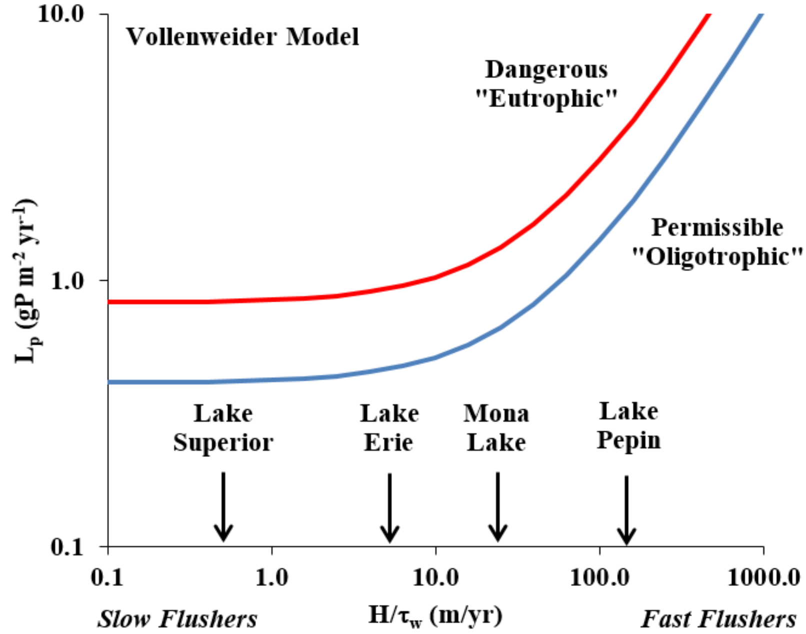

Figure 3-4 A Vollenweider loading plot based on Vollenweider (1975), illustrating the position of four lakes along the x-axis characterizing morphometric and hydraulic residence time.

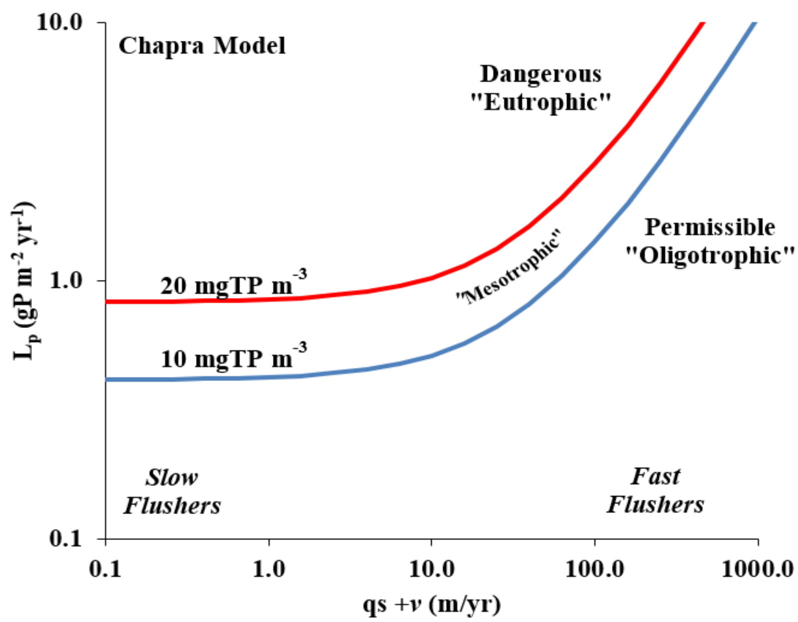

Figure 3-5 A Chapra budget plot based on Chapra and Tarapchak (1976), illustrating the relationship between areal total phosphorus loading, areal hydraulic loading and settling velocity and their interaction in mediating trophic state. The solid lines represent TP concentrations of 10 and 20 mgP m^{-3}; the boundaries between oligotrophy and mesotrophy and mesotrophy and eutrophy, respectively.

3.2.2 Biokinetic Model

The model used in application to Mona Lake, LAKE2K, is part of a family of platforms that also includes QUAL2K (river water quality), SED2K (sediment quality) and AT2K (river benthic algae) developed by Dr. Steven C. Chapra of Tufts University (http://www.qual2k.com). LAKE2K (Chapra and Martin 2004), is a 1D, three-layer, biokinetic model written in Visual Basic that applies a mass balance approach to simulate physical and biogeochemical processes in lakes (Table 3-2). Additionally, the model accommodates different chemical forms (e.g., ammonia and nitrate nitrogen), physical states (e.g., soluble reactive, dissolved organic and particulate phosphorus) and classes (multiple phytoplankton and zooplankton species) of several state variables. A suite of more than 118 mass transport and kinetic coefficients are specified in full application of the model. The model framework, detailing kinetics and mass transfer in simulating carbon, nitrogen, oxygen and phosphorus is presented in Figure 3-6.

Table 3-2 Physical, chemical and biological state variables accommodated in LAKE2K.

Physical	**Chemical**		**Biological**
Light	Carbon	Phosphorus	Phytoplankton
Temperature	Conductivity	Silica	Zooplankton
Secchi Disk	Nitrogen	Suspended Solids	-
-	Oxygen	-	-

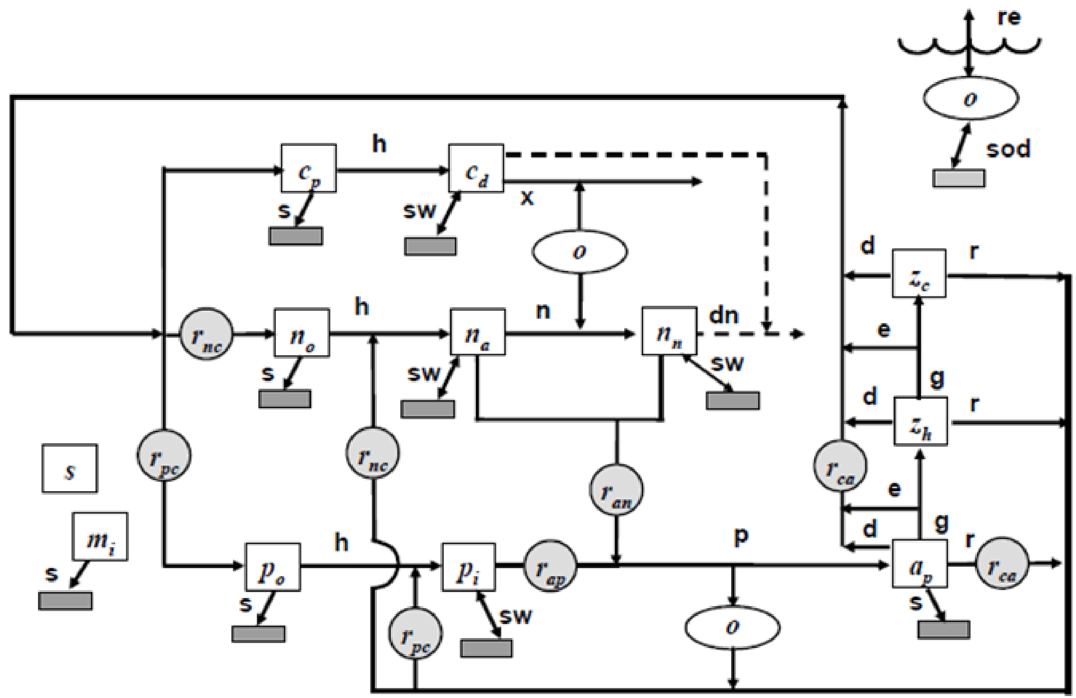

Figure 3-6 Model kinetics and mass transfer framework. Kinetic processes used in this model calibration are oxidation (x), photosynthesis (p), respiration (r), and death (d). Mass transfer processes are reaeration (re), settling (s), sediment oxygen demand (sod), and sediment-water exchange (sw). Other processes not explicitly utilized in this model application are: hydrolysis (h), nitrification (n), denitrification (dn), grazing (g), and egestion (e) (Chapra and Martin 2004).

The modeling performed here targets the total phosphorus analyte and other state variables serving to mediate mass transport, biokinetics and trophic state impacts of that constituent. This requires specification of a physical framework and four submodels: total phosphorus (the target analyte), temperature (vertical mixing and biokinetic rates), dissolved oxygen (trigger for sediment-P flux) and phytoplankton (phosphorus cycling and trophic state response) with attendant provision of model inputs, initial conditions, biokinetic and mixing coefficients and datasets for use in testing model performance.

3.2.2.1 Physical Framework

Physically, the Mona Lake system is divided into three layers (epilimnion, metalimnion and hypolimnion; Figure 3-7) with fully mixed conditions simulated by adjustment of vertical mixing coefficients. While LAKE2K accommodates changing layer volumes due to imbalance between inflow and outflow, it is assumed here that inflow equals outflow and, in the water balance, that precipitation equals evaporation resulting in constant layer volumes. Layer boundaries are user specified through inspection of thermocline and oxycline position determined in monitoring programs. Tributary inflow is directed into one of the three layers (epilimnion, metalimnion, hypolimnion) based on a density algorithm derived from seasonal inflow and layer temperatures.

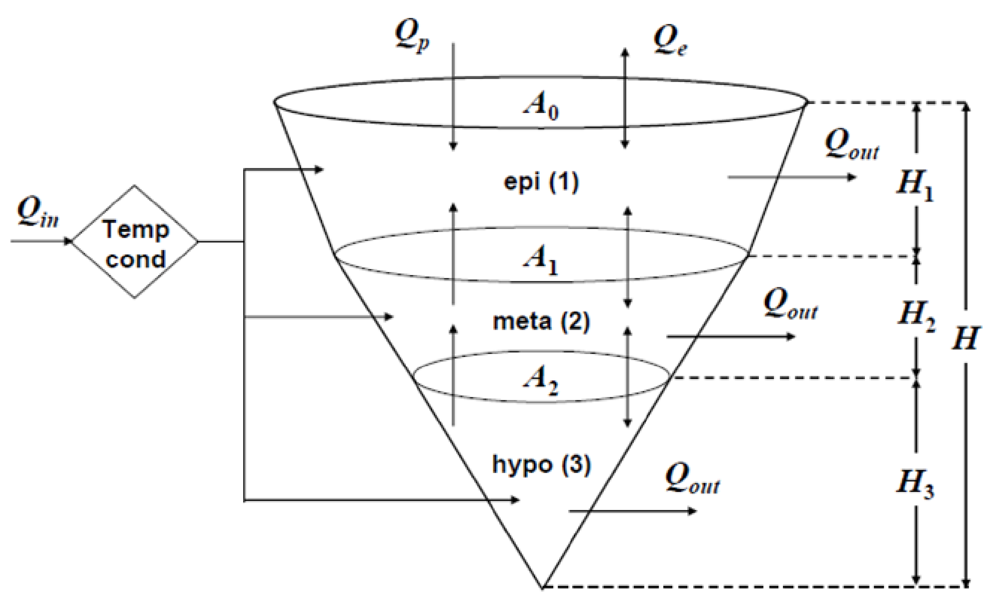

Figure 3-7 Physical framework with water balance and vertical segmentation scheme. (Chapra and Martin 2004).

3.2.2.2 Temperature Submodel

A heat balance is written for each of the three model layers. Where tributary discharge is received by the epilimnion, the balance includes heat inflow and outflow, air-water heat flux and heat exchange between the epilimnion and metalimnion. The heat balance for the metalimnion and hypolimnion is based solely on vertical mass transport between layers. Surface heat exchange is determined as the net effect of five processes, expressed as cal cm^{-2} d^{-1} (Figure 3-8).

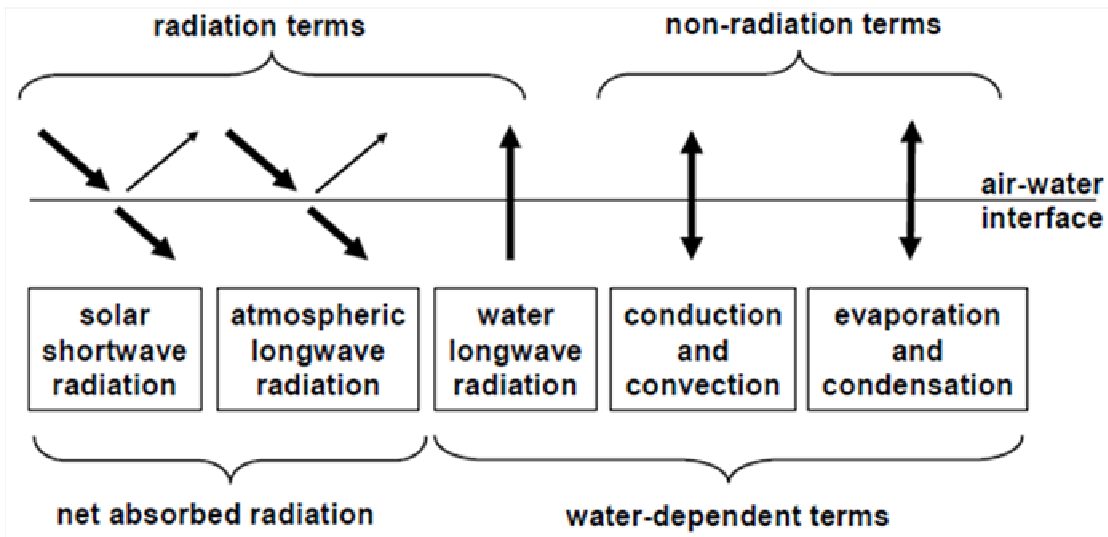

Figure 3-8 Surface heat balance.

Solar radiation is computed as a function of the radiation at the top of the Earth's atmosphere (varying with user-specified latitude) attenuated by atmospheric transmission, cloud cover and reflection. Atmospheric longwave radiation, resulting from heating of the atmosphere by the sun's shortwave radiation, varies with air temperature and the emission efficiency reflectance of the atmosphere. Water longwave radiation is calculated based on the emissivity of water and water temperature. Conduction and convection are heat transfer among molecules and fluids, respectively, and are calculated based on the wind speed and air and water temperatures. Evaporation and condensation are calculated based on wind speed and the vapor pressure of the air. Model inputs required for the heat balance calculation include latitude, cloud cover, air temperature and dew point; water temperature is calculated by the model internally. Meteorological model inputs were obtained from the National Oceanic and Atmospheric Administration station at the Muskegon County Airport. Heat exchange between layers occurs through vertical diffusive mass transport, calculated here for the metalimnion as,

$$\frac{dc_2}{dt} = \frac{E_1'}{V_2}(c_1 - c_2) + \frac{E_2'}{V_2}(c_3 - c_2)$$

where $c_{1,2,3}$ are the heat content (cal) of the individual layers, $E'_{1,2}$ are the bulk turbulent diffusion coefficients at lower boundary of the two layers ($m^3\ d^{-1}$) and V_2 is the metalimnetic layer volume (m^3). Values for E' are determined by calibration to measured layer column temperatures.

3.2.2.3 Oxygen Submodel

The oxygen mass balance includes the contribution from phytoplankton photosynthesis and losses to oxidation of organic carbon and ammonia nitrogen and respiration by phytoplankton and zooplankton. Oxygen is further consumed by the lake bottom through sediment oxygen demand. Oxygen may be gained or lost from the system depending on whether the epilimnion is oversaturated or undersaturated. In this application of LAKE2K, we limit the source-sink components to reaeration and sediment oxygen demand (Figure 3-9).

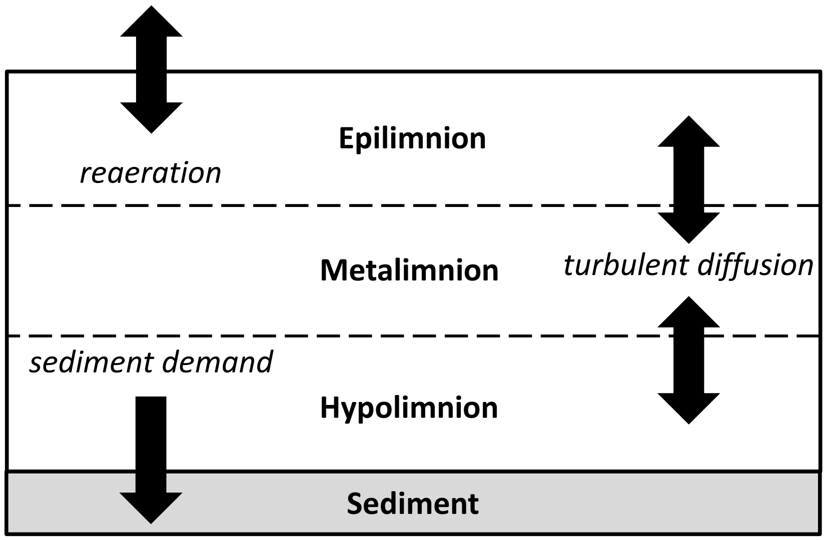

Figure 3-9 Oxygen mass balance.

Here, atmospheric reaeration depends on wind speed (a model input) and temperature (calculated internally). Vertical turbulent diffusion is as determined by model calibration (see Temperature Model) and the rate of sediment oxygen demand is a user input also determined by calibration.

3.2.2.4 Phosphorus Submodel

The primary focus of the modeling effort is total phosphorus. In LAKE2K, the TP analyte is not calculated, but rather determined as the sum of its components (soluble reactive phosphorus (SRP), dissolved organic phosphorus (DOP) particulate organic phosphorus (detritus; POP) and phytoplankton phosphorus (Phyto-P). Mass balances are performed for each of the TP components, accommodating their specific source-sink terms (Table 3-3 and Figure 3-10). Those for POP and DOP are relatively straightforward; both involving external loads and dissolution-hydrolysis processes and POP having a settling sink. The SRP mass balance is more complex as it is linked to both the phytoplankton (losses to algal uptake) and oxygen (trigger for onset of release) models. There is also a sediment release source which may be either user-specified or calculated using a Sediment Diagenesis Submodel (user-specification is employed here). The Phyto-P mass balance is linked to the SRP submodel as well through algal P uptake, calculated as the increase in phytoplankton biomass times the user-specified phosphorus : chlorophyll ratio. Each of these processes utilizes one or more of the more than 118 kinetic coefficients embodied in LAKE2K; most kinetic coefficients have, as well, the option to adjust rates for changes in temperature through a derivation based on the Arrhenius model,

$$k(T) = k(20)\theta^{T-20}$$

where *k(T)* = reaction rate (1/d) at Temperature *T* (°C) and θ = the temperature parameter for a given reaction. The phosphorus mass balances also contain the vertical mass transport and outflow terms common to all of the temperature and constituent mass balances.

Table 3-3 Source-sink terms in the phosphorus TP component mass balances.

Process	POP	DOP	SRP	Phyto-P
tributary load	source	source	source	-
sediment release	-	-	source	-
phytoplankton uptake	-	-	sink	source
POP dissolution	sink	source	-	-
DOP hydrolysis	-	sink	source	-
settling	sink	-	-	sink

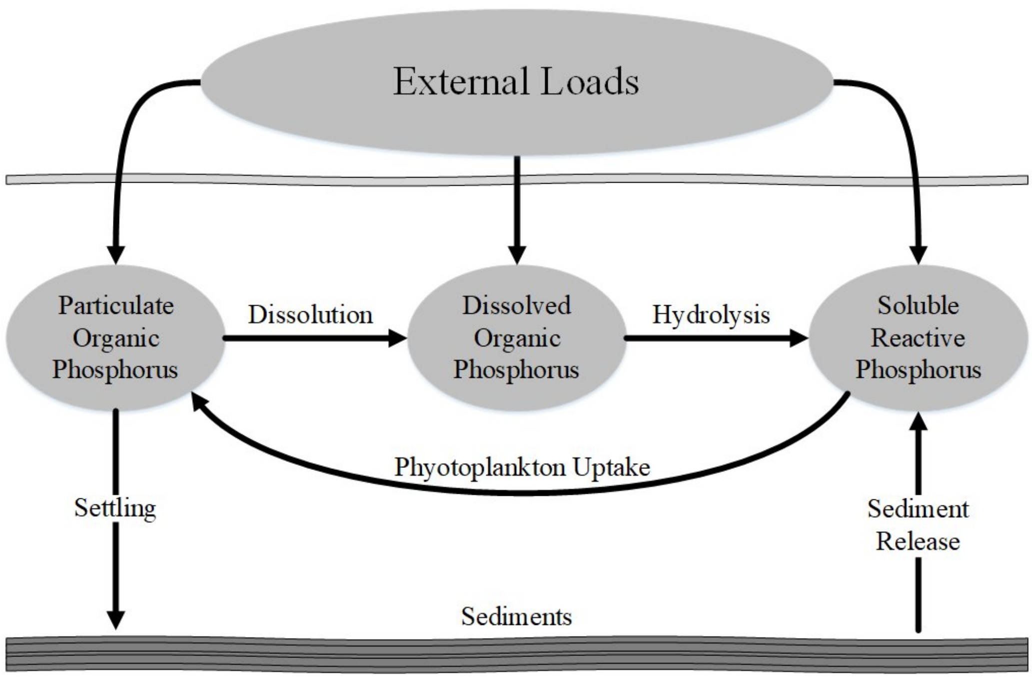

Figure 3-10 Mass balance processes for the components making up the total phosphorus analyte. In this illustration, the particulate organic phosphorus and phytoplankton phosphorus components are grouped together.

3.2.2.5 Phytoplankton Submodel

Phytoplankton are modeled by performing a mass balance on algal carbon considering photosynthesis as a source and respiration, death and zooplankton grazing as sinks. Model output as chlorophyll is determined through a user-specified carbon to chlorophyll ratio. In this application of LAKE2K, respiration and death are treated as a summed term represented by the rate of respiration and the zooplankton sink (grazing) is not included. The rate of gross photosynthesis (μ, d^{-1}) is calculated as the product of a user-specified maximum rate of gross photosynthesis (μ_{max}, d^{-1}), mediated through dimensionless limitation functions describing the impact of temperature, $f(T)$, phosphorus availability, f(P) and light, f(I) on the rate of photosynthesis. LAKE2K makes provision for treating three phytoplankton groups exhibiting different maximum specific rates of photosynthesis and respiration and differing responses to T, P and I. That feature is utilized in this work to accommodate the seasonal succession from small green algae to large green algae to cyanobacteria (Plankton Ecology Group Model applied to Mona Lake, Gillett et al. 2015).

The temperature dependence of photosynthesis, $f(T)$, is described by an asymmetrical bell-shaped curve (Figure 3-11a) where an optimum temperature (T_{opt}) and coefficients describing the slope of the ascending (κ_1) and descending (κ_2) limbs of the response are user-specified,

$$f(T) = e^{-\kappa_1 \cdot (T - T_{opt})^2} \quad \text{for } T \leq T_{opt}$$

$$f(T) = e^{-\kappa_2 \cdot (T - T_{opt})^2} \quad \text{for } T > T_{opt}$$

The nutrient limitation function, $f(P)$, uses a Michaelis-Menten (Monod) approach (Figure 3-11b) based on the SRP concentration (mgSRP m^{-3}), and a user-specified half-saturation constant (mgSRP m^{-3}),

$$f(P) = \frac{SRP}{K_p + SRP}$$

Nitrate and silica limitation are not considered in this application. The light dependency of photosynthesis, $f(I)$ also uses a Michaelis-Menten (Monod) approach (Figure 3-11c) based on the mean daily photosynthetically-available radiation (PAR, langleys d^{-1}), computed as a constant fraction of the solar radiation incident at the water surface, and a user-specified half saturation constant (K_I, langleys d^{-1}),

$$f(I) = \frac{PAR}{K_I + PAR}$$

Epilimnetic mean daily PAR is determined using the Beer-Lambert Law and an internally-calculated vertical light attenuation coefficient. The interrelationship of the physical framework and the temperature, oxygen, phosphorus and chlorophyll submodels in simulating total phosphorus and its impact on phytoplankton abundance (as chlorophyll) is summarized in Figure 3-12.

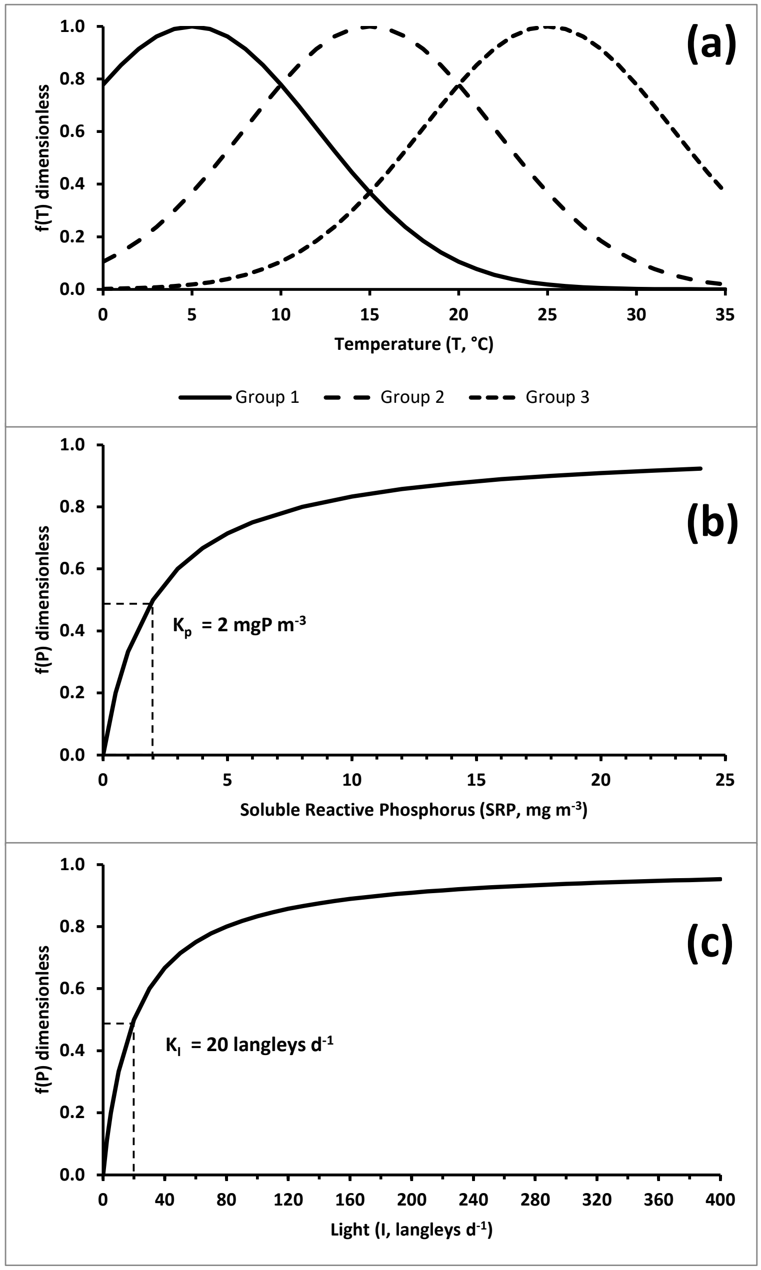

Figure 3-11 Growth mediation functions (*f*) for (a) temperature with T_{opt} = 5, 15 and 25 °C and κ1 and κ2 equal to 0.01 and 0.05, respectively, (b) phosphorus for a value of K_p = 2 mgSRP m^{-3} and (c) light for a value of K_I = 20 langleys d^{-1}.

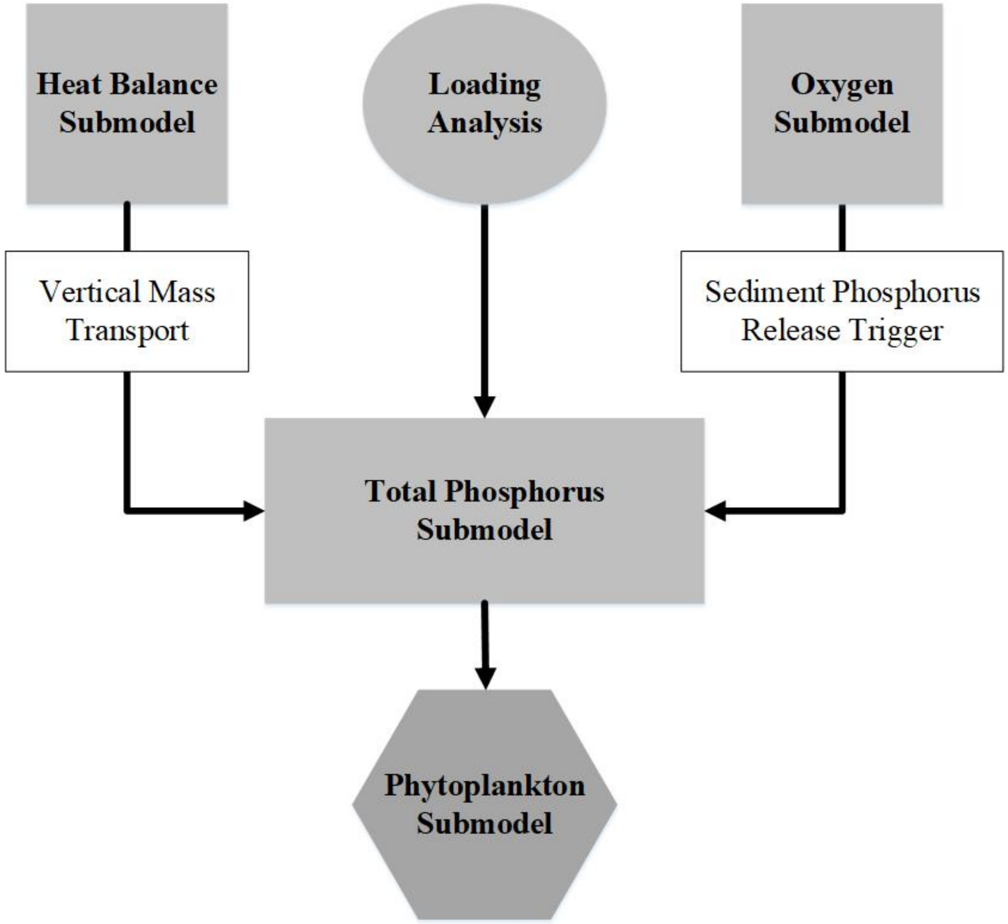

Figure 3-12 Model framework as used in this application of LAKE2K.

3.2.2.6 Solution Technique

The mass balances described above are written in the form of ordinary differential equations and solved using an Euler integrator. Model output is generated in both tabular and graphical form.

4 Results and Discussion

Applying budget trophic state models (Vollenweider Loading Plot, Carlson TSI) to Mona Lake indicate that the current phosphorus loading, after notable reductions (wastewater diversion, ~75%), coupled with its hydrodynamic properties, should result in a mesotrophic body of water. Calculation of trophic state from both past and current nutrient concentrations describe the observable trophic state of Mona Lake, highly eutrophic. The observed trends and impacts offering explanation for the existing trophic state and their drivers are discussed below.

4.1 Spatiotemporal Phenomenon

The morphometry characteristic of drowned river mouth systems like Mona Lake creates hydrologic properties important to remember when performing spatiotemporal analyses. As previously identified (Evans 1992), Mona Lake has seasonally variable retention times, also observed during monitoring in 2017 and 2018 (Table 4-1). With its riverine morphometry, high spring discharge (Figure 4-1) drive a strong flushing effect while the lake is isothermal, rapidly transporting tributary contributions to the larger Lake Michigan system. Low summer discharge allow tributary constituents to remain (settle or assimilate) in the lake longer at a time when conditions support algal growth (higher solar radiation, warmer water) while thermal and oxygen regimes impact temporal, internal lake dynamics (anoxia).

Table 4-1 Varying retention times for 2017 and 2018, periods identified. *January 1st 2018-November 1st 2018 as December 2018 USGS data not yet available.

	Winter/Spring τ (days) **January-June**	**Summer τ (days)** **June-September**	**Annual τ (days)**
2017	35	141	55
2018	37	103	44*

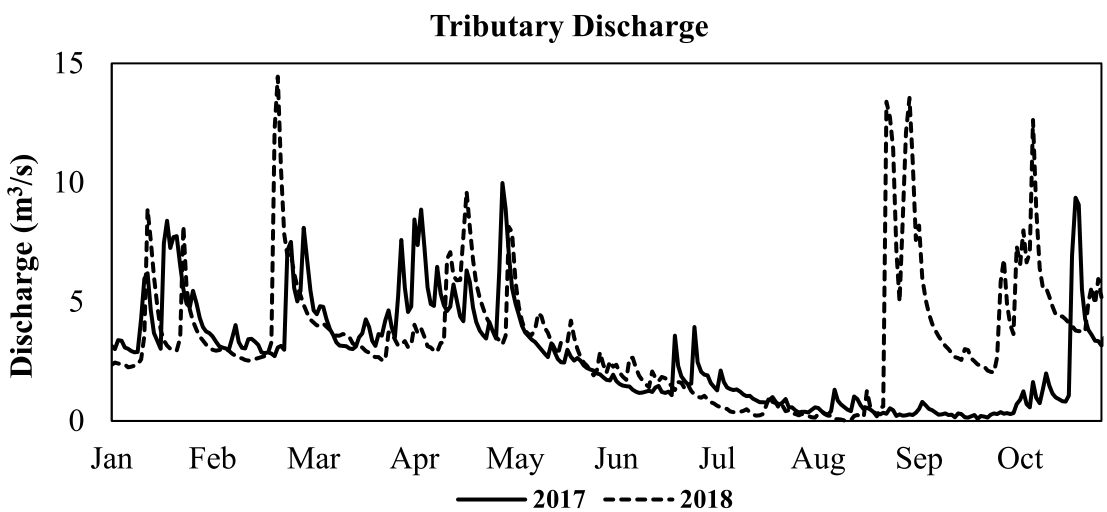

Figure 4-1 Summation of Mona Lake tributary discharge for 2017 and 2018, illustrating seasonal minimum discharge from May through August and maximum discharge occurring in spring and fall.

4.1.1 Stratification and Anoxia

Stratification in both 2017 & 2018 was present by mid-June, with well-defined oxyclines and thermoclines present at sites with sufficient depth to develop a thermal gradient (Mid, Deep East/Deep West/West). This stratification and attendant reduction of vertical mass transport, coupled with sediment oxygen demand, create a hypolimnion devoid of oxygen (anoxia) by the June 21st and June 5th sampling dates in 2017 and 2018, respectively. Generally, in eutrophic dimictic lakes, the thickness of the anoxic layer increases with the strength and duration of stratification, as limited oxygen is transferred to bottom layers, and the sediment oxygen demand greatly exceeds the mass introduced through diffusive mixing. In Mona Lake, the volume of the anoxic hypolimnion mirrored the strength of stratification at all sites deeper than ~4 m (Figure 4-7), indicating the lack of diffusive transport from the epilimnion and/or metalimnion during more heavily stratified periods. Seasonal temperature maps (2018; Figures 4-2, 4-4, and 4-6) indicate expected spatiotemporal warming trends (spatially homogenous within layers) while providing illustration of stochastic events impacting water quality (anoxia and attendant impacts).

During periods of anoxia, lake sediments release highly bioavailable phosphorus (SRP). Phosphorus, like oxygen, is subject to the impacts of water density (stratification) on mass transport between layers. Thus, this SRP accumulates in the hypolimnion while small shear forces (entrainment; Figure 4-8) at the metalimnetic and then epilimnetic boundaries transfer phosphorus to surface waters. Controlled by stochastic wind events, entrainment events (wind, shear) increase mass transport, especially in lakes with a shallow mean depth (low resistance to mixing). The resulting increase in mixing forces and therefore mass transport of phosphorus to the epilimnion (photic zone) can occur under conditions optimal for algal growth (high solar radiation, warm temperatures).

4.1.1.1 East Station

In 2018, conditions at the shallowest sampling site (East, depth ~4 m), warmed with increasing solar radiation, remaining completely mixed with the exception of ephemeral decreases observable in August and September (Figure 4-2). A function of its minimal depth, this area of the lake remains oxic longest (Figure 4-3), with the exception of intermittent anoxic episodes in June, July, and August. These anomalies in an otherwise well-mixed basin (temperature) likely occur during meteorologically quiescent periods (low wind, diffusive transport), wherein the sediment oxygen demand is greater than the mass transport of oxygen from the surface. In mid-July and mid-September, large masses of oxygen present themselves in the epilimnion. Not coinciding with temperature changes (mixing and/or entrainment), these increases are mass photosynthetic production plumes.

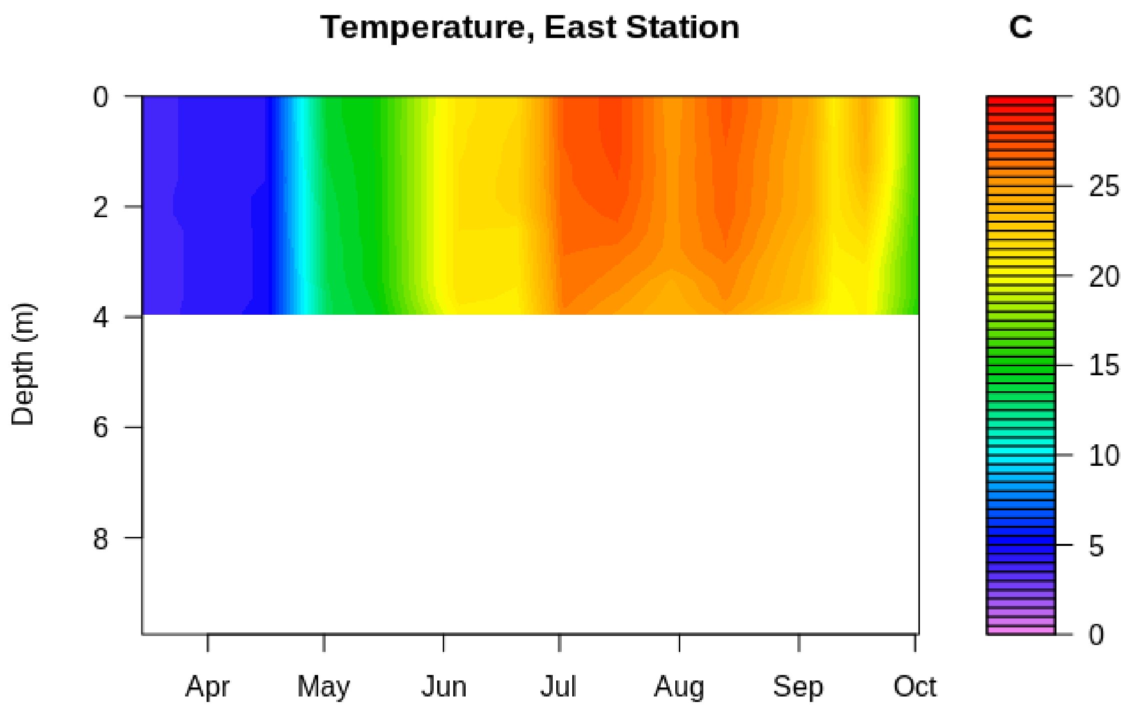

Figure 4-2 East station thermal succession, 2018.

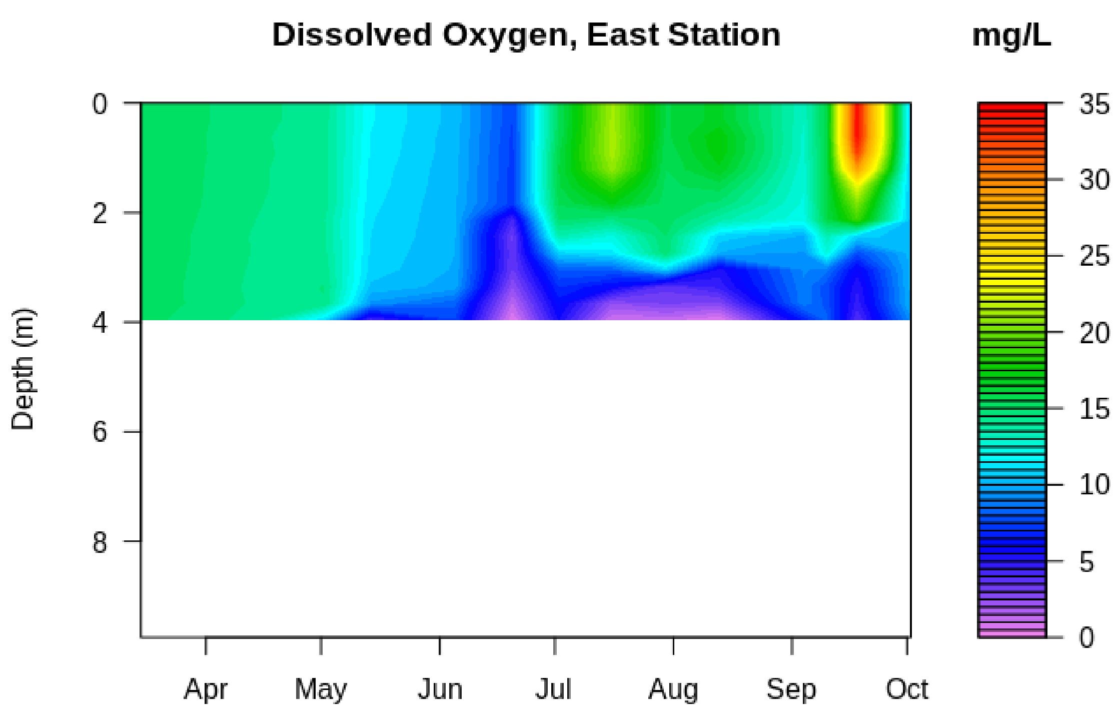

Figure 4-3 East station dissolved oxygen succession, 2018, corrected for saturation.

4.1.1.2 Mid Station

Thermal succession at the Mid station (depth ~6 m) in 2018 illustrates the seasonal behavior expected of a temperate dimictic lake. The completely mixed water column (April), warms with increases in solar radiation (Figure 4-4). The penetration of solar radiation cannot reach the lake bottom as in the East basin, and thus stratification develops. Rates of heat transfer by vertical turbulent diffusion (mixing across layers) decline as stratification strengthens, reducing the transfer of heat and supply of oxygen to the hypolimnion (anoxia). Periods of increased mass transport between the epilimnion and metalimnion via entrainment are observable in mid-July, August, and September. The same supersaturation events observed at the East Station (mid-July and mid-September) are seen at the Mid station.

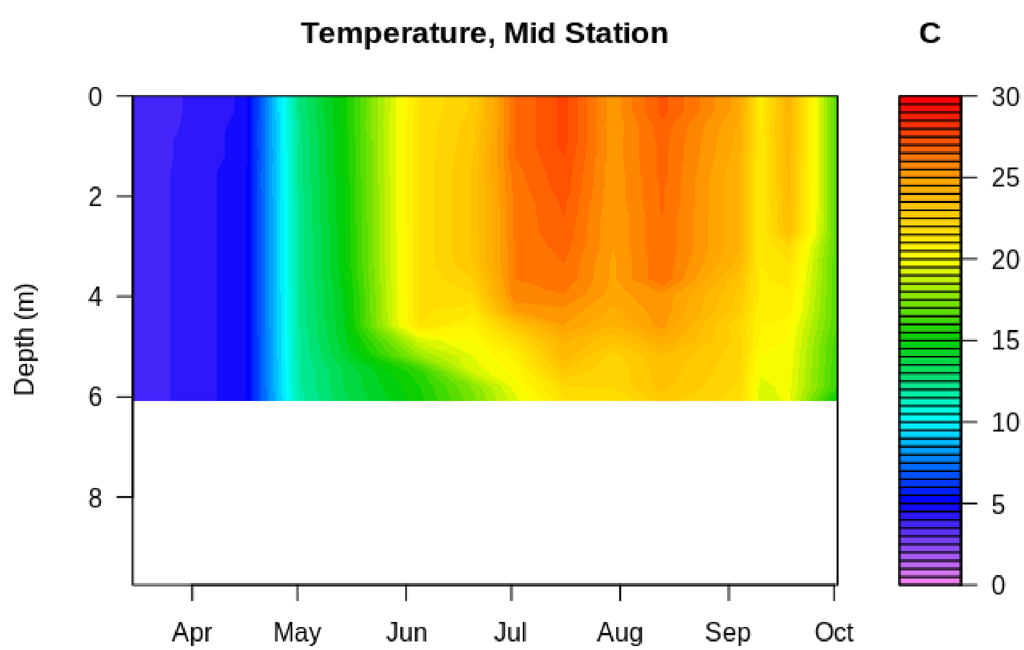

Figure 4-4 Mid station thermal succession, 2018.

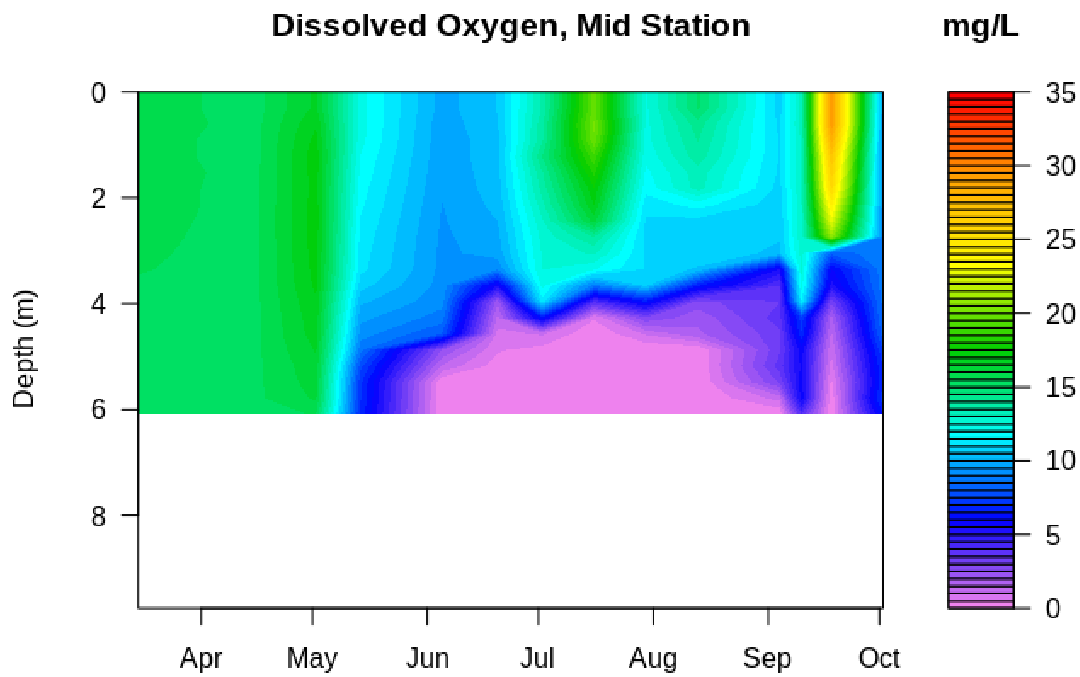

Figure 4-5 Mid station dissolved oxygen succession, 2018, corrected for saturation.

4.1.1.3 Deep Stations

Like the Mid station, the deeper stations (composite of Deep East, Deep West, West) transition from completely mixed waters at ice-out to a strongly stratified system (Figure 4-6), producing an anoxic zone comprising nearly half the water column by mid-July (Figure 4-7). As observed in the East and Mid stations, oxygen supersaturation events (photosynthesis), not ascribable to wind driven mixing (temperature decrease), appear to have taken place in mid-July and mid-September.

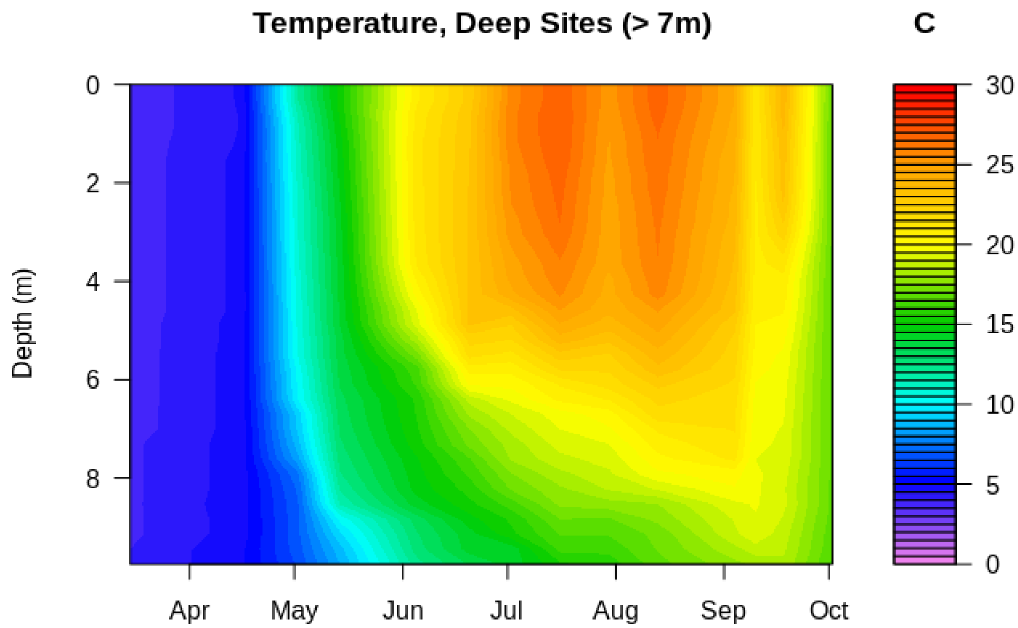

Figure 4-6 Composite of Deep East, Deep West, and West station thermal succession, 2018

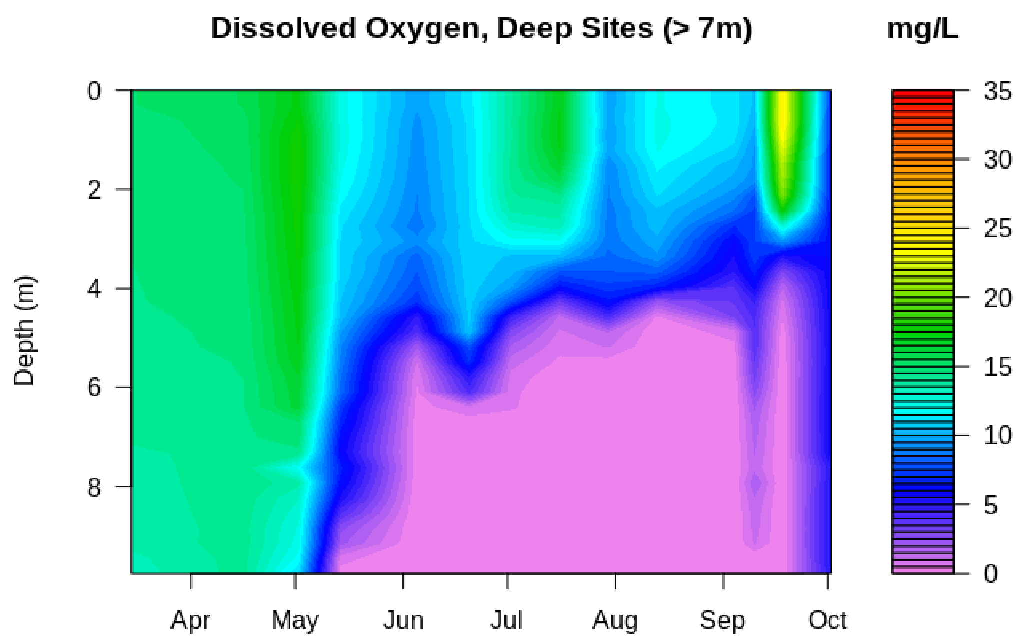

Figure 4-7 Composite of Deep East, Deep West, and West station dissolved oxygen succession, 2018, corrected for saturation.

Further understanding of stochastic water column thermal (mixing) dynamics was accomplished through examination of data from the temperature logger buoy string at East Deep (1 m below the surface, 1 m above lake bottom, midpoint, Figure 4-8). We can observe multiple layer specific and multi-layer entrainment-based mixing events, transferring heat to lower layers. An entrainment event on June 29th (1, Entrainment; explained Figure 4-9) indicates a large, near whole water column mixing event. Epilimnetic and metalimnetic temperatures reach equilibrium with each other, transferring enough heat to warm the hypolimnion ~3°C. A rapid strengthening of stratification on July 20th (2, Intrusion) like occurred as a result of high amounts of solar radiation and quiescent meteorological periods. During this event, surface temperatures warmed drastically while the increasing density gradient prohibited heat transfer to bottom layers, observable in the decreased temperatures in both the metalimnion and hypolimnion. However, the magnitude and rate of heat loss in the metalimnion and hypolimnion is likely too abrupt to have come from decreasing magnitudes of heat transfer from the epilimnion and is likely the result of an intrusion from Lake Michigan, discussed qualitatively later. Another intrusion event on August 4th (3, Entrainment) caused a sharp drop in surface temperatures, transferring large amounts of heat to the metalimnion. The hypolimnion remains largely unaffected, showing only a small and brief increase in temperature. This inability to fully entrain the hypolimnion is likely correlated to the lack of shear force (wind) magnitude and duration during this event. Bursts of shear stress (gusts) may be capable of causing entrainment in surface layers, while more sustained winds may be required for the shear forces to translate to and impact the hypolimnion.

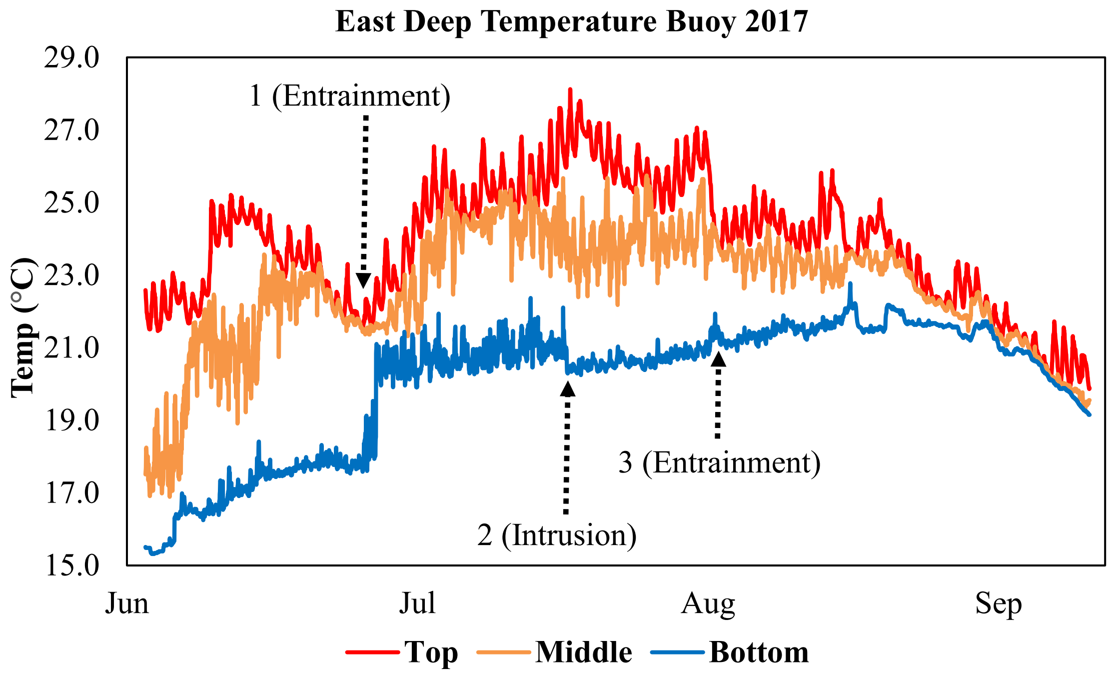

Figure 4-8 Temperature loggers, placed 1 m below surface (Top), the mid-depth point of 3.5 m below surface (Middle), and 1 m above bottom (Bottom) in 2017. Arrows and text indicate examples of observed physical mixing events attributed to entrainment and intrusions.

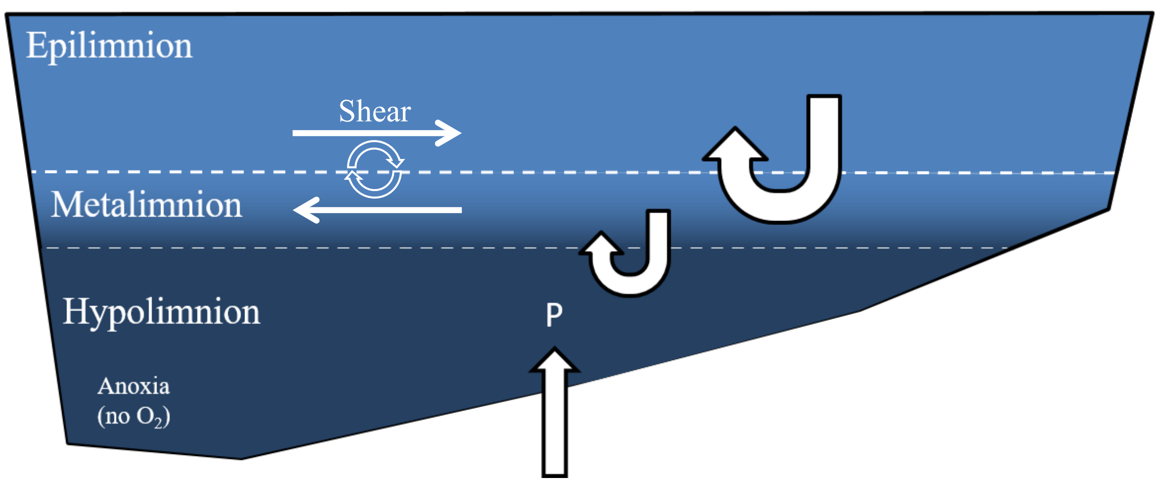

Figure 4-9 Entrainment diagram, illustrating shear forces and phosphorus transport.

4.1.2 Intrusions

In dimictic northern temperate lakes, the epilimnion may see heating and cooling events (oscillating with meteorology, solar radiation) during the ice-free season, but the general trend is that of warming until declines leading up to fall turnover. The metalimnion fluctuates as a function of diffusive heat transfer (entrainment), warming under shear forces (wind) transferring heat from the epilimnion. The metalimnion can also undergo cooling during quiescent periods (lack of diffusion at its epilimnetic boundary) as small amounts of turbulent mixing at the hypolimnetic boundary persist and cooler water is diffused into the metalimnion. Hypolimnetic temperatures are expected to continuously warm until turnover approaches.

The thermal mass of the system must be conserved, however, and a cooling of the hypolimnion prior to fall turnover is not ascribable to entrainment, as this could only transfer warmer water. As previously noted, simultaneous cooling of the metalimnion and hypolimnion was observed (Figure 4-9) at the East Deep continuous temperature monitoring buoy in 2017. The only hydrologic component capable of introducing cooler water to Mona Lake during the stratified period is Lake Michigan. While it was previously hypothesized that Lake Michigan may interact with Mona Lake under wind-driven seiche events (ADCP deployment, 2017), its influence was not expected to be detected 2.4 km (East Deep Buoy) from the confluence with Lake Michigan. While the ADCP deployment offered qualitative insight in to the frequency and range of magnitude Lake Michigan's hydrodynamic linking has, while its data were not able to be quantitatively integrated in this effort (would require robust nearshore Lake Michigan modeling/coupling). Channel temperature monitoring (Figures 4-10 and 4-11) revealed diurnal and stochastic fluctuations in water temperature present in the Mona Lake-Lake Michigan channel. While the channel is shallow (mean depth ~2 m), it was suspected that cooler (more dense) water from Lake Michigan may sometimes remain on the bottom of the channel, seeping into Mona Lake, while the warmer Mona Lake water (less dense) discharge outward. Under larger seiche events, the whole channel water column may be comprised of cooler Lake Michigan water. This dense pulse from Lake Michigan, likely cooler than any existing water in Mona Lake, will create a 'new' hypolimnion, strengthening the stratification regime and subsequent resistance to mixing. In 2018, temperature was monitored at surface, middle, and bottom depths at the channels origin with Mona Lake. On eight occasions in 2018, a temperature gradient of over 6°C from channel surface to bottom was observed (Figure 4-11), coinciding with the observed stratified period in Mona Lake. From this, it is hypothesized that stochastic and ephemeral intrusions from Lake Michigan may introduce cooler (more dense) water to Mona Lake, strengthening the stratification attendant resistance to mixing.

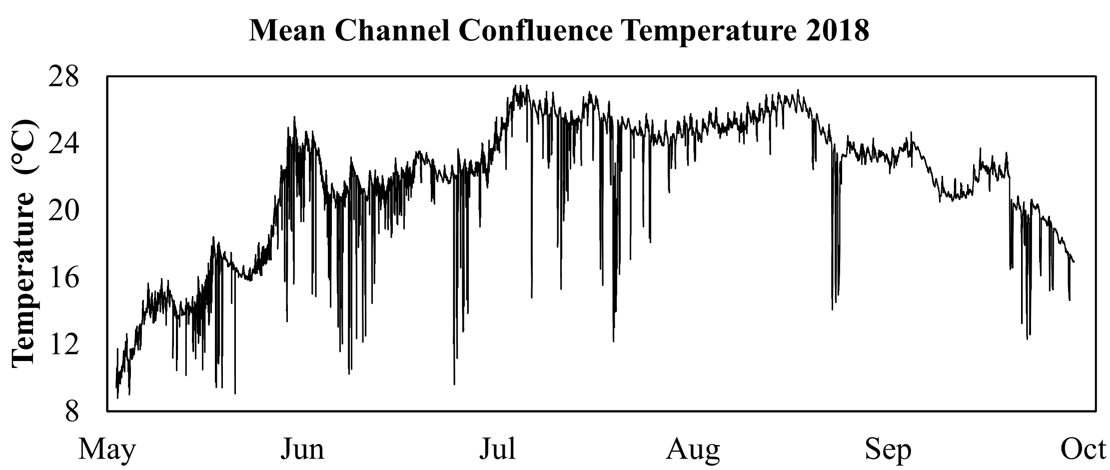

Figure 4-10 Temperature logger vertical post mean temperature data, placed in the confluence of Mona Lake and it's channel to Lake Michigan, illustrating intrusion event frequency.

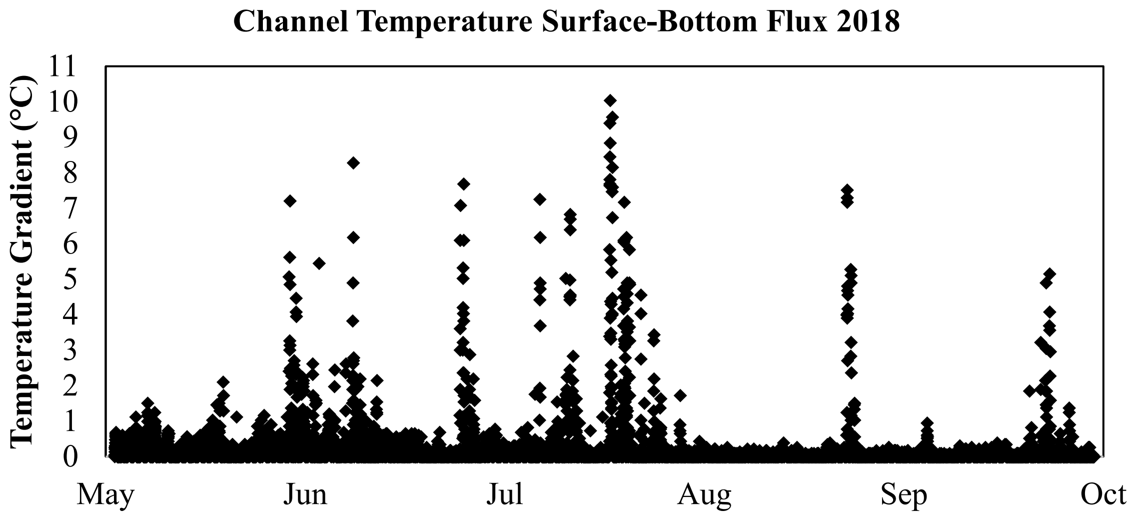

Figure 4-11 Temperature logger vertical post mean temperature data, placed in the confluence of Mona Lake and it's channel to Lake Michigan. Three temperature loggers were placed at top, middle, and bottom in ~2 m of water. Data displayed indicates observed difference between top and bottom loggers.

4.1.3 Chlorophyll and Cyanobacteria

In dimictic eutrophic lakes wherein biomass production is high, surface Chlorophyll (Chl-*a*; algae) levels generally increase during the ice-free period, until turnover. Decades of elevated biomass production lead to large amounts of respiration, creating a demand for oxygen as the decaying organisms settle downward in the water column (sediment oxygen demand). A large stratification gradient (cold hypolimnion) creates a lack of diffusion based mass transport (oxygen). With an inability to obtain more oxygen, the mass of oxygen in the hypolimnion is quickly consumed by the respiration demand in the sediments. This leads to the anoxic periods observed in the seasonal oxygen mapping above, which rids Fe^{3+} (ferric ion) molecules of their ability to sorb phosphorus particles, reducing itself to Fe^{2+} (ferrous ion) and releasing PO_4^{3-} (SRP; Ramm and Scheps 1997) . This highly bioavailable phosphorus accumulates in the hypolimnion, with entrainment forces responsible for diffusing it upwards to the epilimnion where biomass production can occur.

The transport of phosphorus and subsequent growth in Mona Lake is observable in regression of mean lake surface TP against observed Chl-*a* concentrations (Figure 4-12; Dillon and Rigler 1974), which peaked during a Microcystis bloom containing 360 μg/L Microcystin-LR (Michigan Department of Environmental Quality Staff Report; Figure 4-13). following lake turnover. Microcystins are neuro and/or hepatic toxin produced by cyanobacteria. In 2015, the Michigan Department of Environmental Quality (MDEQ) revised their definition of a harmful algal bloom to align with the World Health Organization Guidelines (Chorus et. al. on behalf of WHO 1999) that algal blooms in recreational waters pose a human risk at levels exceeding 20 μg/L microcystin, which is 1/18 the Mona Lake concentration on 9/16/18. Cyanobacteria capable of producing microcystins (i.e. *Anabaena)* are often capable of nitrogen fixation (Dolman et al. 2012), offering them a competitive advantage in a lake with low dissolved inorganic nitrogen (Xie et al. 2012). This allows them to persist in the seasonal algal succession through initial ice-free depletion of nutrients (nitrogen, phosphorus), often coinciding with entrainment-based upwellings of SRP in lakes with anoxic sediment release and allowing them to undergo rapid growth with minimal competition for nutrients. Microcystin concentrations have been correlated to total phosphorus in Mona Lake (Xie et al. 2012).

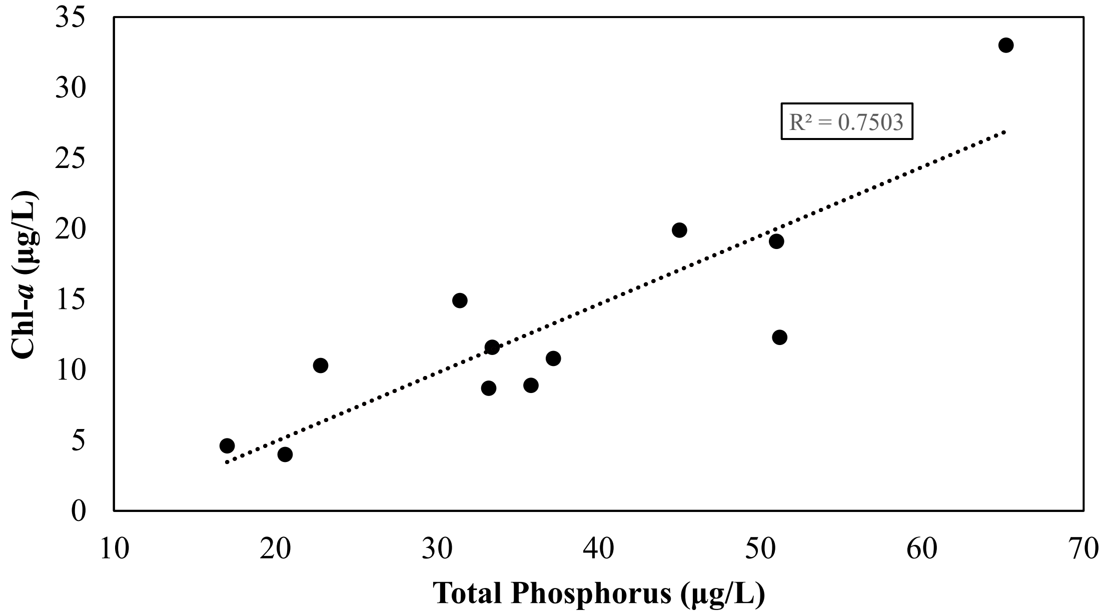

Figure 4-12 Total phosphorus and Chlorophyll-a relationship, 2018.

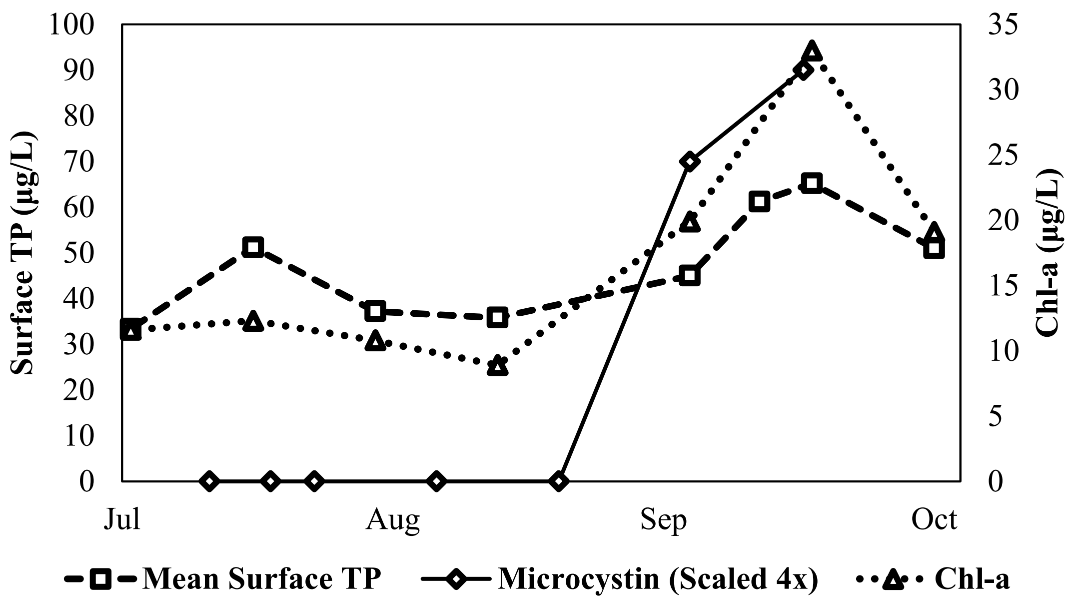

Figure 4-13 Lake surface total phosphorus, Chlorophyll a, and Microcystin concentrations observed in 2018, illustrating correlation.

4.2 External Loading

A temporal analysis of tributary hydrology indicated the first year of field sampling (2017) was a decadal minimum phosphorus load, while the second year of field monitoring (2018) was the second highest phosphorus load since 2008 (Figure 4-14). No significant relationship between tributary discharge and phosphorus concentration was observed during the field monitoring (see 4.2.2), and thus an average concentration from 2017 & 2018 was applied to each respective tributary for external load calculation. A 10-year mean daily load analysis (Figure 4-15) was in agreement with previous hydrologic analysis (Evans 1992, Steinman et al. 2009) regarding Black Creek delivering over 70 percent of the phosphorus load to Mona Lake. For the monitored years 2017 and 2018, Little Black Creek was found to represent 12 percent of the load, an increase from previously published loading analyses. This was attributed to an upstream source of SRP, detected in this field monitoring and discussed in detail below. A temporal loading plot (Figure 4-16) again illustrates the seasonal minimum external load delivered from May through August, while spring and fall high discharge are responsible for higher rates of external loading.

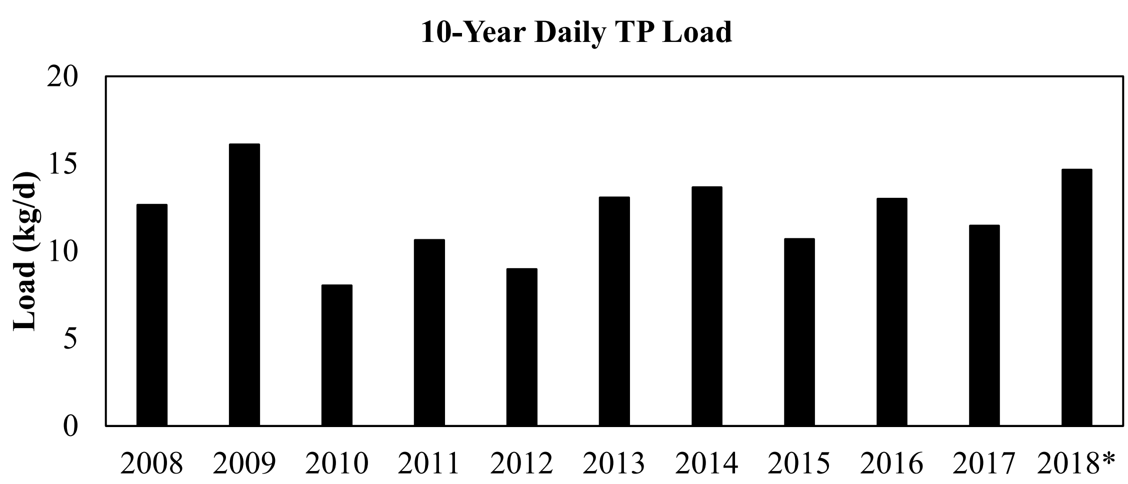

Figure 4-14 External loading daily average for years 2008-2018. *USGS December 2018 data unavailable.

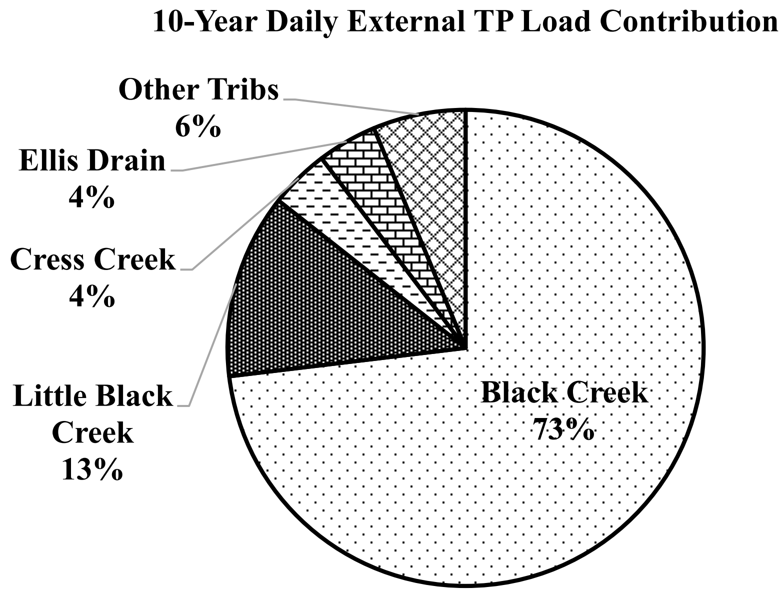

Figure 4-15 Total phosphorus load fractions for each tributary in the Mona Lake Watershed. ‘Other Tribs’ refers to small creek area as presented in the Mona Lake Watershed Atlas (Annis Water Resources Institute 2003).

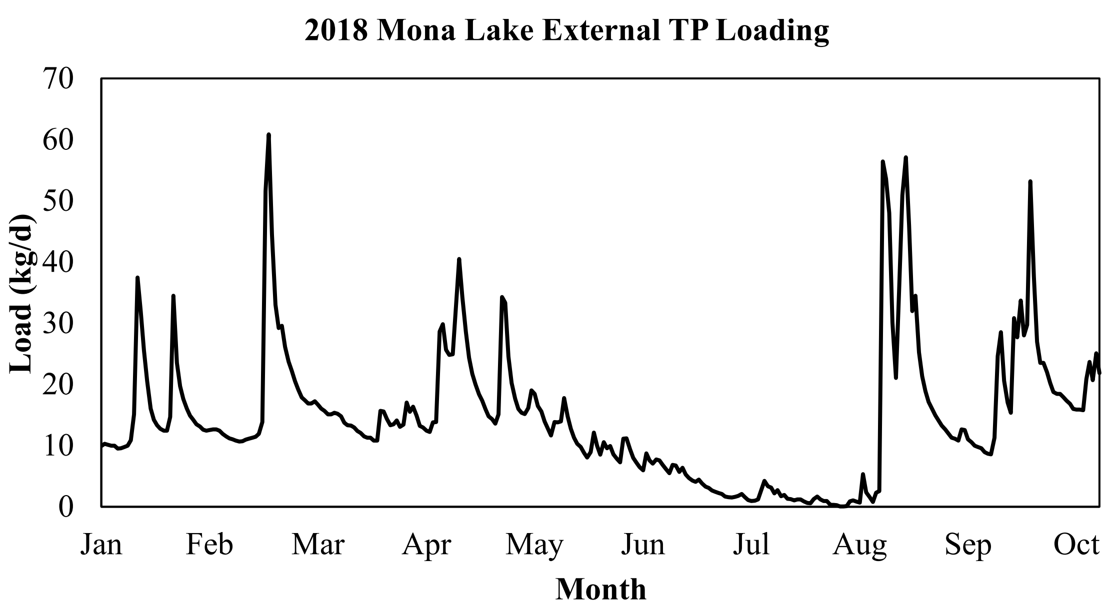

Figure 4-16 External loading (tributary summation) in 2018.

4.2.1 Little Black Creek

Upon detection of elevated SRP concentrations (2017, relative to other tributaries in the watershed) in Little Black Creek, discrete spatial monitoring was conducted in an attempt to locate a source capable of delivering a concentration ~2x higher than nearby tributaries. Samples collected 3 km upstream from the Little Black Creek monitoring program sampling site contained 196 μgSRP/L and 277 μgSRP/L (Figure 4-17) while concentrations 500-800 meters further upstream contained 10-20 μgSRP/L (other watershed tributary mean: 16 μgSRP/L). Concentrations downstream from the peak detections point showed a plausible dilution effect over ~1 km. Sources of water quality impairment (storm sewers from metal finishing industries, metal plating Superfund site, spills from a wastewater pump station) in Little Black Creek (U.S. EPA section 303(d) listed) have been documented previously (Steinman et al. 2006), while elevated SRP levels were not among the detected impairments. The documented sources capable of producing this nutrient point-source contribution would seem to be the abandoned landfill without a leachate collection system, or various stormwater discharges (MDEQ 2000). However, the pollution detected in this effort is upstream of documented contamination sites and monitoring wells (Figure 4-17; map oriented North-South, discharge occurs east-west). Because of this, exact source attribution was not made in this research, but its spatial resolution provides justification for further spatiotemporal analysis of Little Black Creek phosphorus loading. The impacts of its contribution and/or potential reduction to loading and therefore trophic state of Mona Lake is discussed later in this document (Section 5).

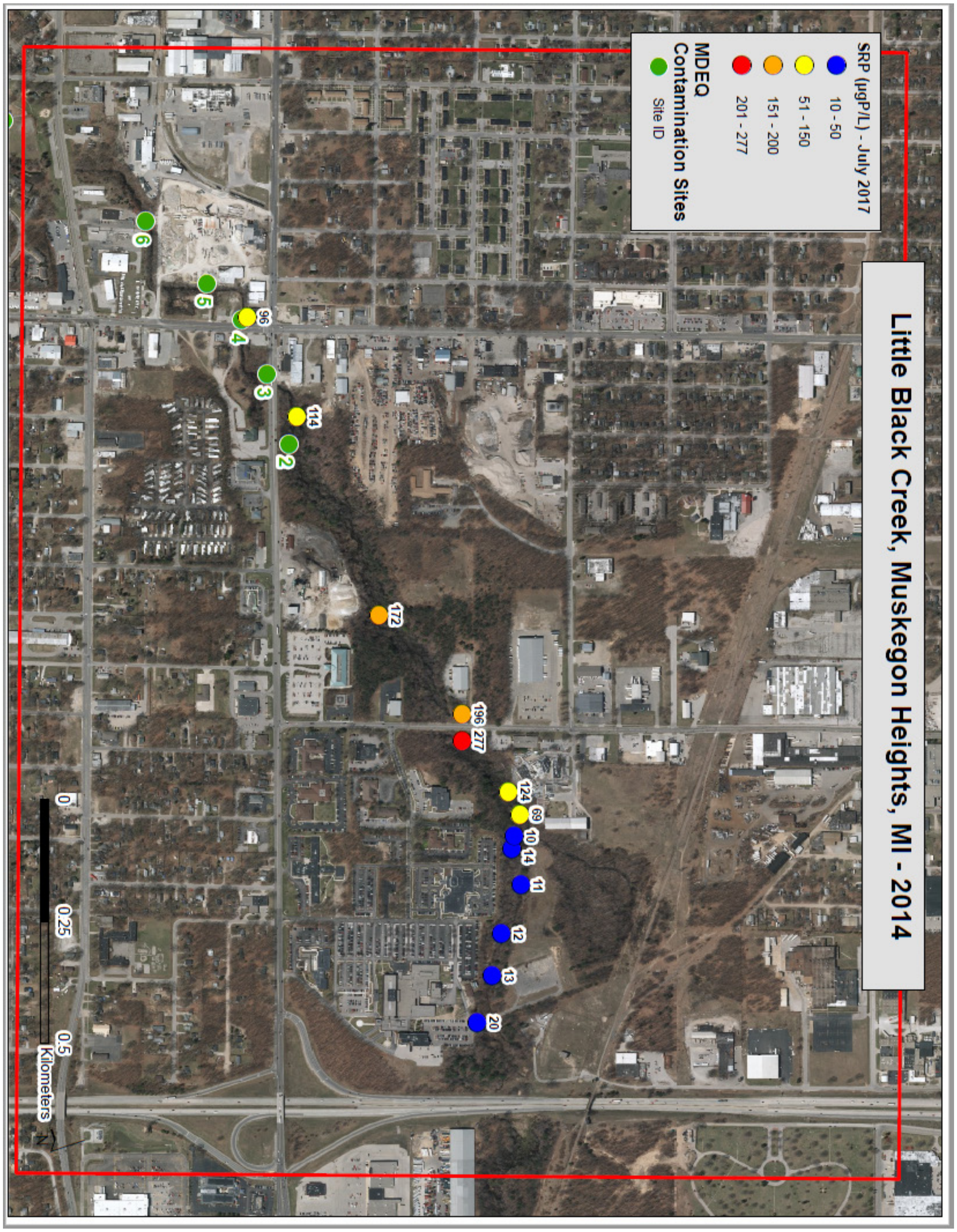

Figure 4-17 Little Black Creek upstream SRP sampling results, with documented MDEQ contamination sites downstream. Map is oriented North-South, while tributary discharge occurs East-West.

4.2.2 Concentration and Discharge Relationships

No significant relationships were seen in regression analysis of tributary discharge and concentration for either SRP or TP (Figures 4-18, 4-20, and 4-21). However, the observed high discharge two-year peak TP value for Black Creek (9.5 m^3/s at 142 μg/L) is hypothesized that the precipitation event causing this decadal high discharge would have likely resulted in abnormal contributions of particulate phosphorus (sediment or algae bound). This is confirmed in regressing the particulate phosphorus pool for Black Creek (Figure 4-19), indicating the fraction of phosphorus bound to particles for the high discharge event to be 26 percent higher than the average observed during monitoring. 2017 and 2018 observed mean phosphorus pools (Figure 4-22) indicate that Black Creek has the highest tributary particulate and dissolved organic phosphorus concentrations, while Little Black Creek contains the highest concentration of soluble reactive phosphorus. Analysis of celery flat TP loading to Black Creek (upstream and downstream of celery flats) indicate no significantly different increase in concentrations (Figure 4-23), remaining magnitudes lower than TP values for the celery flats (Steinman and Ogdahl 2011).

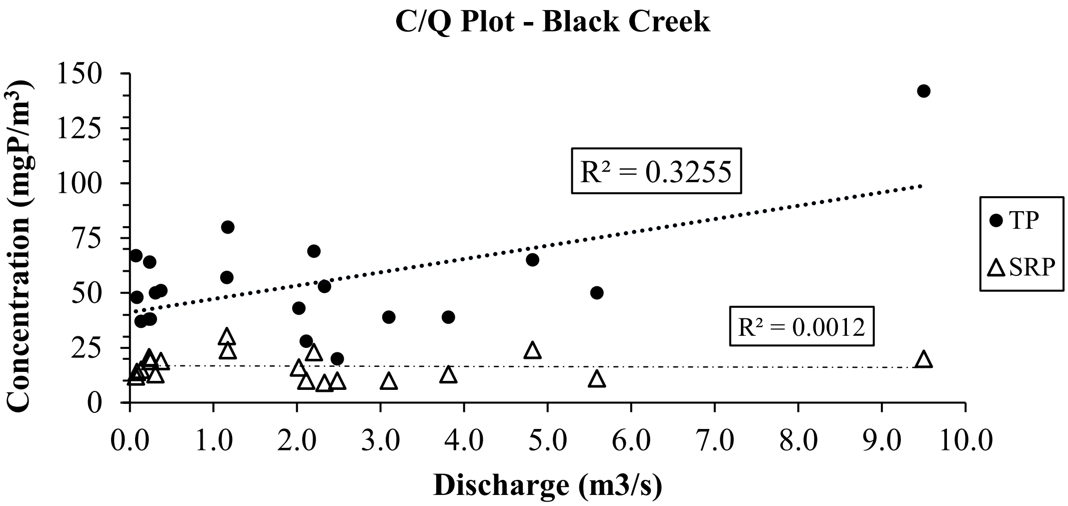

Figure 4-18 Black Creek TP/SRP versus discharge plot for 20 total sampling events in 2017 and 2018.

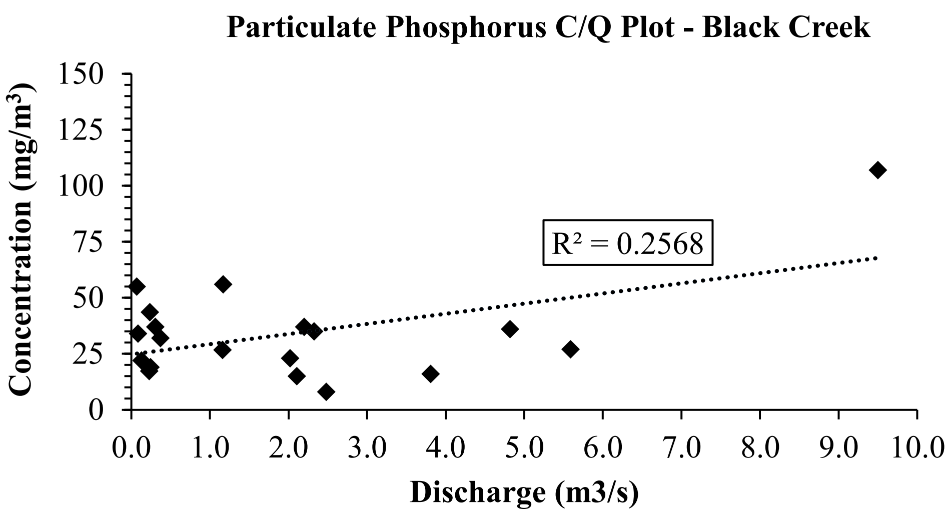

Figure 4-19 Black Creek PP versus discharge plot for 20 total sampling events in 2017 and 2018, explaining the observed TP increase as a PP increase at the outlier (large storm) discharge data point.

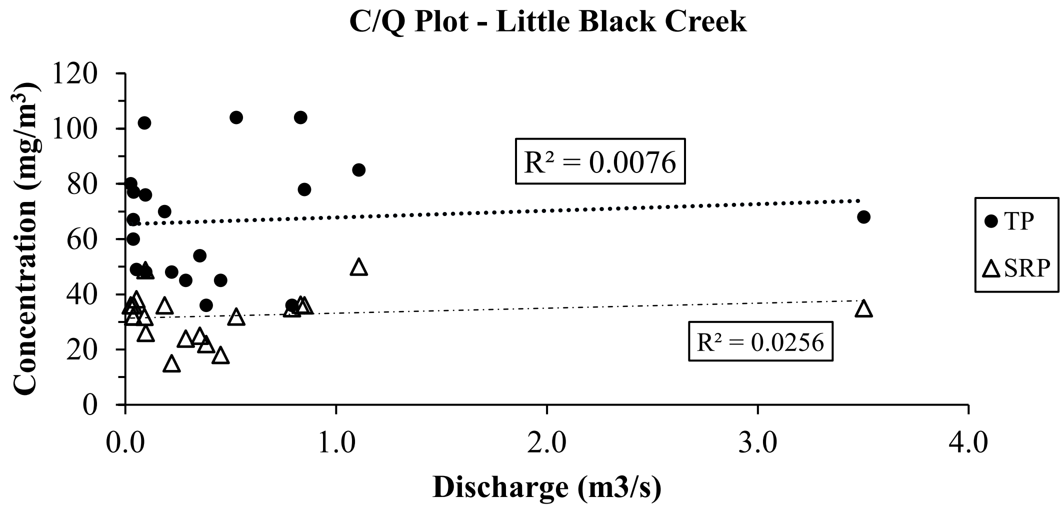

Figure 4-20 Little Black Creek TP/SRP versus discharge plot for 20 total sampling events in 2017 and 2018.

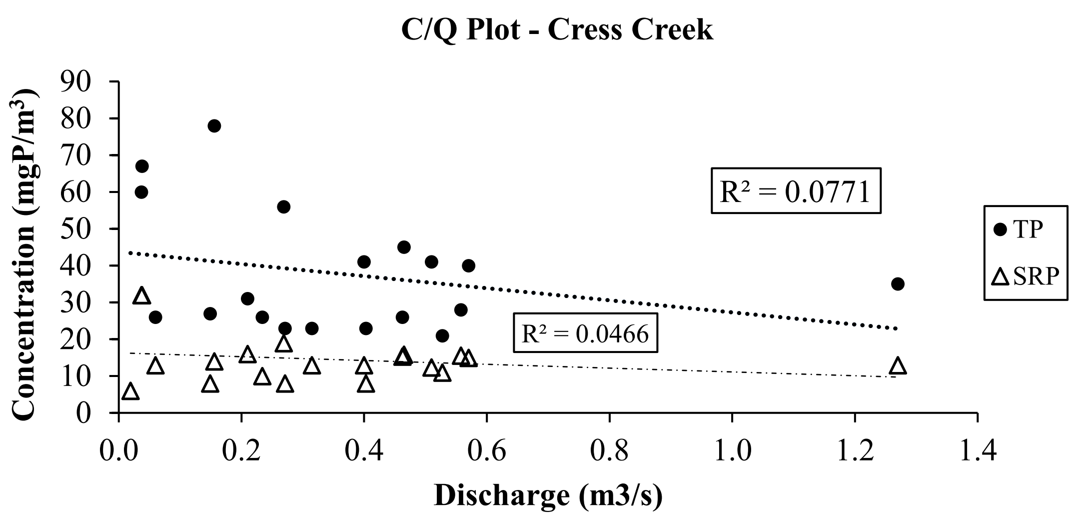

Figure 4-21 Cress Creek TP/SRP versus discharge plot for 20 total sampling events in 2017 and 2018.

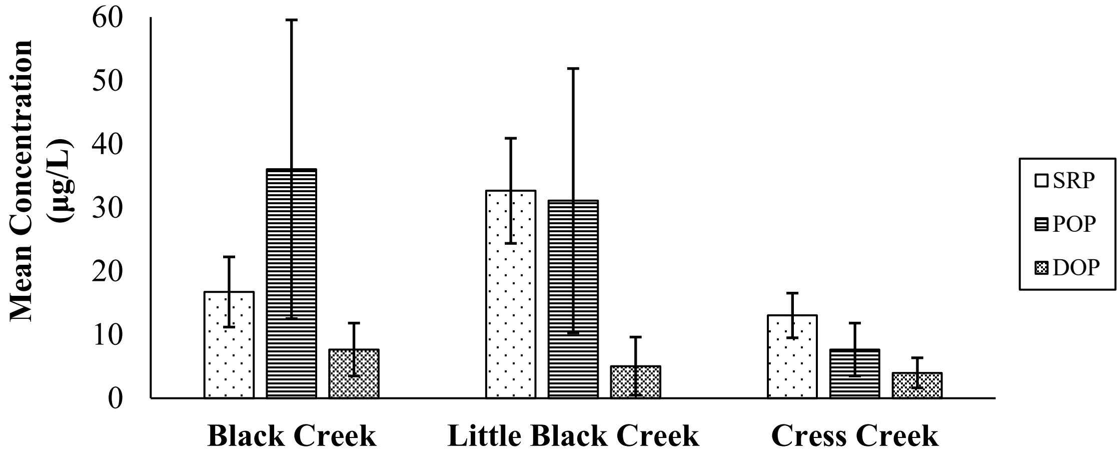

Figure 4-22 Mean SRP, POP, and DOP pools, with standard deviation, for 20 total sampling events in 2017 and 2018.

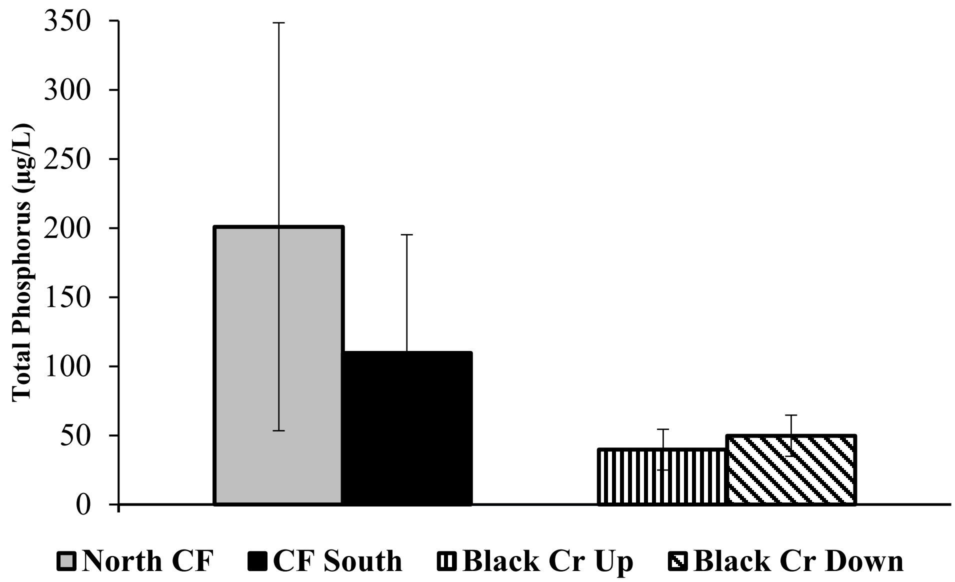

Figure 4-23 Observed differences in mean TP concentrations in Black Creek, upstream and downstream of the celery flats control structures. Celery flat TP concentrations (Steinman 2009) presented for comparison.

4.3 Screening Models

Synthesis of initial conclusions from the above results begins with application of updating screening models previously applied in water quality assessment (Vollenweider and Chapra loading models, Trophic State Index). Contemporary conditions (2017 and 2018) place the expected trophic state of Mona Lake between mesotrophy and eutrophy per the Vollenweider and Chapra plots (Figure 4-24). The same trophic state was predicted in applying the same models to data from 1981, the first post-wastewater diversion study (Limnotech 1982), suggesting little change in nearly four decades. Application of 10 year mean tributary loading (2008-2018; averaged), indicates 2017 and 2018 monitoring years to be representative of the decadal status and agree with the Vollenweider and Chapra model-based consensus that external loads to Mona Lake should result in near mesotrophy (Figure 4-25).

The trophic state observed in years 2017 and 2018 is classifiably eutrophic, as verified by TSI/TP concentration analysis (Figures 4-26 and 4-27), also observed by MDEQ (staff report on Algal Toxin Monitoring in Michigan Inland Lakes 2017). While a decrease in mean lake TP (during monitoring) was observed in 2018, it is believed to have been influenced by a series of large precipitation events in September, significantly flushing the lake of its seasonally accumulated phosphorus and reducing the observed seasonal mean TP concentration. Furthermore, it remains 5x above the eutrophic threshold. As was identified to be a main objective, the discrepancy between trophic state prediction models seen in both historical and contemporary assessments directs modeling and management actions toward the manifestations of legacy deposits (internal loading).

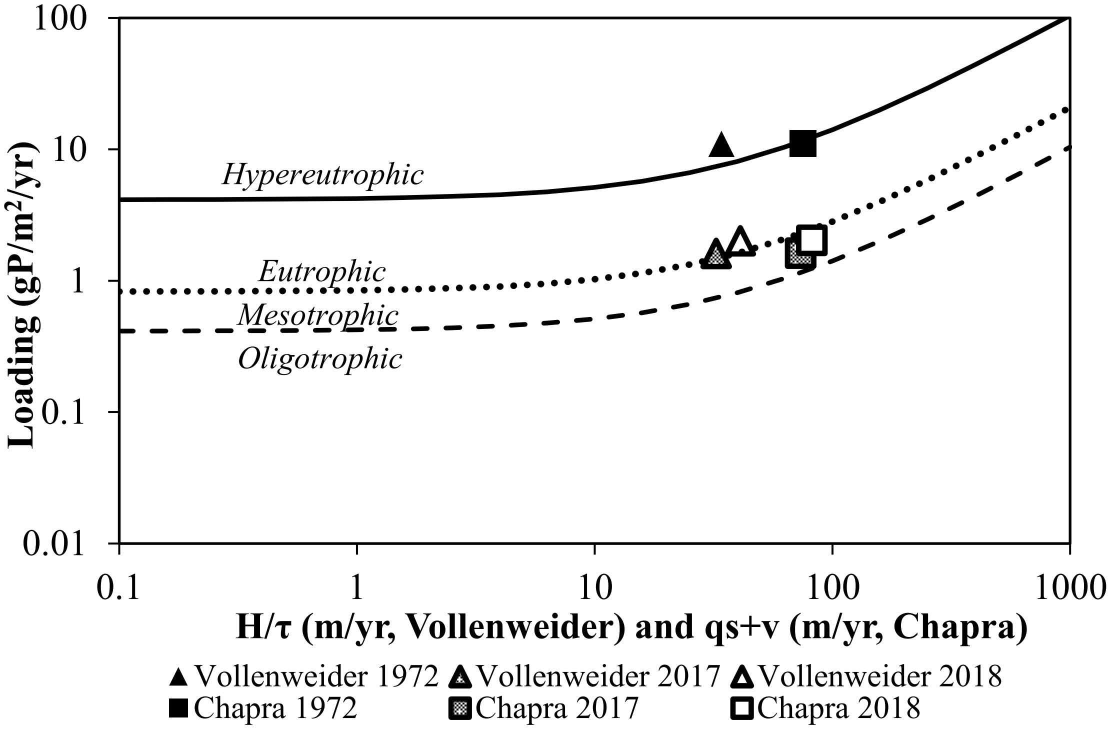

Figure 4-24 Vollenweider and Chapra plots for historical 1972, 2017 and 2018 trophic state predictions.

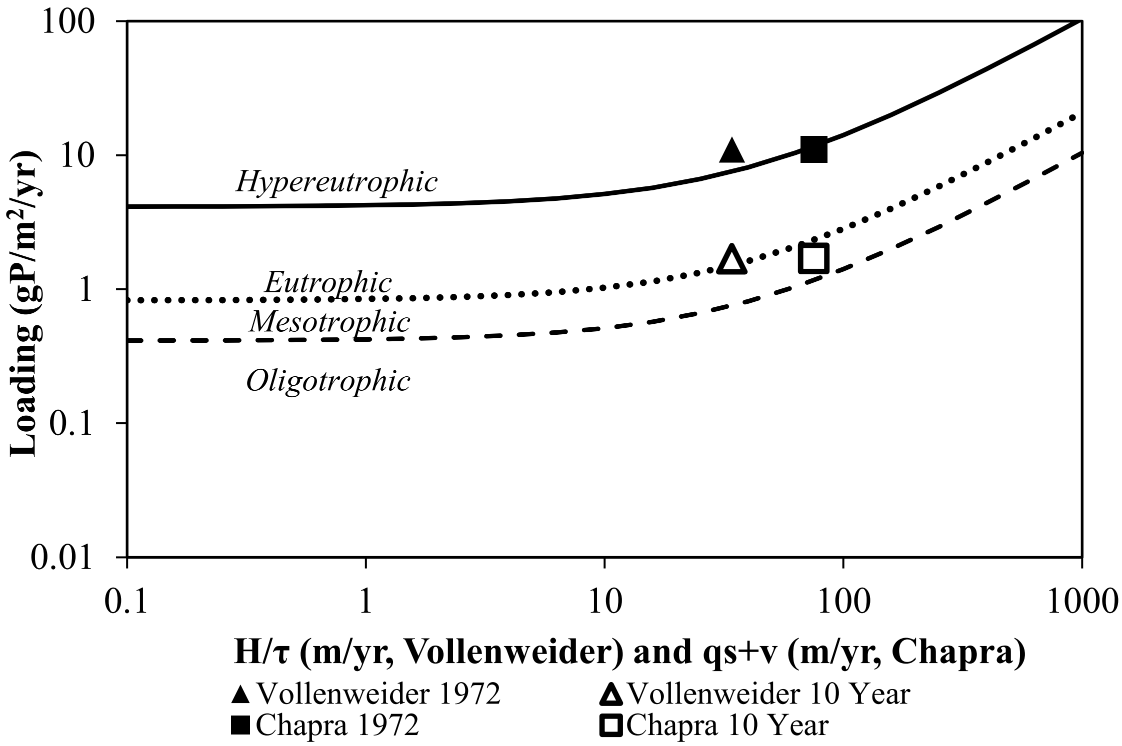

Figure 4-25 Vollenweider and Chapra plots from 10 year average loading estimates.

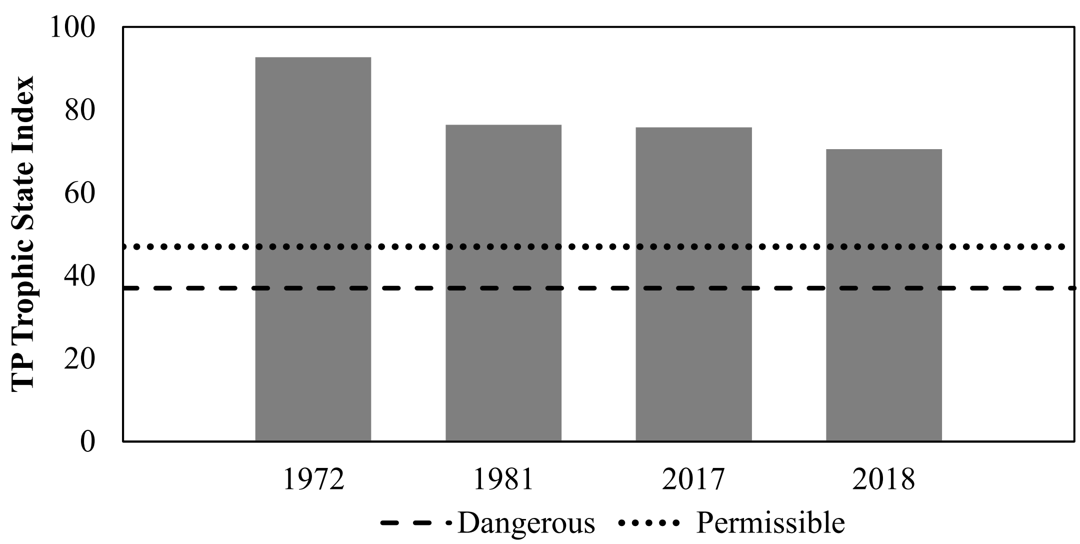

Figure 4-26 Trophic state index calculation for historical data, 1972 (Freedman et al 1979), 1981 (Limnotech 1982), and monitoring years observations (2017 and 2018).

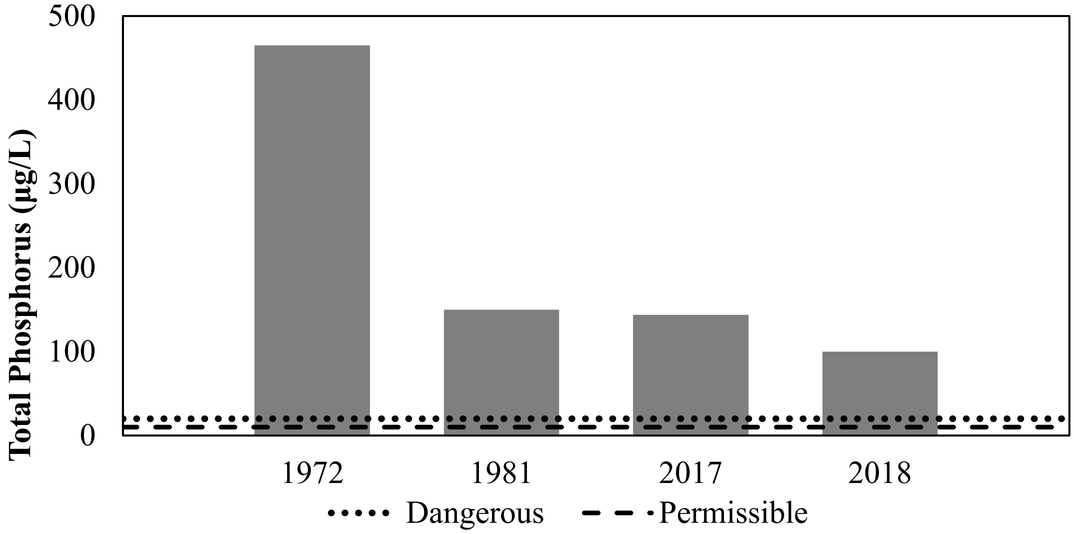

Figure 4-27 Total phosphorus historical data, 1972 (Freedman et al 1979), 1981 (Limnotech 1982), and monitoring years observations (2017 and 2018).

4.3.1 Internal Loading

As previously noted, spring discharge delivers higher phosphorus loads to Mona Lake. Mean tributary TP in April 2018 was 24 µg/L, 35 percent less than the mean lake concentration. While monitoring began later in 2017 (June), the same tributary-lake discrepancy existed, with mean lake TP being 28 percent higher than mean tributary TP (40 µg/L versus 29 µg/L). The departure of mean lake TP from tributary TP provides initial monitoring evidence that there is an in-lake source of phosphorus. Temporal analysis of mean tributary TP versus mean epilimnetic TP (Figure 4-28) show distinct instances in which lake concentrations were greater than tributary concentrations. These instances coincide with entrainment events, transferring phosphorus released from lake sediments to surface waters. Entrainment was greater in 2017, as evidenced by epilimnetic TP concentrations remaining above the tributary average from July through turnover. The period of epilimnetic TP decrease between entrainment events in 2018 is attributable to settling during a meteorologically quiescent period. Comparing mean tributary TP to mean hypolimnetic TP gives further proof of a potent source of internally loaded phosphorus (Figure 4-29), entrained to surface waters by stochastic mixing events. Observations of mean hypolimnetic SRP (Figure 4-30) provide proof of a clear internal source of phosphorus (sediment released). Entrainment forces (mixing) migrate this completely bioavailable form of phosphorus (SRP) to surface waters, wherein it is quickly consumed and observed analytically as total phosphorus (majority particulate phosphorus, Figure 4-31). A temporal analysis of percent TP as SRP for 2018, aligned temporally with the dissolved oxygen map (Figure 4-32), offers tertiary proof of sediment released SRP under anoxic conditions.

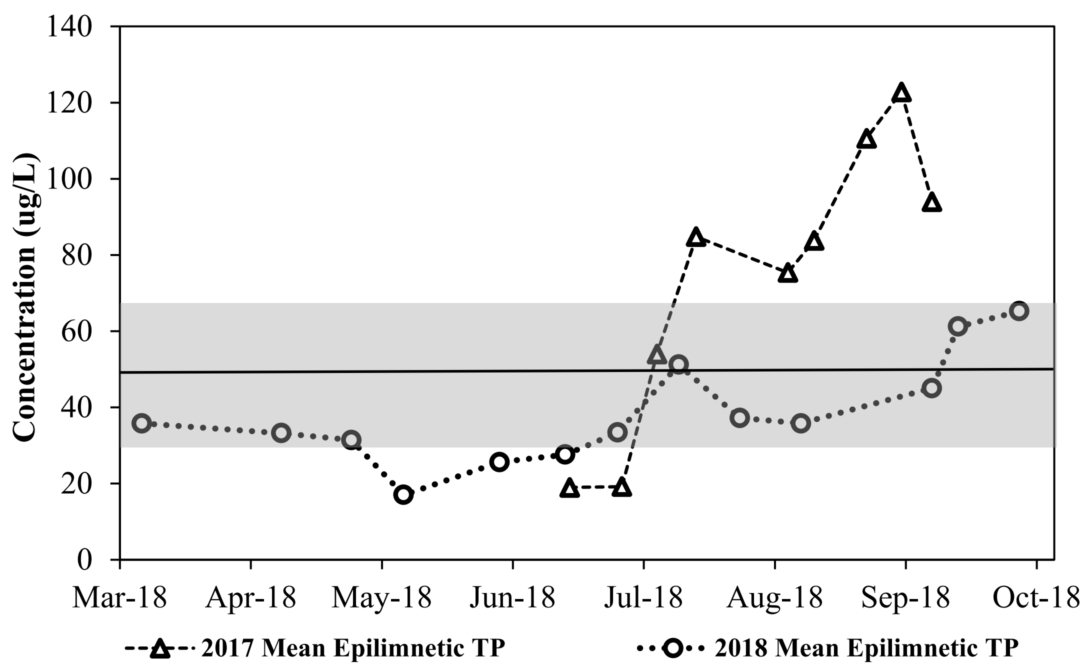

Figure 4-28 Mean tributary TP (2017/2018) and mean epilimnetic TP (2017 and 2018), illustrating lake surface water concentrations higher than discharge concentrations, pointing to internal loading sources. Solid line indicates tributary mean while shaded area illustrates tributary TP range (mean plus and minus the standard deviation).

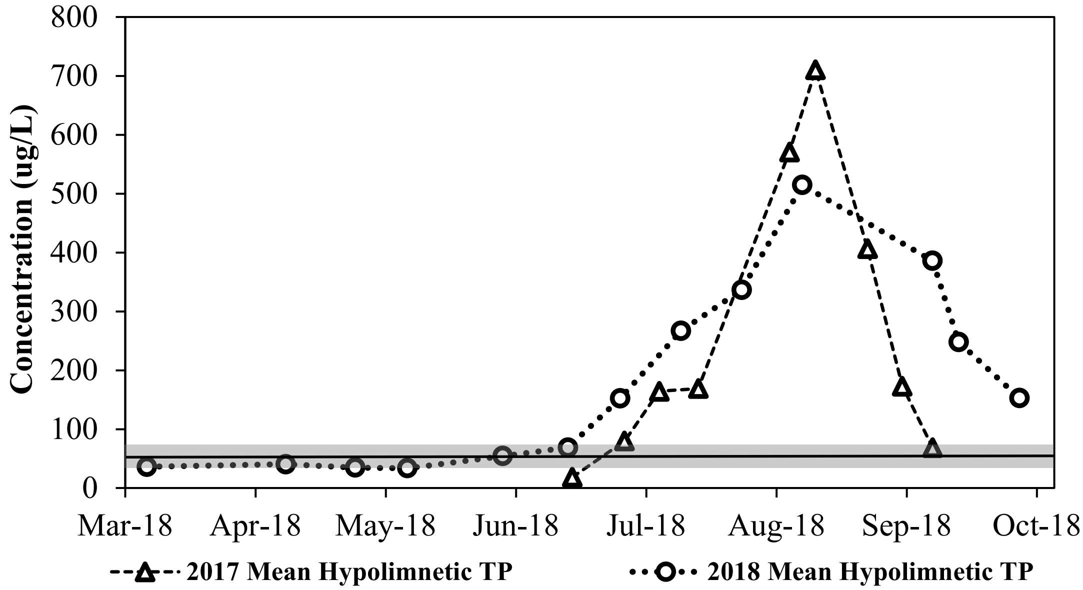

Figure 4-29 Mean tributary TP (2017/2018) and mean hypolimnetic TP (2017 and 2018), illustrating lake bottom water concentrations higher than discharge concentrations, pointing to the source of internal loading. Solid line indicates tributary mean while shaded area illustrates tributary TP range (mean plus and minus the standard deviation).

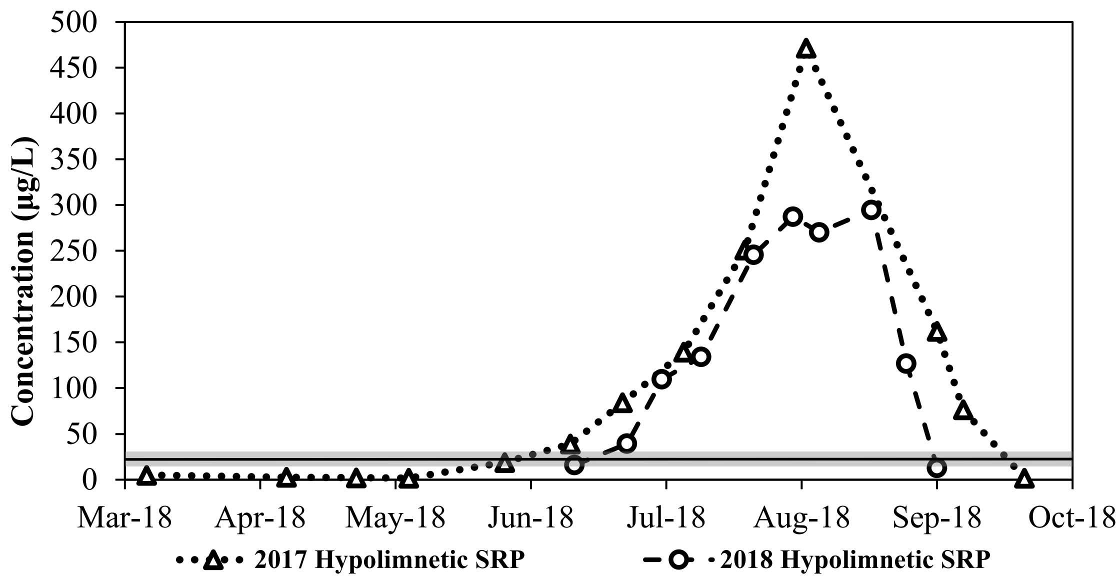

Figure 4-30 Mean tributary SRP (2017/2018) and mean hypolimnetic SRP (2017 and 2018), illustrating lake bottom water concentrations higher than discharge concentrations, pointing to the source of internal loading. Solid line indicates tributary mean while shaded area illustrates tributary SRP range (mean plus and minus the standard deviation).

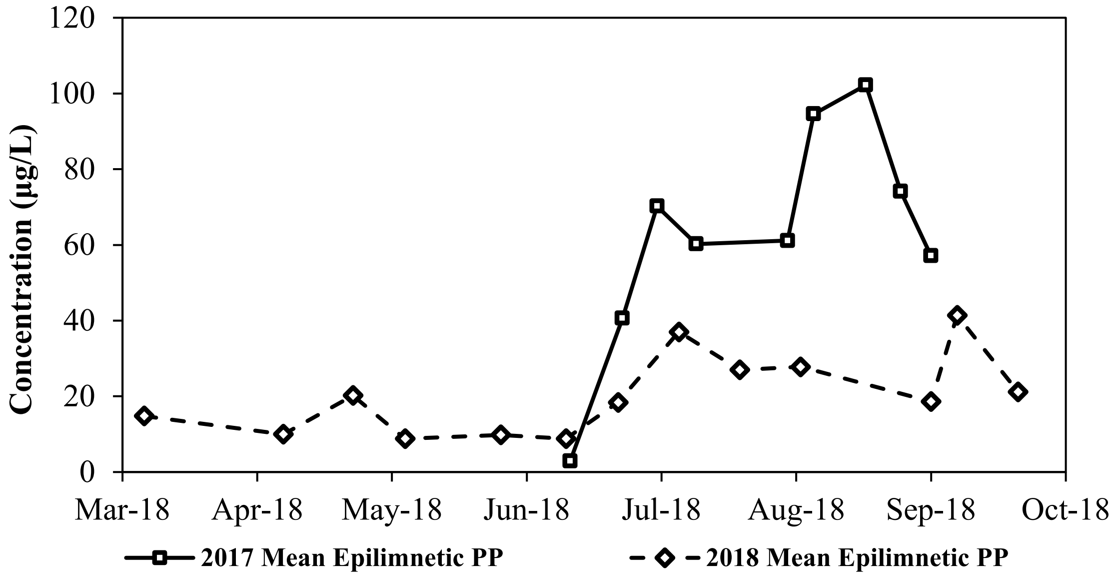

Figure 4-31 Mean tributary particulate phosphorus (2017/2018) and mean epilimnetic particulate phosphorus (2017 and 2018), illustrating lake bottom water concentrations higher than discharge concentrations, attributing the internal source to increases in PP.

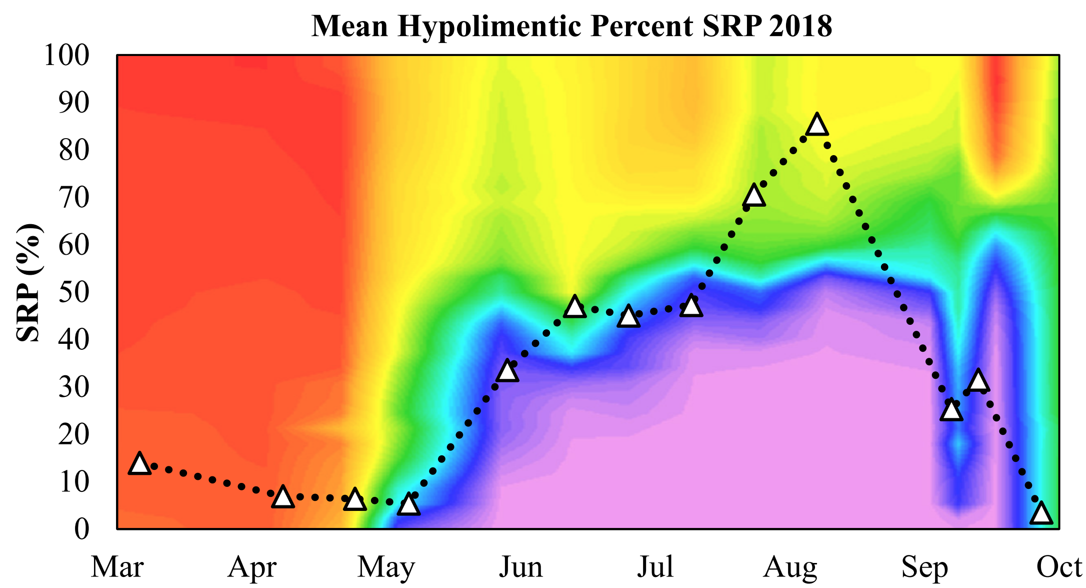

Figure 4-32 Percent TP as SRP for 2018, aligned temporally with the deep sites (East Deep, West Deep, West) dissolved oxygen succession map.

4.4 Biokinetic Model

Screening models, such as those developed by Vollenweider (1975) and Chapra and Tarapchak (1976), have found favor in supporting water quality assessment for over 40 years. These are simple frameworks, with input requirements well within reach of most stakeholders. Additionally, they may be used together with empirical models to quantify other manifestations of eutrophication (e.g., Chlorophyll, Secchi disk transparency, hypolimnetic oxygen demand; Chapra 1997). Yet, screening models are applied with the knowledge that they do not take into account all of the source/sink processes important to some systems; in the case of Mona Lake, for example, sediment phosphorus release. Application in support of engineering design and management, where the economic impact of decision-making comes into play, suggests that a more sophisticated platform would be appropriate. Chapra (1997) has described the trade-offs between model complexities, model reliability and funds available for model development and application (Figure 4-32). In essence, those relationships show that model reliability increases with complexity to a point and then declines as the framework moves past the modeler's capacity to parameterize processes. Additional funds may allow accommodation of additional complexity, thus achieving the required reliability. It is part of the modeling craft to incorporate a degree of complexity consistent with both the required reliability and the funds available. The utilization of a biokinetic framework here is in the spirit of that objective.

One of the objectives in applying the biokinetic model, here LAKE2K, is to test model performance by comparing model output with field observations. In this process, termed calibration, model parameters are adjusted over a reasonable range to yield a solution that yields a best fit to observations. A ‘best fit’ may be defined subjectively as the model’s ability to visually track the magnitude and spatial or temporal pattern of a constituent. Alternatively, a quantitative approach may be selected where the modeler seeks to minimize residuals between output and observations (e.g. root mean square error). The subjective approach is chosen here, as the ability to predict the magnitude of concentrations and seasonal/spatial patterns are of primary importance to the management of Mona Lake. While this goal may be achieved through an objective approach, such an outcome is not guaranteed.

The LAKE2K platform as applied here (Figure 3-12) includes a physical framework and four submodels: Temperature, Oxygen, Phosphorus and Phytoplankton (Chlorophyll). The development of the physical framework, model inputs (e.g. meteorological conditions, hydrologic and constituent loads) and initial conditions have been described previously. Kinetic coefficients relating to the four submodels, as specified through the calibration process, are presented in Table 4-2. Output generated by each submodel forms the basis of the performance evaluation and, subsequently, model runs in management applications.

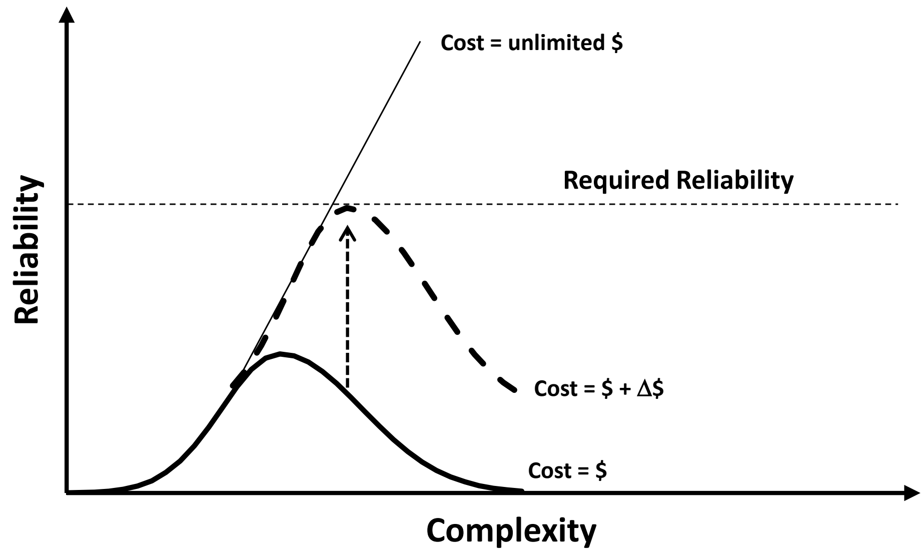

Figure 4-33 The trade-off between model complexity, model reliability and funding for model development and application. Adapted from Chapra (1997).

Table 4-2 Biokinetic coefficients utilized in this application of LAKE2K. Bold face indicates coefficients adjusted in model calibration. Phytoplankton groups are small green algae (SG), large green algae (LG) and cyanobacteria (Cy).

Parameter	*Units*	*Value*
Stoichiometry:		
Dry weight	gD	100
Carbon	gC	**40**
Nitrogen	gN	7.2
Phosphorus	gP	**1**
Chlorophyll	gA	**1**
Water Column Particulate organic phosphorus:		
Dissolution rate	d^{-1}	**0.05**
Temperature parameter for organic P dissolution	d'less	1.07
Settling velocity	m d^{-1}	**1**
Water Column Dissolved organic phosphorus:		
Hydrolysis rate	d^{-1}	**0.015**
Temperature parameter for organic P hydrolysis	d'less	1.07
Sediment Flux:		
Diagenesis model		**No**
SOD	g m^{-2} d-1	**1.1**
SOD temperature correction	d'less	1.08
Oxygen attenuation of SOD	L mgO_2^{-1}	0.5
SRPFlux	mgP m^{-2} d^{-1}	**20**
SRP release temperature correction	d'less	1.1
Oxygen trigger of SRP release	L mgO_2^{-1}	0.15

Phytoplankton:				
Type		SG	LG	Cy
Maximum growth rate	d^{-1}	**2.5**	**1**	**2**
Temperature model for growth		Optimal		
Theta or Topt	°C	**10**	**18**	**20**
Kappa1	d'less	**0.02**	**0.0075**	**0.055**
Kappa2	d'less	**0.8**	**0.035**	**0.05**
Respiration rate	d^{-1}	**0.02**	**0.02**	**0.02**
Temperature parameter for respiration	d'less	1.07	1.07	1.07
Fraction organic for respiration	d'less	0.5	0.5	0.5
Death rate	d^{-1}	**0**	**0**	**0**
Temperature parameter for death	d'less	1.08	1.08	1.08
Nitrogen half saturation	μgN L^{-1}	65	65	65
Phosphorus half saturation	μgP L^{-1}	**1**	**1**	**1**
Silica half saturation	μgSi L^{-1}	50	50	50
Light model		Half saturation		
Light parameter	langleys/d	**70**	**70**	**70**
Settling velocity @ 20oC	m d^{-1}	**0.1**	**0.1**	**0**
Cell density	g/cm3	1.027	1.027	1.027
Ammonia preference parameter	μgN L^{-1}	25	25	25
Grazability	d'less	0	0	0
Silica content	gSi	**0**	**0**	**0**

4.4.1 Temperature Submodel

The model was calibrated to 2018 monitoring data, as field efforts in 2018 began in March as opposed to mid-June in 2017 and provided a more complete calibration dataset. Meteorological data (air temperature, dew-point temperature, wind speed, cloud cover, and atmospheric turbulence) are input as required for the heat balance calculation. Continuous tributary temperature is also user input in support of the thermal load calculation while lake layer (3-layer) initial condition temperatures are derived from early season field data. Tributary heat and meteorological (solar radiation) inputs are received by the user-defined epilimnion, with heat transfer to other layers controlled by vertical turbulent mixing coefficients for the epilimnion-metalimnion and metalimnion-hypolimnion boundaries, respectively. The frequency and magnitude of the mixing coefficients is user-input and adjusted to achieve a best fit to the modeled heat balance (lake layer temperature). The excellent model-data fit noted here (Figure 4-35) is generally expected of physical submodels, with more variability expected with the introduction of chemical and biological state variables. However, the satisfactory fit of the heat budget confirms that the vertical mass transport, crucial in simulating more complex state variables (phosphorus, dissolved oxygen), is very well characterized by the model.

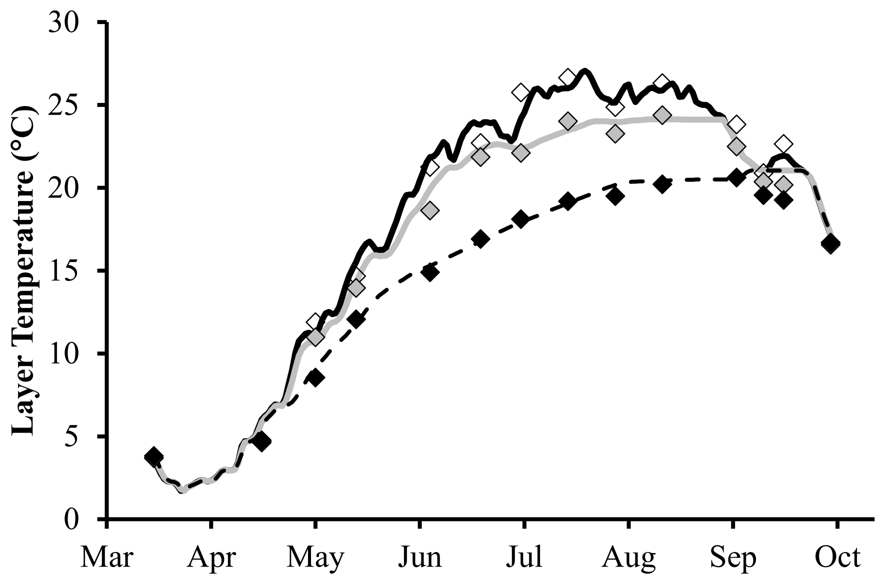

Figure 4-34 Comparison of measured (symbols) and modeled (lines) layer-average water temperature for 2018. The epilimnion is represented by open symbols and a solid black line, the metalimnion by gray symbols and a gray line and hypolimnion by black symbols and a dashed black line.

4.4.2 Oxygen Submodel

Tributary discharge (oxygen loading, assuming saturation) and meteorological data inputs (wind speed; reaeration calculation) are also utilized in the Oxygen Submodel (Figure 4-35). The Oxygen Submodel mass balance includes tributary loads to the epilimnion, reaeration of the epilimnion, sediment oxygen demand in the hypolimnion, and vertical mass transport between the adjoining layers. Vertical mass transport coefficients are called on from the Temperature Submodel. A measured dissolved oxygen concentration is specified as an initial condition for each of the three layers and layer specific concentrations are calculated as a function of time. The combination of these submodels creates a dynamic tension between surface reaeration and sediment oxygen consumption, mediated by vertical mass transport. This is vital, as the key role of the

Oxygen Submodel is to provide a quantification of the trigger for the onset of sediment phosphorus release in the Phosphorus Submodel.

As thermal stratification strengthens, vertical mass transport is reduced and hypoxia and anoxia are observed in the metalimnion and hypolimnion (Figure 4-35). Model output for epilimnetic oxygen tracks the seasonal temperature trend impacting saturation well, but under-predicts observations. This occurs because measurements are made near mid-day (capturing photosynthetically-driven oversaturation), while the model generates daily average output. Model output for the hypolimnion tracks the depletion rate and onset of anoxia satisfactorily, indicating that vertical mass transport coefficients (Temperature Submodel) and the user-specified rate of sediment oxygen demand serve well in describing bottom water oxygen dynamics. Lastly, model output also tracks oxygen in the metalimnion well, a location where concentration is mediated by vertical mass transport and conditions in the epilimnion and hypolimnion. This result offers further support for the value of the vertical mass transport coefficients determined in the Temperature Submodel.

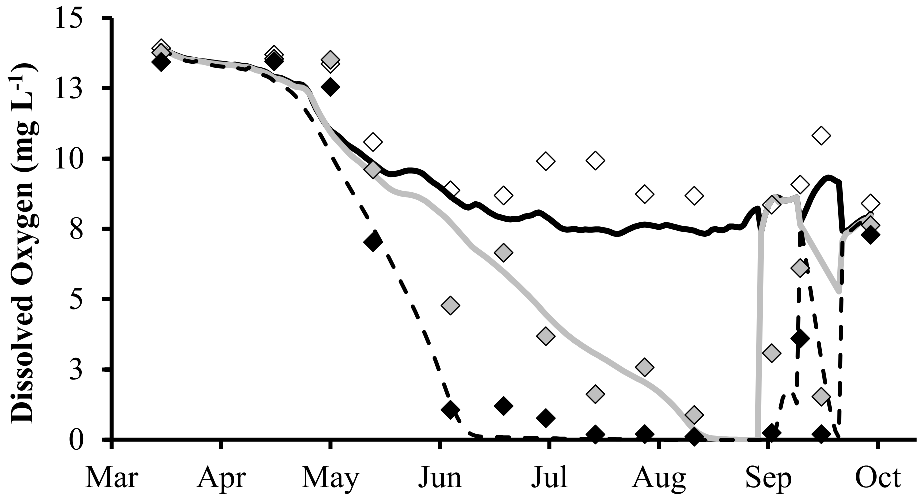

Figure 4-35 Comparison of measured (symbols) and modeled (lines) layer-average dissolved oxygen concentration for 2018. The epilimnion is represented by open symbols and a solid black line, the metalimnion by gray symbols and a gray line and the hypolimnion by black symbols and a dashed black line.

4.4.3 Phosphorus Submodel

The Phosphorus Submodel begins with a mass balance on soluble reactive phosphorus, accommodating inputs from tributary loads, conversion of dissolved organic phosphorus and sediment release, as well as sinks including phytoplankton uptake and lake flushing. SRP is distributed across layers through the vertical mass transport defined in previous submodels. The SRP component of the Phosphorus Submodel plays a critical role in mediating trophic state conditions, as it is expected to be a reflection of the sediment release phenomenon, a driving force for the Phytoplankton (Chlorophyll) Submodel. The SRP mass balance tracks the (low) epilimnetic and (high) hypolimnetic concentrations well (Figure 4-36). Characteristics of the simulation include low concentrations in the epilimnion due to phytoplankton uptake and high concentrations in the hypolimnion due to sediment release, with an expanded scale (Figure 4-37) better representing conditions in the epilimnion.

Dissolved organic phosphorus is the second of three components of the Phosphorus Submodel, with a mass balance accommodating inputs from tributary loads and conversion of particulate organic phosphorus. DOP sinks include hydrolysis to soluble reactive phosphorus and lake flushing while vertical mass transport distributes DOP across layers. The primary significance of dissolved organic phosphorus is as part of the recycle of phosphorus taken up by phytoplankton and returned to the SRP component through dissolution of particulate and dissolved organic phosphorus. The modeled mass balance tracks DOP concentrations well in both magnitude and stability (Figure 4-38).

The particulate phosphorus mass balance accommodates inputs from tributary loads and accounts for uptake of soluble reactive phosphorus by phytoplankton. As a particle bound form of phosphorus, it settles, in addition to hydrolysis and flushing. Its distribution across layers is a function of vertical mass transport forces. The primary significance of particulate phosphorus is in its tributary load contribution, as well as its role as a reservoir/storage (through phytoplankton) for SRP transported from the hypolimnion. Recycle of PP contributes back to the SRP pool through dissolution and hydrolysis of DOP. The PP mass balance (Figure 4-39) tracks concentrations well over the season, both in magnitude and temporal structure, responding to tributary loads and spring phytoplankton growth in the early part of the season and increases in phytoplankton abundance in the late summer.

The mass balances for SRP, PP, and DOP are summed to yield the TP mass balance. TP is the primary state variable for evaluating trophic state response to management actions, integrating tributary loads, sediment phosphorus release and in-lake processes. Thus the Phosphorus Submodel plays a critical role in engineering design. As with soluble reactive phosphorus, total phosphorus results emphasize the discrepancy between (low) epilimnetic and (high) hypolimnetic concentrations (Figure 4-40); with an expanded scale presentation (Figure 4-41) for the epilimnion better illustrating the goodness of fit.

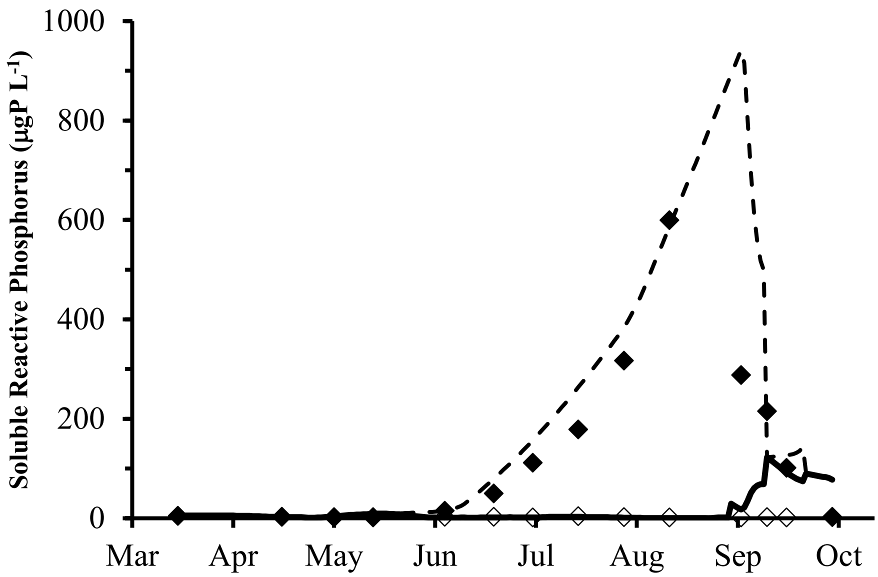

Figure 4-36 Comparison of measured (symbols) and modeled (lines) layer-average soluble reactive phosphorus for 2018. The epilimnion is represented by open symbols and a solid black line and the hypolimnion by black symbols and a dashed black line.

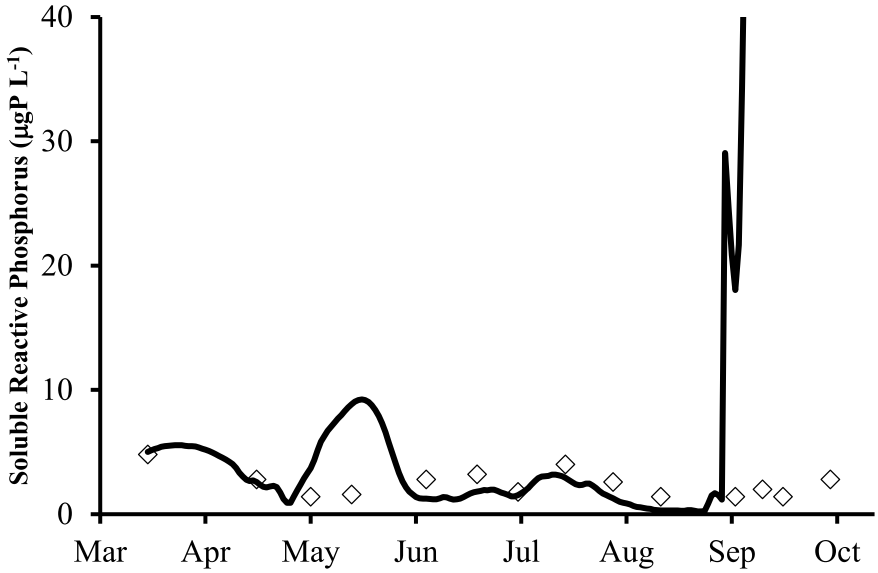

Figure 4-37 Comparison of measured (symbols) and modeled (line) epilimnetic, layer-average soluble reactive phosphorus for 2018. This figure provides a scale expansion from the figure illustrating both epilimnetic and hypolimnetic concentrations.

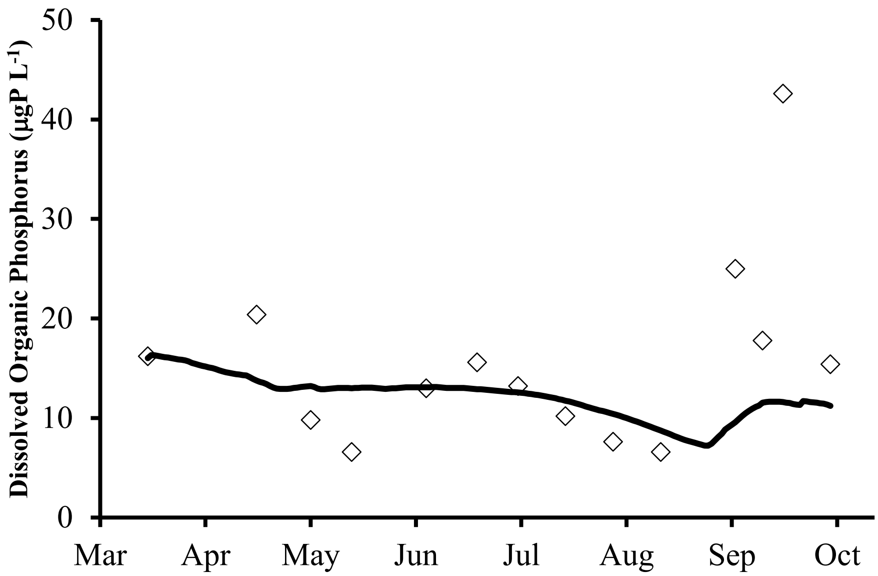

Figure 4-38 Comparison of measured (symbols) and modeled (line) epilimnetic, layer-average dissolved organic phosphorus for 2018.

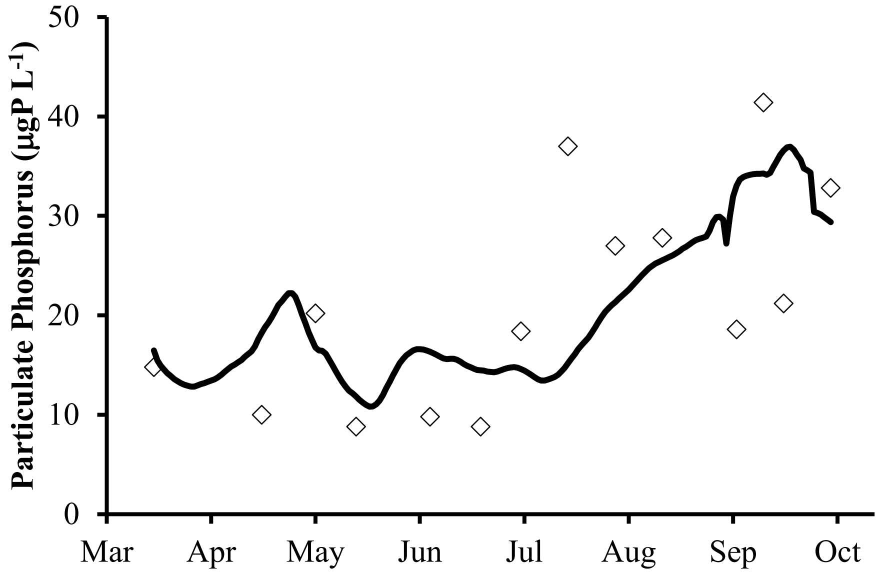

Figure 4-39 Comparison of measured (symbols) and modeled (line) layer-average, epilimnetic particulate phosphorus for 2018.

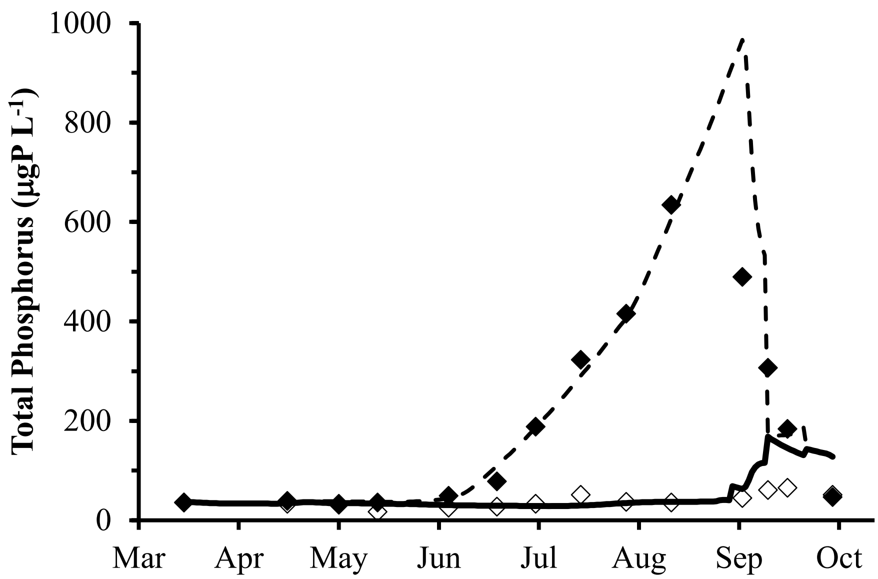

Figure 4-40 Comparison of measured (symbols) and modeled (lines) layer-average total phosphorus for 2018. The epilimnion is represented by open symbols and a solid black line and the hypolimnion by black symbols and a dashed black line.

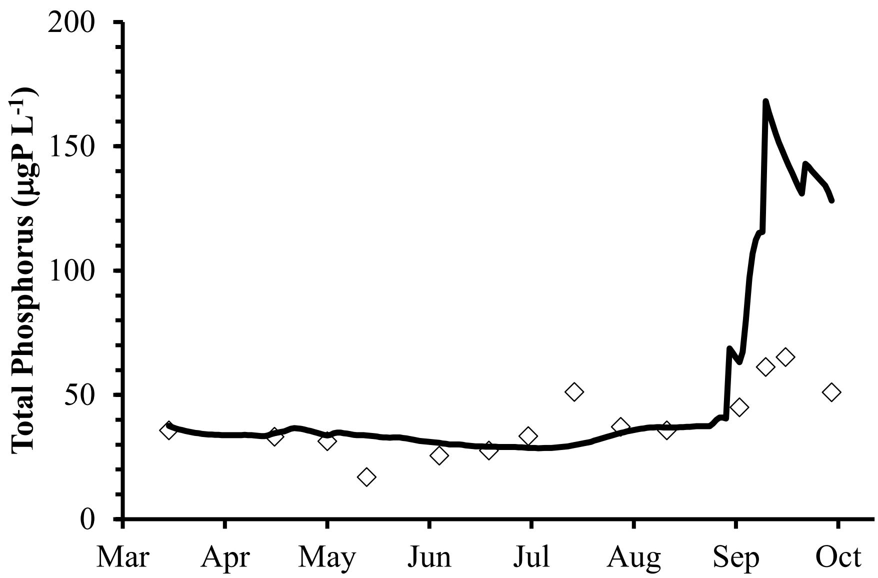

Figure 4-41 Comparison of measured (symbols) and modeled (line) epilimnetic, layer-average total phosphorus for 2018. This figure provides a scale expansion from the figure illustrating both epilimnetic and hypolimnetic concentrations.

4.4.4 Phytoplankton (Chlorophyll) Submodel

In the Phytoplankton (Chlorophyll) Submodel, up to three phytoplankton groups, each having a characteristic assemblage of growth-mediating kinetic coefficients, may be user-identified. In this model application, three groups are simulated: small green algae, large green algae and cyanobacteria (Figure 4-42), with key differences among the groups including the maximum specific growth rate, the temperature optimum for growth, and settling velocity (cyanobacteria do not sink; buoyancy effect). Inclusion of three groups facilitates tracking of total chlorophyll concentrations, while recognizing seasonal changes in phytoplankton composition. The overall Phytoplankton (Chlorophyll) Submodel mass balance includes gains through gross photosynthesis and losses to respiration and settling. First-order rate coefficients are provided for each of these processes as user input. Gross photosynthesis is mediated by attenuation factors reflecting the effects of light, temperature, and soluble reactive phosphorus concentration. The light effect is influenced by the flux of solar radiation (Temperature Submodel) and an internally-calculated vertical extinction coefficient. The effects of temperature are simulated through a temperature optimum and internally calculated (Temperature Submodel) layer temperatures. Soluble reactive phosphorus levels, calculated in the Phosphorus Submodel, are included through a Michaelis-Menten function. The Phytoplankton (Chlorophyll) Submodel serves well in tracking the planktonic algal community (Figure 4-43), both as phytoplankton biomass and in the seasonal pattern: a spring bloom followed by a clearing phase, a stable midsummer period and, finally, a late summer-early fall bloom (cyanobacteria).

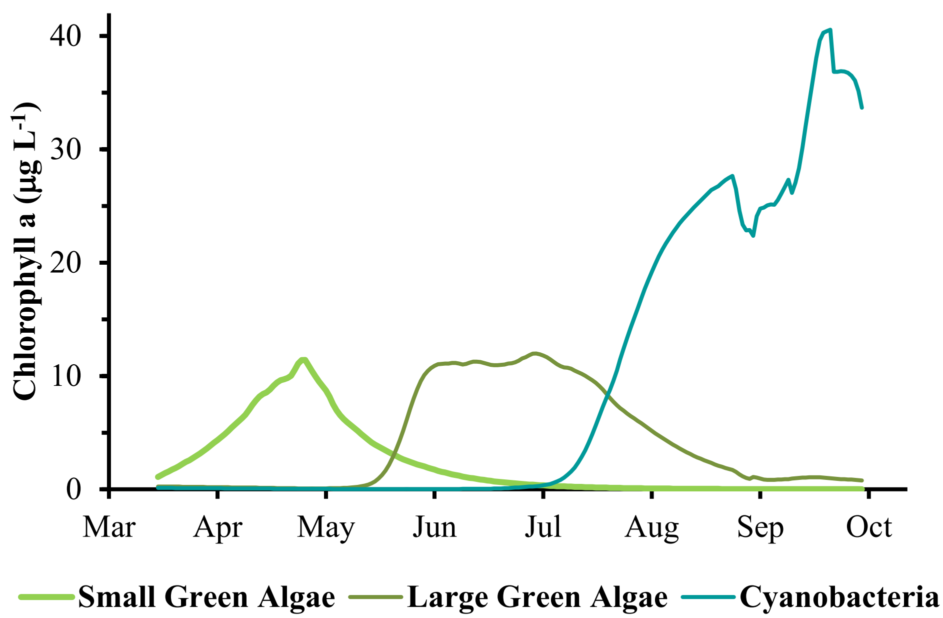

Figure 4-42 Model-predicted contributions to epilimnetic chlorophyll by each of three phytoplankton groups over the 2018 field season

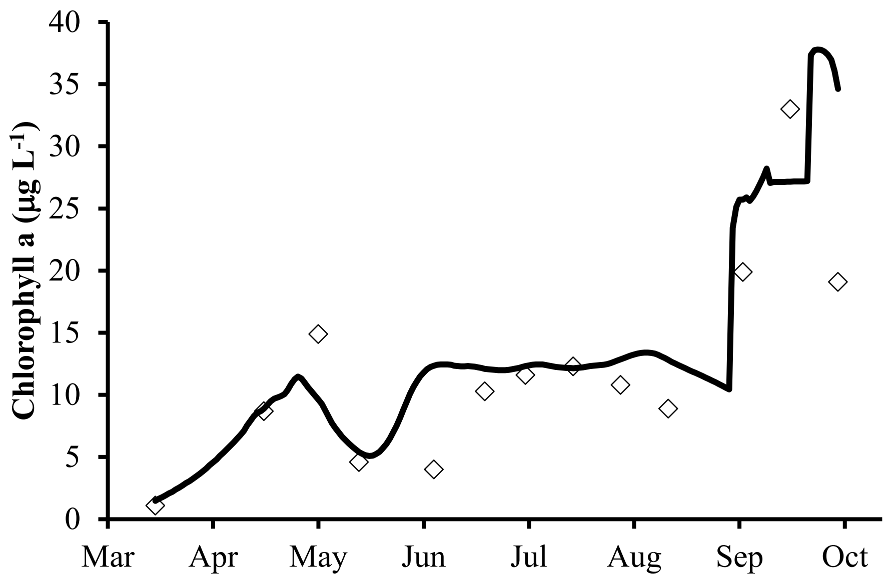

Figure 4-43 Comparison of measured (symbols) and modeled (lines) epilimnetic chlorophyll for 2018. Measurements are represented by symbols and model output by a line.

4.5 Management Scenario Modeling

As was outlined previously, stakeholders desired assembly of a model framework capable of simulating phosphorus management scenarios for Mona Lake. Successful model calibration (Section 4.4) allows for confidence in the ability to predict trophic state impacts under hypothetical phosphorus load reduction strategies able to aid and direct management resources.

4.5.1 Internal Loading Reduction

In the absence of anoxia induced sediment phosphorus release, model predictions indicate a 19 percent decrease in average epilimnetic TP concentrations (Figure 4-44), reflected also in a predicted Chlorophyll-a decrease of 48 percent (Figure 4-45). With large spring discharge delivers the epilimnetic TP concentration observed in March, we can conclude that in the absence of internal loading, under existing external loading scenarios, Mona Lake would reach mesotrophy by mid-June. Chlorophyll-a concentrations (Figure 4-45) are predicted to enter eutrophic levels during April green algae abundance, declining as temperatures increase and growth optima change between phytoplankton groups, recovering to near eutrophic levels in May. While these are both significant improvements, interannual variance in discharge (external loading) could shift the temporal occurrence of the below-threshold dates, aligning it with seasonal algal succession capable of cyanobacteria proliferation.

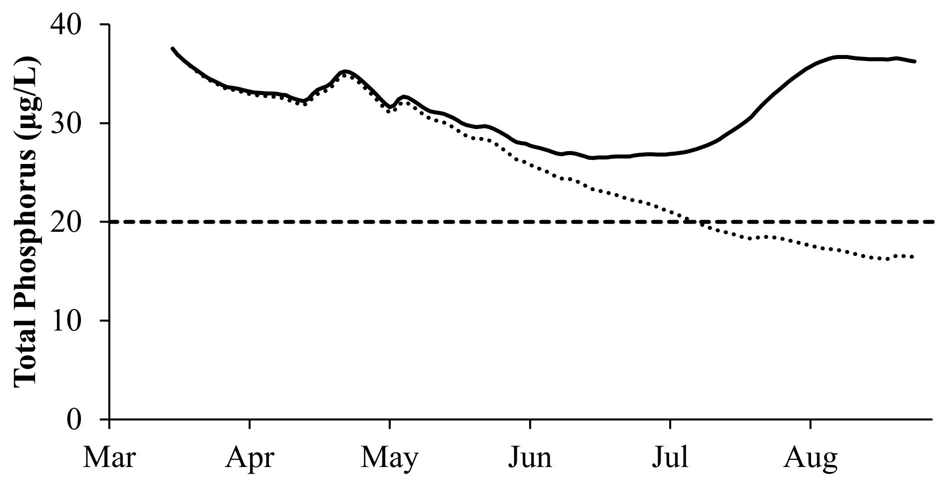

Figure 4-44 Model predicted total phosphorus concentrations if sediment released phosphorus were managed (zero). Black line indicates baseline (calibrated model) while grey line indicates prediction of baseline model sans sediment release. Eutrophic threshold indicated by at 20 µg/L.

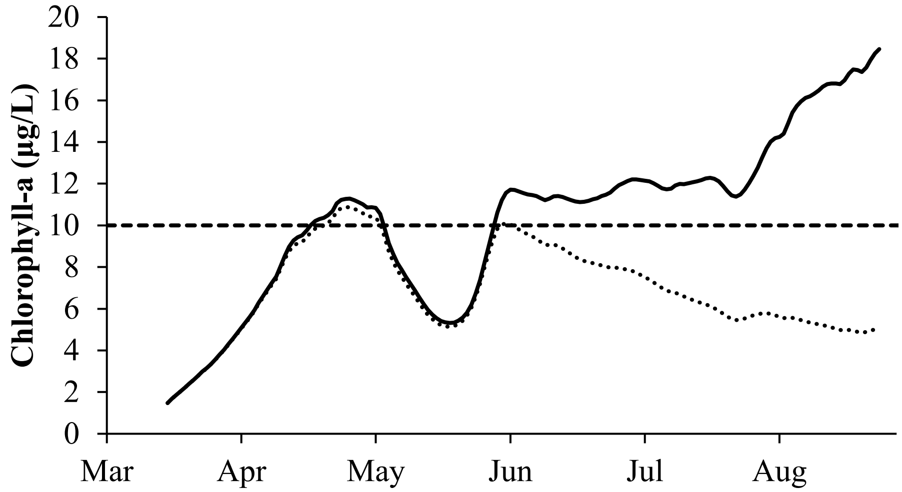

Figure 4-45 Model predicted Chlorophyll-a concentrations if sediment released phosphorus were managed (zero). Black line indicates baseline (calibrated model) while grey line indicates prediction of baseline model sans sediment release. Eutrophic threshold indicated at 10 µg/L.

4.5.2 External Loading Reduction

With the above management simulation illustrating the governance of seasonal loading (high spring load), external load reduction scenarios of 10, 25, 50, and 75 percent were simulated (Figure 4-46) while sediment phosphorus release remained at its calibrated baseline contribution. Predicted external loading reductions of 10 and 25 percent indicate the epilimnetic TP concentration to remain above the eutrophic threshold. A 50 percent reduction would bring about mesotrophy while a 75 percent reduction predicts oligotrophy. These same reduction strategies show considerable decreases in Chlorophyll-a predictions (Figure 4-47), with 25, 50, and 75 percent reduction strategy predictions remaining in mesotrophy for much of the year. However, Chlorophyll-a response under all reduction strategies reach eutrophy as internal loading dominates trophic state dynamics by July. Lastly, external loading reductions of 50 and 75 percent, while not impossible, would be very difficult in the Mona Lake watershed.

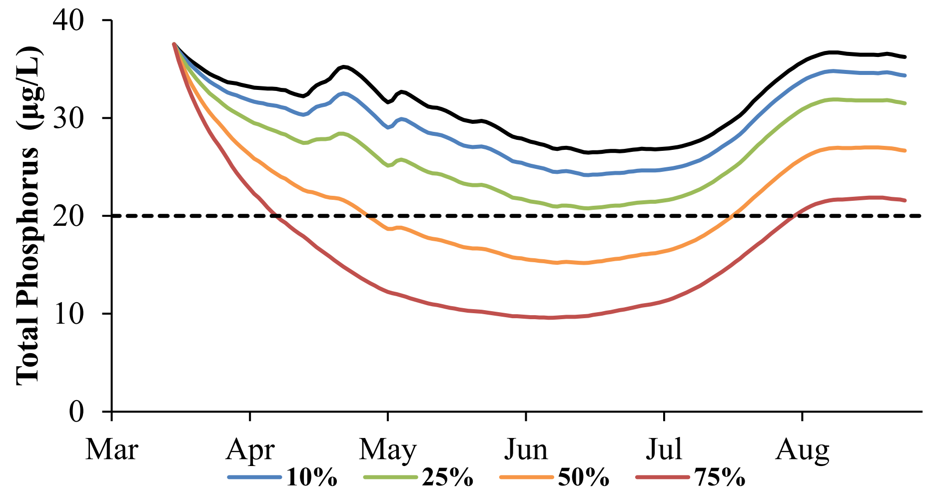

Figure 4-46 Total phosphorus predictions resulting from external load reductions of 10, 25, 50, and 75 percent. Baseline shown in black and eutrophic threshold indicated at 20 µg/L.

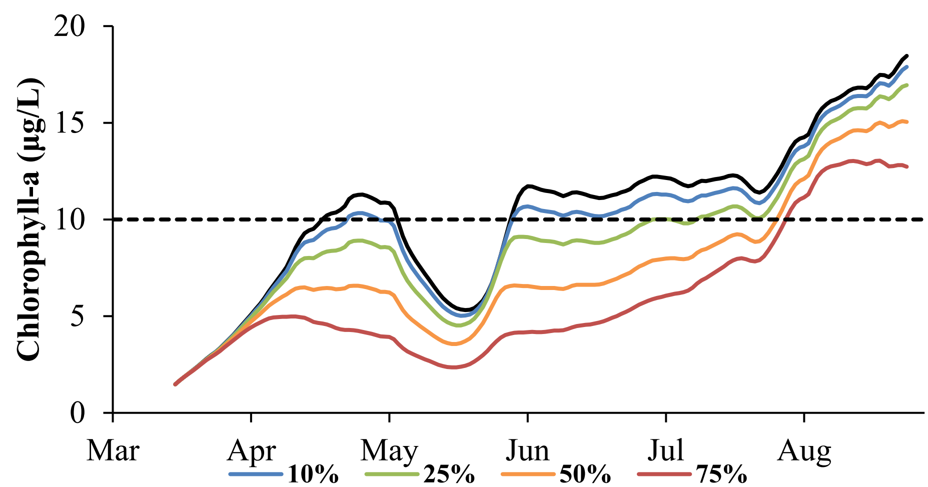

Figure 4-47 Chlorophyll-a predictions resulting from external load reductions of 10, 25, 50, and 75 percent. Baseline shown in black and eutrophic threshold indicated at 10 µg/L.

4.5.3 Combined Reduction

Previously tested management scenarios, addressing external and internal loading independently, showed promising improvements in predicted water quality. However, neither predicted an entirely satisfactory improvement in trophic state (eutrophic to mesotrophic) for the whole ice-free period. As a result, a plausible external loading reduction of 25 percent was paired with hypothetical internal loading treatment (no sediment release), with model predictions confirming this to be a satisfactory management strategy (Figures 4-48 and 4-49). The absence of sediment phosphorus loading, combined with an external loading reduction of 25 percent predicts mesotrophy from May onward. The lake is able to remain in mesotrophy (characterized by TP and Chlorophyll-a concentrations) as a result of no internally loaded and stochastically entrained phosphorus reaching the epilimnion. Furthermore, the epilimnetic concentrations for the "Existing IC" result from a model prediction using existing (baseline) lake TP concentrations as the initial condition and not those that would result from the reduction. Extending the baseline model runtime and applying resulting concentrations from the respective reduction percentage as a new initial condition further improves the trophic state of Mona Lake, as seen in the "New IC" simulations. Under the revised initial condition, a mean lake total phosphorus concentration of 17 μg/L is predicted (mesotrophic), reflected in mean Chlorophyll-a concentrations of 5 μg/L (1 μg/L above mesotrophy).

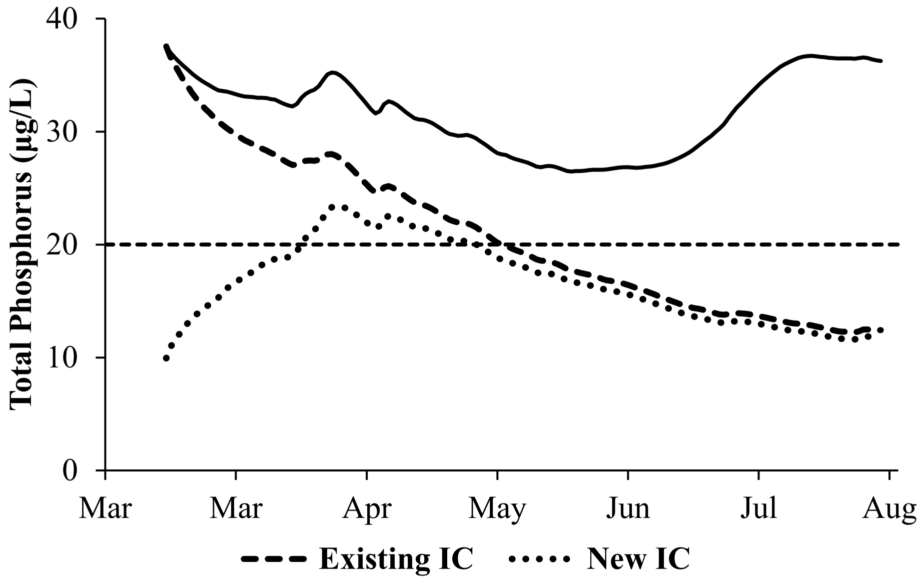

Figure 4-48 Total phosphorus predictions resulting from an external load reduction of 25 percent paired with internal loading control (no sediment release). Baseline shown by solid line and eutrophic threshold indicated at 20 µg/L.

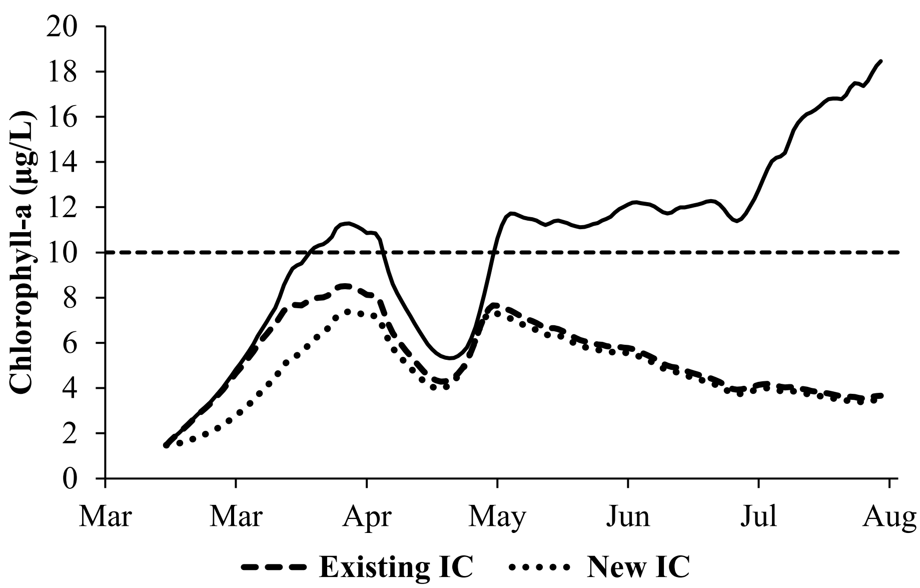

Figure 4-49 Chlorophyll-a predictions resulting from an external load reduction of 25 percent paired with internal loading control (no sediment release). Baseline shown by solid line and eutrophic threshold indicated at 10 µg/L.

5 Summary and Recommendations for Future Work

As Dr. Steve Chapra has noted, "Lakes function as watershed settling basins in which man's past and present impacts are recorded." Project objectives and accomplishments are detailed below, followed by recommendations for future work.

5.1 Summary

Decades of nuisance algal growth in the Mona Lake watershed are the result of cultural eutrophication (urbanization, agriculture). Historical external loading (tributaries prior to wastewater diversion) delivered high loads of phosphorus, stimulating high amounts of seasonal biomass production. Resulting decomposition (death and settling) has created a high sediment-oxygen demand. Combined with spatiotemporal phenomenon creating and contributing stochastically to its stratification and subsequent anoxia, particle bound phosphorus in the sediments begins its release and transport to the surface. Entrained to the photic zone, this internally loaded phosphorus arrives just following assimilation of high spring nutrient loads that stimulate initial algal growth. As external loading decreases with minimal summer discharge, internal loading manifests just as blue-green algae flourish, lacking competition for nutrients. Previous reduction efforts in external loading have offered improvement (wastewater diversion, celery flat discharge restriction), while decades of their historical prevalence continue to dictate the trophic state of Mona Lake in the form sediment phosphorus release (SRP).

5.1.1 Black Creek

Prior to discharge restriction, the celery flats were shown to contribute 1.6x and 2.6x downstream SRP and TP increases, respectively (Steinman & Ogdahl 2011). In this effort, the first study after the installation of discharge restrictors (2015), a non-significant difference ($p<0.10$) was found between upstream and downstream concentrations. From this, initial conclusions on the efficacy of celery flat discharge restriction (contribution to Black Creek) are positive, but suggest the need for further monitoring.

5.1.2 Little Black Creek

While only 9 percent of the hydrologic contribution to Mona Lake, Little Black Creek is responsible for 12 and 18 percent of the TP and SRP load, respectively. With management solutions likely still requiring external loading reduction, the upstream potential point-source detection, shown here to be spatially separate from prior contamination, offers a potential reduction in loading of 4 and 12 percent for TP and SRP, respectively. This load reduction was calculated by paired differences (10 sampling events in 2018) in concentrations between the original downstream sampling site and a site upstream of the source detection area.

5.1.3 Internal Loading

Sediment released phosphorus has been shown to account for ~68 percent of the mass total phosphorus to Mona Lake (Steinman et al. 2009). The impacts (both in the presence and absence of) this internal source of phosphorus have been quantified in the modeling effort, offering both a management tool for an internal loading treatment method feasibility study, and further conclusive evidence that sediment released phosphorus dominates the trophic state dynamics at a time when the lake is most vulnerable (blue-greens).

5.2 Recommendations

Multiple stochastic and ephemeral forces (meteorological) impact the dynamics of Mona Lake. Its erratic behavior applies greatly to its geochemical characteristics (external loading, variable retention time). Thus, a management approach aimed at improving its trophic state must be multifaceted, taking care to acknowledge the presence of idiosyncratic watershed components and events with consideration given to how they may impact management methods.

5.2.1 Tributary Monitoring

As noted above, there exists initial evidence for celery flat discharge control structure success. However, without continuous monitoring, final conclusions should not be drawn on the percent efficacy. Prior to discharge control structure installation, downstream-upstream differences in SRP were significantly correlated to antecedent precipitation, yet upstream-downstream load differences in SRP and TP were not significantly correlated (Steinman and Ogdahl 2011). This forms the basis for the recommendation that an updated, hydrologically robust, monitoring of the celery flats be a component of external load reduction efforts. For example, continuous discharge monitoring paired with discharge-triggered autosampling would offer true loading contribution analysis. Lastly, representing 77 percent of the hydrologic contribution, the Black Creek watershed is the most obvious candidate for further external loading reductions (best management practices) to couple with internal loading treatment/remediation.

5.2.2 Intrusion Monitoring

Detection of intrusions from Lake Michigan (physically and chemically) propose an area of thought crucial in considering when evaluating sediment release treatment and respective effectiveness. While hypothesized to strengthen stratification, intrusions could also impact the residence time of chemical treatment and/or inactivation technologies by diluting a treatment dosage, or rendering it insufficient. It is recommended the potential for these stochastic phenomenological be considered during internal loading treatment technology feasibly studies.

5.2.3 Sediment Release Study

In the management modeling presented above, it was shown that while external loading reductions (some unrealistic) would drastically improve the mean trophic state of Mona Lake, sediment release control (the absence of internal loading) would continue to govern late season growth dynamics. From this, a pairing of management actions, both external and internal, are recommended. Optimal best management practices for the watershed would require further analysis of land use not accomplished in this study, but should be conducted.

Various internal lake management techniques will have ranging efficacies, due to the stochastic mixing properties of Mona Lake. It is recommended that internal loading treatment technologies be evaluated based on their ability to treat and interact with the governing, dynamic components: anoxia and attendant phosphorus release, intrusion frequency and associated repercussions, and resiliency/usefulness of seasonal high-discharge flushing events. Lastly, treatment technology costing should consider the unique bathymetry of Mona Lake in that only an estimated 42 percent of its area is capable of stratification and attendant anoxia leading to phosphorus release – meaning only a relatively small area of the western half of the lake may require the decided upon treatment method.

Phosphorus release inactivation may be accomplished through chemical flocculation, oxidation, and/or binding methods:

- Aluminum salts (alum; Cooke et al. 2005), forms an aluminum hydroxide barrier that persists even in the presence of continued anoxia, although nearby Spring Lake has shown diminishing inactivation with this method in an 11 year post-treatment study (Annis Water Resources Institute Report 2017).
- Phoslock, a lanthanum modified bentonite clay, bonds with phosphorus released during anoxia (SRP) and has been shown to maintain its binding capacity longer than alum (Robb et al. 2003).

- Sediment oxidation (Riplox) enhances denitrification, retaining the phosphorus binding capabilities of iron in the sediments (Cooke et al. 2005).

Physical manipulation leading to phosphorus release inactivation may be accomplished through aeration or mixing:

- Hypolimnetic aeration, effective at increasing dissolved oxygen in the hypolimnion without causing destratification accomplished through submersion of a lift device, bringing hypolimnetic water to the surface, exchanging it with gases (oxygen), and returning it to the hypolimnion.
- Artificial circulation, preventing stratification, improves water column dissolved oxygen (prevents anoxia). Furthermore, this technique can alter the seasonal succession of algae, neutralizing seasonal nutrient dynamics favoring blue-greens later in the year by continuously providing for more desirable green algae (Cooke et al. 2005).
- Hypolimnetic withdrawal, accomplished through siphoning or pumping of hypolimnetic water to areas of low-nutrient concentration have been shown to accelerate phosphorus export (flushing) while reducing the entrained phosphorus capabilities (Cooke et al. 2005). This may be a unique method to consider regarding withdrawal to the Mona Lake channel.

5.3 Conclusion

The above summary of observations and subsequent production of a model capable of simulating management strategies, offers a contemporary, system-wide understanding of spatiotemporal trophic state dynamics. While the impact of legacy deposits is felt heavily in Mona Lake – it is not anomalous in that regard – and the work presented here, combined with recommendations for future work, ensure the capability to improve its water quality for current and future stakeholders.

"Let us put our minds together and see what kind of life we can make for our children."

Sitting Bull

6 Reference List

Annis Water Resources Institute. (2003). Mona Lake Watershed Atlas. Charles Stewart Mott Foundation.

Annis Water Resources Institute. (2017). Report. Internal Phosphorus Loading in Spring Lake 11 Years Following Alum Treatment. Submitted to Progressive AE.

APHA, AWWA, WEF, 2005. Standard Methods for the Examination of Water and Wastewater, 21st ed. American Public Health Association, Washington, D.C.

Carlson, R. E. (1977). A trophic state index for lakes. Limnology and Oceanography.

Chapra, S. C. (1997). Surface Water-Quality Modeling. Waveland Press.

Chapra, S. C., & Dobson, H. F. H. (1981). Quantification of the Lake Trophic Typologies of Naumann (Surface Quality) and Thienemann (Oxygen) with Special Reference to the Great Lakes. Journal of Great Lakes Research, 7(2), 182–193.

Chapra, S. C., and Martin, J.L., 2004. LAKE2K: A Modeling Framework for Simulating

Lake Water Quality (Version 1.2): Documentation and Users Manual. Civil and Environmental Engineering Dept., Tufts University, Medford, MA

Chapra, S. C., & Tarapchak, S. J. (1976). A chlorophyll model and its relationship to phosphorus loading plots for lakes. Water Resources Research, 12(6), 1260–1264.

Chorus, I. & Bartram, J. (1999). Toxic Cyanobacteria in Water—A Guide to Their Public Health Consequences, Monitoring, and Management, E & FN Spon, published on behalf of the World Health Organization, New York.

Cooke, G.D., Welch, E.B., Peterson, S.A., & Nichols, S.A. (2005). Restoration and Management of Lakes and Reservoirs. Third Edition. CRC Press.

Dillon, P. J., & Rigler, F. H. (1974). The phosphorus-chlorophyll relationship in lakes1,2. Limnology and Oceanography, 19(5), 767–773.

Dolman, A. M., Rücker, J., Pick, F. R., Fastner, J., Rohrlack, T., Mischke, U., & Wiedner, C. (2012). Cyanobacteria and Cyanotoxins: The Influence of Nitrogen versus Phosphorus. PLoS ONE, 7(6), e38757.

Evans, E. D. (1992). Mona, White and Muskegon Lakes in Muskegon County: The 1950's-1980's.

Freedman, P.L., Canale, R.P., and Auer, M. T. (1979). Applicability of land treatment of wastewater in the Great Lakes area basin: Impact of wastewater diversion, spray irrigation on water quality in the Muskegon County, Michigan, lakes.

Gillett, N. D., Luttenton, M. R., & Steinman, A. D. (2015). Spatial and temporal dynamics of phytoplankton communities in a Great Lakes drowned river-mouth lake (Mona Lake, USA). Journal of Limnology.

Jacoby, J.M., Collier DC, Welch EB, Hardy J, Crayton M (2000). Environmental factors associated with a toxic bloom of Microcystis aeruginosa. Canadian Journal of Fisheries and Aquatic Sciences 57: 231–240.

James, L.A. (2013). Legacy sediment: definitions and processes of episodically produced anthropogenic sediment. Anthropocene, 2 (2013), pp. 16-26.

Limnotech. (1982). The Effect of Wastewater Land Treatment on Eutrophication in Muskegon County Lakes.

Madison Metropolitan Sewerage District Staff. (2016). Yahara WINS Pilot Project: Final Report.

Michigan Department of Environmental Quality. (2017). ALGAL TOXIN MONITORING IN MICHIGAN INLAND LAKES: 2017 RESULTS.

Michigan Department of Environmental Quality. (2000). Total Maximum Daily Load for Biota for Little Black Creek: Muskegon County, Michigan.

Nürnberg, G. K., (2009). Assessing internal phosphorus load - Problems to be solved. Lake and Reservoir Management.

Nürnberg, G.K., (2004) Quantified hypoxia and anoxia in lakes and reservoirs. The Scientific World Journal, 4, 42–54.

Nürnberg, G. K., & LaZerte, B. D. (2016). Trophic state decrease after lanthanum-modified bentonite (Phoslock) application to a hyper-eutrophic polymictic urban lake frequented by Canada geese (*Branta canadensis*). Lake and Reservoir Management, 32(1), 74–88.

Ramm, K., & V. Scheps, (1997). Phosphorus balance of a polytrophic shallow lake with the consideration of phosphorus release. Hydrobiologia 342: 43–53.

Rawson, D.S., (1956). Algal indicators of trophic lake types. Limnology & Oceanography 1: 18–25.

Robb M., Greenop B., Goss Z., Douglas G., Adeney J. (2003). Application of Phoslock, an innovative phosphorus binding clay, to two Western Australian waterways: preliminary findings. In: Kronvang B. (eds) The Interactions between Sediments and Water. Developments in Hydrobiology (Vol 169).

Sherman, B., Whittington, J., & Oliver, R. (2000). The impact of artificial destratification on water quality in Chaffey Reservoir. Archiv Für Hydrobiologie. Special Issue Advances in Limnology, 55 (January 2000), 15–29.

Smith VH, Bennett SJ (1999): Nitrogen, phosphorus supply ratios and phytoplankton community structure in lakes. Arch Hydrobiol., 146, 37–53.

Sonzogni, W. C., Fitzgerald, G. P., & Lee, G. F. (1975). Effects of Wastewater Diversion on the Lower. Water Pollution Control Federation (Vol. 47).

Steinman, A. D., & Ogdahl, M. E. (2011). Does converting agricultural fields to wetlands retain or release P? Journal of the North American Benthological Society.

Steinman, A.D., Chu, X., & Ogdahl, M. (2009). Spatial and temporal variability of internal and external phosphorus loads in Mona Lake, Michigan. Aquatic Ecology.

Steinman, A., Rediske, R., Chu, X., Denning, R., & Nemeth, L. (2003). Preliminary Watershed Assessment: Mona Lake Watershed.

Steinman, A. D., Rediske, R., Denning, R., Nemeth, L., Chu, X., Uzarski, D., Luttenton, M. (2006). An environmental assessment of an impacted, urbanized watershed: the Mona Lake Watershed, Michigan. Arch. Hydrobiol., 166.

Vollenweider, R. A. (1975). Input-output Models. Hydrologie.

Wetzel, R. G. (2001). Limnology (3rd ed.). Academic Press.

Xie, L., Rediske, R. R., Hong, Y., O'Keefe, J., Gillett, N. D., Dyble, J., & Steinman, A. D. (2012). The role of environmental parameters in the structure of phytoplankton assemblages and cyanobacteria toxins in two hypereutrophic lakes. Hydrobiologia, 691(1), 255–268.